People's Democratic Republic of Algeria

Ministry of High Education and Scientific Research

University M'hamed BOUGARA- Boumerdes

Faculty of sciences of engineer

Department of Industrial Maintenance
Engine's Dynamics and Vibroacoustics Laboratory

In Partial Fulfillment
Of the Requirements for the Master
Degree in Mechanics and systems engineering

TOPIC

Study of the mechanical behavior of single edge notched tension (SENT)

Realized by:

- ***CHAFAI Oussama***
- ***KAABOUCHE Ali***

***Supervised by*:**
Dr. ***SETTET Ahmed Tidjani***

2016/2017

Acknowledgments

This work was done in laboratory of L.D.M. V (laboratoire dynamique des moteurs et vibroacoustique) (Engine's dynamic and vibroacoustics laboratory).

First, we thank God Almighty for giving us the will and patient to do this research.

We are grateful for the consistent guidance and support of our advisor ***Dr. SETTET Ahmed Tidjani****, who made this experience enjoyable as well as challenging. Without him, this work would never have been possible. we also want to thank him for helping us improve our selves professionally. Also, we would like to thank juries members for their interest to our work.*

Above all, we want to thank our families; our parents, for helping us becoming men that we are today, and for their support and understanding. And my gratitude is extended to our brothers and sisters.

we also would like to thank all the staff of the laboratory LDMV under direction of Professor ***NOUR Abdelkader*** *for their help and support, we enjoyed working for our classes, we are also grateful for the support of our friends and colleagues in mechanic and engineering systems group and all peoples that knows us*

without forgetting to think the Algerian Airlines Compony and its staff especially the composite atelier staff and our supervisors in it mister ***Samir*** *chief of composite atelier and mister* ***GHARBI Amar****.*

Dedication

I would like to dedicate this work to:

my parents, brothers and my sister.

my friends and all people I love.

All my teachers that I learned under their hands, especially those of maintenance department and mechanical and engineering of systems.

To everybody that helped me from near or far to reach what I'm today.

OUSSAMA

Dedication

I dedicate this modest work to:

My beloved mother and father

All my family

All my friends

All department's teachers, students and

Administrative staff and whoever helped to achieve this work

Ali

الملخص

في هذا العمل حاولنا فهم وتقييم التشققات في المواد المركبة وكيفية تفاعلها مع مختلف قياسات هذه التشققات وبالأخص المواد المصنوعة بواسطة دمج ألياف الكربون مع البروكسي (المرصوفة التي تلصق الألياف) ودمج ألياف الزجاج مع الألياف وهكذا قمنا بصناعة النماذج مستخدمين هذه المواد ثم قمنا بإحداث شقوق عليها بمختلف الأحجام والزوايا لأجل ملاحظة انتشار وتطور هذه التشققات بعد تعريضها لقوة شد وجذب وهذا قصد الحصول على والتشوه ومختلف الجهود والقوى.

قمنا بمحاكات النماذج التي لا تحتوي على تشققات مع تلك النماذج التي أعطتنا أضعف النتائج باستخدام برنامج المحاكات (Ansys).

قمنا بمقارنة هذه النتائج المحصلة من التجربة مع النتائج المحصلة باستخدام برنامج المحاكات.

Abstract

In this work, we tried to understand and estimate the composite material's rupture and how it reacts in the presence of different fracture dimensions especially for composite materials that are made by carbon/epoxy and glass/epoxy, so we prepared specimens using this two materials then we created different crack sizes and angles in the aim to see the propagation of the cracks and deduce the displacement, the deformation and stresses.

We simulated plan specimens (without crack) and specimens that gave us the weakest results using the simulation program 'Ansys'.

then we tried to compare theses experimental results with the other results that are obtained using simulation study of the critical specimens.

Résumé

Dans ce travaille on a essayé de comprendre et d'estimer la rupture du matériau composite et comment il réagit avec les différentes dimensions de fracture et spécialement pour les matériaux composites structuré en fibre de carbone et résine (époxy polymère) et fibre de verre et résine (époxy polymère), alors on a préparé des éprouvettes par ces matériaux, ensuite on a créé des fractures des différentes dimensions et angle afin de voir la propagation de ses fractures et déduire le déplacement, la déformation et les contraintes.

On a simulé les éprouvettes plane (sans fractures) et celles qui nous a données des résultats défavorables en utilisant le programme de simulation 'Ansys'.

On a comparé ses résultats expérimentaux avec des résultats obtenus après qu'on a utilisé la simulation

الكلمات الدلالية: المواد المركبة، المركبة، الكسر، التشقق، الشق، أليف الكربون، ألياف الزجاج، الأيبوكسي، المواد، الألياف، كربون/إيبوكسي، زجاج/إيبوكسي.

Key words: composite materials, composite, fracture, rupture, crack, cracked, carbon fiber, glass fiber, epoxy, materials, fibers, carbon/epoxy, glass/epoxy.

Mots clés : matériaux composites, composites, fracture, rupture, crack, cracker, fibre de carbone, fibre de verre, époxy, matériaux, fibres, carbone/époxy, verre/époxy.

TABLE OF CONTENTS

Table of contents

Abstract IV
Table of contents V
List of figures VI
List of tables VII
List of symbols VIII
General introduction 2

Chapter I : GENERALITIES ON COMPOSITE MATERIALS

I.1. Introduction 4
I.2. Definitions 4
I.3. Historical development 5
I.4. Advantages and disadvantages of composite material 6
I.4.1. Advantages of composite 6
I.4.2. The drawbacks of composite materials 7
I.5. Matrix 8
I.5.1. Definition 8
I.5.2. Role of the matrix 8
I.5.3. Types of matrices 9
a) Polymer Matrix Composites 9
b) Metal Matrix 11
c) Ceramic Matrix Composites 13
I.6. Reinforcement 14
I.6.1. Definition 14
I.6.2. Types of reinforcement 14
I.7. Classification of composite materials 16
I.8. Application of composite materials 16
I.9. Lamina and Laminate 17
I.9.1. Laminae 17
I.9.2. Laminates 20
I.10. Mechanical terminology 21
I.10.1. Introduction 21
I.10.2. Historic 21

I.10.3. Mechanics of materials approach ... 22
a) Determination of longitudinal modulus E_1 ... 22
b) Determination of transverse modulus E2 ... 23
c) Determination of major Poisson's ratio ... 24
d) Determination of in-plane shear modulus G_{12}: ... 24
e) 2D stiffness and compliance matrix for unidirectional lamina in terms of constants matrix: ... 25
f) Coefficients of stiffness matrix ... 25
g) Coordinates transformation stress and strain transformation are required: ... 26
I.10.4. Finite element approach ... 26
I.11. Conclusion: ... 27

Chapter II: FRACTURE IN COMPOSITE MATERIALS

II.1. Introduction ... 29
II.2. Definition ... 29
II.3. Historical perspective ... 30
II.4. The reason of the failure of structures ... 30
II.5. Relevance of fracture mechanics for damage analysis ... 33
II.6. Basic Principles of Fracture Mechanics ... 33
II.7. Application of Fracture Mechanics to Composite Materials ... 35
II.8. Other Analysis and Behavior Topics ... 37
II.9. Fracture criteria ... 40
II.10. The stress intensity criterion ... 40
II.11. The energy criterion ... 41
II.12. Crack separation modes ... 42
II.13. Crack surface displacements ... 42
II.14. Fracture Mechanics Analyses of Through-Thickness Cracks ... 43
II.15. Stress Intensity Factor Approach ... 46
II.16. Conclusion ... 49

Chapter III: EXPERIMENTAL STUDY

III.1. The aim of this work 51
III.2. The machine of test 51
III.3. Materials tested by Z250 machine 52
III.4. Tensile test 52
III.5. Material and geometry of Specimen used 52
III.6. Process of fabrication of CFRP & GFRP 52
III.6.1. Tools of work 52
III.6.2. The process 53
III.7. Result and discussion 62
III.7.1. Glass/epoxy result graphs (different crack sizes) 62
III.7.2. Glass/epoxy result graphs (different crack angles) 70
III.7.3. Carbon/epoxy result graphs (different crack sizes) 76
III.7.4. Carbon/epoxy result graphs (different crack sizes) 84
III.8. Conclusion 91

Chapter IV: NUMERICAL SIMULATION

IV.1. Introduction 93
IV.2. Definition of ANSYS 93
IV.3. FEA of specimen using ANSYS WORKBENCH 94
IV.4. Simulation process 94
IV.4.1. ACP (pre) 94
IV.4.2. Engineering data 95
IV.4.3. Geometry 96
IV.4.4. Meshing 97
IV.4.5. Setup 98
IV.4.6. load and boundary conditions 99
IV.5. Results and discussion of specimen in deferent crack angle 100
IV.5.1. Results for a carbon/epoxy specimen (without crack) 100

a) Total deformation ... 100
b) Maximum principal stress ... 100
c) Normal elastic strain ... 100
IV.5.2. Results for a carbon/epoxy specimen with a=15mm & $\theta = 90^{\circ}$ crack ... 101
a) Total deformation ... 101
b) Maximum principal stress ... 102
c) Normal elastic strain ... 102
IV.5.3. Results for a carbon/epoxy specimen (with a=15mm & crack $\theta = 60^{\circ}$) ... 103
a) Total deformation ... 103
b) Maximum principal stress ... 103
c) Normal elastic strain ... 104
IV.5.4. Results for a carbon/epoxy specimen with a=15mm & θ=45°crack ... 104
a) Total deformation ... 104
b) Maximum principal stress ... 105
c) Normal elastic strain ... 105
IV.5.5. Results for a carbon/epoxy specimen with a=15mm & θ=30° crack ... 106
a) Total deformation ... 106
b) Maximum principal stress ... 106
c) Normal elastic strain ... 107
IV.5.6. Discussion ... 107
a) Total deformation [mm] ... 107
b) Maximum principal stress [Mpa] ... 108
c) Normal elastic strain ... 109
IV.6 Results and discussion of specimen in deferent crack size ... 110
IV.6.1 Results for a glass/epoxy specimen with a=10mm & $\theta = 90^{\circ}$ crack ... 110
a) Total deformation ... 110
b) Maximum principal stress ... 111

c) Normal elastic strain 111

IV.6.2 Results for a glass/epoxy specimen with a=5mm & $\theta=90^{\circ}$ crack 112

a) Total deformation 112

b) Maximum principal stress 112

c) Normal elastic strain 113

IV.6.3 Results for a glass/epoxy specimen without crack 113

a) Total deformation 113

b) Maximum principal stress 114

c) Normal elastic strain 114

IV.6.4 Discussion 115

a) Total deformation [mm] 115

b) Maximum principal stress 116

c) Normal elastic strain 117

IV.7 Conclusion 117

General conclusion 120

LISTE OF FIGURES

Liste of figures

Chapter I

Figure. I.1: a composite material 4
Figure. I.2: ancient sword composite 6
Figure. I.3: making bricks with straw and mud 6
Figure. I.4: making bricks with straw and mud 6
Figure. I.5: matrix surrounds fillers 8
Figure. I.6: types of matrix 9
Figure. I.7: sport equipment made of polymer composite material 10
Figure. I.8: shows Gas turbine engine components made of metal matrix composites. 12
Figure. I.9: Reinforcements types 14
Figure. I.10: Two Principal Types of Laminae 18
Figure. I.11: Effect of Broken Fiber on Matrix and Fiber 19
Figure. I.12: Various Stress-Strain Behaviors 19
Figure. I.13: Unbounded View of Laminate Construction 20
Figure. I.14: Composite loaded in fiber direction. 23
Figure. I.15: Composite loaded in transverse direction. 24
Figure. I.16: Composite loaded with shear stress. 25
Figure. I.17: Transformation of coordinate 26

Chapter II

Figure. II.1 Schematic Roman bridge design. The arch shape of the bridge causes loads to be transmitted through the structure as compressive stresses. 33
Figure. II.2 Kings College Chapel in Cambridge, England. This structure was completed in 1515… 33
Figure. II.3 Crack-Extension Modes 35
Figure. II.4 Cracked Plate and Load-Deformation Diagram 35
Figure. II.5 Wu's Load Paths and Crack Orientations 37
Figure. II.6 Cracked Unidirectionally Reinforced Plate under Tension Perpendicular to fibers 37
Figure. II.7 Composite Laminate Crack Growth 38
Figure. II.8 Cracked Plate with Symmetric and Skew-Symmetric Stresses at Infinity 40
Figure. II.9 Edge crack in a plate in tension. 42

Figure. II.10 Crack separation modes: (a) opening; (b) sliding; and (c) tearing. 43
Figure. II.11 Crack opening displacement for a crack of size "2a.".. 44
Figure. II.12 The Griffith crack: A through-thickness crack in a uniaxially stressed plate of infinite width.. 45
Figure. II.13 stresses at the tip of a crack under plane stress. 47

Chapter III

Figure. III.1 ZWICK ROELL 250 KN machine 51
Figure. III.2 carbon fiber 53
Figure. III.3 glass fiber tissue 53
Figure. III.4 epoxy box 53
Figure. III.5 hardener box 53
Figure. III.6 vacuum bag 53
Figure. III.7 pumping felt 53
Figure. III.8 peeling film 53
Figure. III.9 vacuum bache 53
Figure. III.10 measure and cut the carbon fiber tissue 53
Figure. III.11 preparing the space of work 54
Figure. III.12 molding resin on plies 54
Figure. III.13 use peeling film to absorb resin 55
Figure. III.14 use the pumping felt to increase heat and pressure 55
Figure. III.15 use vacuum bache as a final rug 56
Figure. III.16 use vacuum bag to throwaway air and provoke pressure 56
Figure. III.17 tracing and cutting the obtained composite material 57
Figure. III.18 carbon fiber and glass fiber specimen 57
Figure. III.19 glass/epoxy specimens with different crack sizes 58
Figure. III.20 glass/epoxy specimens with different crack angles 59
Figure. III.21 carbon/epoxy specimens with different crack sizes 59
Figure. III.22 carbon/ epoxy specimens with different crack angles 59
Figure. III.23 the dimension of specimens 60
Figure. III.24 different carbon/epoxy crack seizes specimens after tensile test 60
Figure. III.25 different carbon/epoxy crack angles after tensile test 61
Figure. III.26 different glass/epoxy crack sizes after tensile test 61
Figure. III.27 different glass/epoxy crack angles tensile test 62

Figure. III.28 tensile test's graph on glass/epoxy specimen without crack 62
Figure. III.29 tensile test's graph on glass/epoxy specimen with crack a=2.5mm 63
Figure. III.30 tensile test's graph of glass/epoxy specimen with crack a=5mm 64
Figure. III.31 tensile test's graph of glass/epoxy specimen with crack a=7.5mm 64
Figure. III.32 tensile test's graph of glass/epoxy specimen with crack a=10mm 65
Figure. III.33 tensile test's graph of glass/epoxy specimen with crack a=12.5mm 66
Figure. III.34 tensile test's graph of glass/epoxy specimen with crack a=15mm 66
Figure. III.35 the effect of glass /epoxy material's different crack sizes on the maximum stress 67
Figure. III.36 the effect of glass/epoxy different crack sizes on the stress of rupture by tensile test 68
Figure. III.37 the effect of glass/epoxy different crack sizes on the strain of max stress of specimens by tensile test 68
Figure. III.38 the effect of glass/epoxy different crack sizes on the strain of rupture of specimens by tensile test 69
Figure. III.39 tensile test's graph of glass/epoxy specimen with crack a=15mm, θ=30° 70
Figure. III.40 tensile test's graph of glass/epoxy specimen with crack a=15mm, θ=45° 71
Figure. III.41 tensile test's graph of glass/epoxy specimen with crack a=15mm, θ=60° 72
Figure. III.42 tensile test's graph of glass/epoxy specimen with crack a=15mm, θ=90° 72
Figure. III.43 the effect of glass/epoxy different crack angles on the maximum stress........... 73
Figure. III.44 the effect of glass/epoxy different crack angles on the stress of rupture 74
Figure. III.45 the effect of glass/epoxy different crack angles on the strain of max stress of specimens by tensile test 75
Figure. III.46 the effect of glass/epoxy different crack angles on the strain of rupture of specimens by tensile test 75
Figure. III.47 tensile test's graph of carbon/epoxy specimen without crack 76
Figure. III.48 tensile test's graph of carbon/epoxy specimen with crack a=2.5mm. 77
Figure. III.49 tensile test's graph of carbon/epoxy specimen with crack a=5mm. 78
Figure. III.50 tensile test's graph of carbon/epoxy specimen with crack a=7.5mm. 78
Figure. III.51 tensile test's graph of carbon/epoxy specimen with crack a=10mm. 79
Figure. III.52 tensile test's graph of carbon/epoxy specimen with crack a=12.5mm. 80
Figure. III.53 tensile test's graph of carbon/epoxy specimen with crack a=15mm. 81
Figure. III.54 the effect of carbon fiber's different crack sizes on the maximum stress.......... 82
Figure. III.55 the effect of carbon fiber's different crack sizes on the stress of rupture 82
Figure. III.56 the effect of carbon/epoxy different crack sizes on the strain of maximum stress 83
Figure. III.57 the effect of carbon/epoxy different crack sizes on the maximum strain 84

Figure. III.58 tensile test's graph of carbon/epoxy specimen with crack a=15mm, θ=30° 84
Figure. III.59 tensile test's graph of carbon/epoxy specimen with crack a=15mm, θ=45° 85
Figure. III.60 tensile test's graph of carbon/epoxy specimen with crack a=15mm, θ=60° 86
Figure. III.61 tensile test's graph of carbon/epoxy specimen with crack a=15mm, θ=90° 87
Figure. III.62 the effect of carbon fiber's different crack angles on the maximum stress 88
Figure. III.63 the effect of carbon/epoxy different crack angles on the stress rupture 89
Figure. III.64 the effect of carbon/epoxy different crack angles on the stress rupture 90
Figure. III.65 the effect of carbon/epoxy different crack angles on the stress rupture 90

Chapter IV

Figure IV.1 ACP (pre) ANSYS window information 96
Figure IV.2 Engineering Data Sources 97
Figure IV.3 outline of composite materials in engineering data source 97
Figure IV.4 specimen with crack 98
Figure IV.5 specimen without crack 98
Figure IV.6 a meshed specimen (without crack) 99
Figure IV.7 a meshed specimen (with crack) 99
Figure IV.8 ACP Setup window 100
Figure IV.9 static structural as new window 100
Figure IV.10 load and boundary condition (specimen without crack) 101
Figure IV.11 load and boundary condition (specimen with crack) 101
Figure IV.12 total deformation of carbon/epoxy specimen (without crack) 102
Figure IV.13 Maximum principal stress of carbon/epoxy specimen (without crack) 102
Figure IV.14 normal elastic strain of carbon/epoxy specimen (without crack) 103
Figure IV.15 total deformation of carbon/epoxy specimen (with a=15mm & θ = 90° crack)..103
Figure IV.16 Maximum principal stress of carbon/epoxy specimen (with a=15mm & θ=90° crack) 104
Figure IV.17 normal elastic strain of carbon/epoxy specimen (with a=15mm & $\theta = 90^\circ$ crack) 104
Figure IV.18 total deformation of carbon/epoxy specimen (with a=15mm & $\theta = 60^\circ$ crack) 105
Figure IV.19 Maximum principal stress of carbon/epoxy specimen (with a=15mm & $\theta = 60^\circ$ crack) 105

Figure IV.20 normal elastic strain of carbon/epoxy specimen (with a=15mm & $\theta = 60°$ crack) 106

Figure IV.21 total deformation of carbon/epoxy specimen (with a=15mm & $\theta = 45°$ crack) 106

Figure IV.22 Maximum principal stress of carbon/epoxy specimen (with a=15mm & $\theta = 45°$crack) 107

Figure IV.23 normal elastic strain of carbon/epoxy specimen (with a=15mm & $\theta = 45°$ crack) 107

Figure IV.24 total deformation of carbon/epoxy specimen (with a=15mm & $\theta = 30°$ crack) 108

Figure IV.25 Maximum principal stress of carbon/epoxy specimen (with a=15mm & $\theta = 30°$crack) 108

Figure IV.26 normal elastic strain of carbon/epoxy specimen (with a=15mm & $\theta = 30°$ crack) 109

Figure IV.27 total deformation for carbon/epoxy & glass/epoxy specimens under tensile ... 110

test with deferent angle of crack 110

Figure IV.28 Maximum principal stress of carbon/epoxy &glass/epoxy specimen vs deferent angle of crack under tensile test 111

a) Figure IV.29 Normal elastic strain carbon/epoxy & glass/epoxy specimens under tensile test with deferent angle of crack 112

Figure IV.30 total deformation of glass /epoxy specimen (with a=10mm & $\theta = 90^\circ$ crack). 112

Figure IV.31 Maximum principal stress of glass /epoxy specimen (with a=10mm & $\theta = 90^\circ$ crack)........ 113

Figure IV.32 normal elastic strain of glass /epoxy specimen (with a=10mm & $\theta = 90^\circ$ crack) 113

Figure IV.33 total deformation of glass /epoxy specimen (with a=5mm & $\theta = 90^\circ$ crack)... 114

Figure IV.34 Maximum principal stress of glass /epoxy specimen (with a=5mm & $\theta = 90^\circ$ crack) 114

Figure IV.35 normal elastic strain of glass /epoxy specimen (with a=5mm & $\theta = 90^\circ$ crack) 115

Figure IV.36 total deformation of glass /epoxy specimen (without crack) 115

Figure IV.37 Maximum principal stress of glass /epoxy specimen (without crack) 116

Figure IV.38 normal elastic strain of glass /epoxy specimen (without crack) 116

Figure IV.39 total deformation for carbon/epoxy & glass/epoxy specimens under tensile test with deferent angle crack 117

Figure IV.40 Maximum principal stress of carbon/epoxy & glass/epoxy in deferent size of crack 118
Figure IV.41 Normal elastic strain carbon/epoxy & glass/epoxy specimens under tensile test with deferent crack size 119

LIST OF TABLES

List of tables

Table. I.1: the difference between thermosets and thermoplastics…………………………......16

Table. I.2: comparison of fracture toughness between different materials………………….......19

Table. III.1 carbon/epoxy and Glass/epoxy mechanical proprieties………………………….69

Table III.2 results of tensile test on specimens of glass fiber with different crack sizes……..74

Table. III.3 results of tensile test on specimens of glass fiber with different crack angles…...80

Table. III.4 results of tensile test on specimens of carbon/epoxy with different crack sizes…88

Table III.5 results of tensile test on specimens of carbon/epoxy with different crack angles..95

Table IV.1 total deformation of cracked specimen in different angle of crack……..………107

Table IV.2 total maximum principle stress of cracked specimen in different angle of crack............108

Table IV.3 total Normal elastic strain cracked specimen in different angle of crack……….109

Table IV.4 total deformation of cracked specimen in different size of crack ...……………115

Table IV.5 Maximum principal stress of glass/epoxy and glass/epoxy in different size of crack 116

Table IV.6 normal elastic strain of glass/epoxy and glass/epoxy in different size of crack...117

LIST OF SYMBOLS AND NOMENCLATURE

List of symbols and nomenclature

A: Area

A_m: area of matrix

A_f: area of fiber

a : $crack\ size$

b : thickness

CMC: Ceramic Matrix Composite

Δ : shear deformation

Δ_m : shear deformation in matrix

Δ_f : shear deformation in fiber

E_1 : Young's modulus following the x axis

E_2 : young s modulus following the y axis

E_m : matrix's young s modulus

E_f : fiber's young s modulus

ε : strain

ε_f: fiber strain

ε_m : matrix strain

ε_{max}: maximum strain

ε_1 : stain following x axis

ε_2 : stain following y axis

F: force

FEM: Finite Element Method

FE: Finite Element

G : the release strain energy

G_{12}: shear modulus

G_m: shear modulus of the matrix

G_f: shear modulus of the fiber

G_c: $critecal\ value\ of\ strain\ energy$

g :energy release

k : stress intensity

l: length

MMC: Metal Matrix Composite

PMC: polymer Matrix Composite

PEEK: Poly Ether-Ether-Ketone

PPS: Poly Phemy lens Sulfide

MMA: Mechanics of Material Approach

RVE: Respective Volume Element

ρ : $density$

δ_1: Stress following axis 1

δ_2: Stress following axis 2

σ_c^∞: criteria stress

δ_m: Stress of the matrix

δ_f: Stress of the fiber

σ_{rup}: Stress of rupture

σ_{max} Maximum stress

V: volume fraction

V_m: Matrix volume fraction

V_f: Fiber volume fraction

ν_{12} : Poisson's ration in the (x, y) plan

ν_m : Matrix s poisson ratio

ν_f : Fiber's Poisson's ratio

γ_{12} : Strain in plane

γ_m : Shear stress in the matrix

γ_f : Shear stress in the fiber

θ : $crack\ angle$

w : width

GENERAL INTRODUCTION

General introduction

Man knew materials and used it since long years ago, he didn't stop his development from that time until now and also to the future, development of human's life style, environment and surroundings won't stop, so the need of new upgraded tools and materials is not an option but it is the issue, it is a necessary need.

Man knew composite materials from centuries ago, he used it in some life's parts after he discovered its benefits against simple materials, due to their characteristics and performance it took day after day a more space of his interests.

Nowadays, composite materials take the majority of scientists and engineers researches, their wide field of use made it the axis of development of the other goods.

We can find composite material everywhere in trees, seeds (like alpha), birds and even humans body is a composite material, also we use composite materials in several domains such as means of transportation like aircrafts, trains, submarines, cars, building, arms and a lot of other applications.

The enemy of each material in first degree is fracture, it reduces its life time, characteristics and performance so we can find several researches in this issue, we tried also in this work to study the rupture of laminar composite material using some methods and technics to analyze this phenomenon.

Our work is structured as follow

Chapter 1: generalities on composite materials: definition, advantages, domain of use, classification…

Chapter 2: fracture of composite materials: definition of fracture, modes, laws and criteria

Chapter 3: experimental study using carbon/epoxy and glass/epoxy specimens submitting tensile test.

Chapter 4: simulation using Ansys.

General conclusion.

CHAPTER I

GENERALITIES ON COMPOSITE MATERIALS

I.1. Introduction

The objective of this chapter is to demystify the three basic things about the composite materials and structures the essence of the composite material the use of the composite materials instead of metals and the manner that composite materials used in structures, as part of the Essence, the general set of composite materials will be defined. classified. and characterized. Then, our attention will be focused on laminated fiber-reinforced composite materials. In the Use, we will investigate the advantages of composite materials over metals from the standpoints of strength. stiffness. weight and cost among others. Finally, in the Manner, we will look into examples and short case histories of important structural applications of composite materials to see even more reasons so that composite materials play an ever-expanding role in today's and tomorrow's structures.

I.2. Definitions

The word "composite" usually signifies that two or more separate materials are combined on a macroscopic scale to form a structural unit for various engineering applications.

Each of the material components may have distinct thermal, mechanical, electrical, magnetic, optical, and chemical properties. It is noted that a composite composed of an assemblage of these different materials gives us a useful new material whose performance characteristics are superior to those of the constituent materials acting independently.

One or more of the material components are usually discontinuous, stiffer, and stronger and known as the reinforcement; the less stiff and weaker material is continuous and called the matrix. Sometimes, because of chemical interactions or other processing effects, an additional distinct phase, called an interphase, exists between the reinforcement and the matrix material Composite materials have some advantages when compared to their components or metal parts. Some material properties that can be improved by forming a composite material are

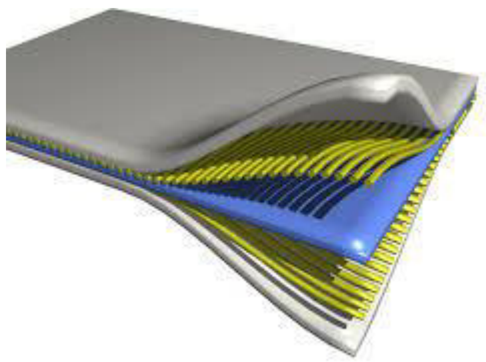

Figure. I.1 a composite material [9]

- Strength
- Stiffness
- Wear resistance
- Weight
- Fatigue life

- Extreme temperature response
- Thermal insulation or conduction
- Electrical insulation or conduction
- Acoustical insulation or conduction
- Response to nuclear, X-ray, or magnetic radiation
- Chemical response or inertness to an environment (corrosion resistance)
- Electromagnetic and radar insulation or conduction
- Crack (fracture) resistance and arrest
- Cost
- fabrication
- Temperature-dependent behavior
- Attractiveness. [1]

I.3. Historical development

Although it is difficult to say when or where people first learned about composites, nature and literature provide us with numerous examples. About 3000 BC, people used brick made of straw and mud for construction. Mud reinforced with bamboo shoots and glued laminated wood were used in houses built by the Egyptians in 1500 BC. Mongols invented the first composite bow in 1200 AD. Glass–polyester radomes were introduced in 1938 for application in aerospace structures here, the fiberglass was combined for the first time with good unsaturated polyester resins. The first molded fiberglass boat was built in 1942. The U.S. government patented the first filament winding process in 1946, followed by missile applications in the 1950s. In 1952, Herring and Galt (I952) described the mechanical properties of thin whiskers of Sn, and inferred that whiskers were single crystals. Boeing 727 started to employ reinforced plastic components in 1960. The first boron and high-strength carbon fibers were introduced in the early 1960s. It was not until 1969 that carbon/
epoxy materials were applied to operational fighter aircraft structures. Metal matrix composites (MMC) such as boron/aluminum were introduced in 1970. DuPont developed Kevlar fibers in early 1970s (Greenwoo and Rose, 1974). Starting in the late 1970s, the application of composites has greatly increased and expended to tennis rackets, large-diameter thin-walled pipes, civilian structural members, golf clubs, automobile and truck components, skis, fiber-reinforced concrete, epoxy-impregnated concrete, composite-pressure vessels, armor, space vehicles, boats, and airplanes, due to the development of new fibers such as carbon, boron, and nanotube and new composite systems with matrix made of polymers and metals. [1]

Figure. I.2 ancient sword composite [10]

Figure. I.3 making bricks with straw and mud [11]

Figure. I.4 plywood composite material [12]

I.4. Advantages and disadvantages of composite material

I.4.1. Advantages of composite

• High resistance to fatigue and corrosion degradation.

• High ‘strength or stiffness to weight’ ratio. As enumerated above, weight savings are significant ranging from 25-45% of the weight of conventional metallic designs.

• Due to greater reliability, there are fewer inspections and structural repairs.

• Directional tailoring capabilities to meet the design requirements. The fiber pattern can be laid in a manner that will tailor the structure to efficiently sustain the applied loads.

• Fiber to fiber redundant load path.

• Improved dent resistance is normally achieved. Composite panels do not sustain damage as easily as thin gage sheet metals.

• It is easier to achieve smooth aerodynamic profiles for drag reduction. Complex double-curvature parts with a smooth surface finish can be made in one manufacturing operation.

• Composites offer improved torsional stiffness. This implies high whirling speeds, reduced number of intermediate bearings and supporting structural elements. The overall part count and manufacturing & assembly costs are thus reduced.

• High resistance to impact damage.

• Thermoplastics have rapid process cycles, making them attractive for high volume commercial applications that traditionally have been the domain of sheet metals. Moreover, thermoplastics can also be reformed.

• Like metals, thermoplastics have indefinite shelf life.

• Composites are dimensionally stable i.e. they have low thermal conductivity and low coefficient of thermal expansion. Composite materials can be tailored to comply with a broad range of thermal expansion design requirements and to minimize thermal stresses.

• Manufacture and assembly are simplified because of part integration (joint/fastener reduction) thereby reducing cost.

• The improved weatherability of composites in a marine environment as well as their corrosion resistance and durability reduce the down time for maintenance.

• Close tolerances can be achieved without machining.

• Material is reduced because composite parts and structures are frequently built to shape rather than machined to the required configuration, as is common with metals.

• Excellent heat sink properties of composites, especially Carbon-Carbon, combined with their lightweight have extended their use for aircraft brakes.

• Improved friction and wear properties.

• The ability to tailor the basic material properties of a Laminate has allowed new approaches to the design of aero-elastic flight structures.

The above advantages translate not only into airplane, but also into common implements and equipment such as a graphite racquet that has inherent damping, and causes less fatigue and pain to the user.

I.4.2. The drawbacks of composite materials

Some of the associated disadvantages of advanced composites are as follows

• High cost of raw materials and fabrication.

• Composites are more brittle than wrought metals and thus are more easily damaged.

• Transverse properties may be weak.

• Matrix is weak, therefore, low toughness.

• Reuse and disposal may be difficult.

• Difficult to attach.

• Repair introduces new problems, for the following reasons

- ♣ Materials require refrigerated transport and storage and have limited shelf life.

- ♣ Hot curing is necessary in many cases requiring special tooling.
- ♣ Hot or cold curing takes time.
- ♣ Analysis is difficult.
- ♣ Matrix is subject to environmental degradation.

However, proper design and material selection can circumvent many of the above disadvantages. **[2]**

I.5. Matrix

I.5.1. Definition

The matrix supports the fibers and keeps them in the proper position, transfers the load to the strong fibers, protects the fibers from damage during manufacture and use of the composite, and prevents cracks in the fiber from propagating throughout the entire composite. The matrix usually provides the major control over electrical properties, chemical behavior, and elevated temperature use of the composite. [3]

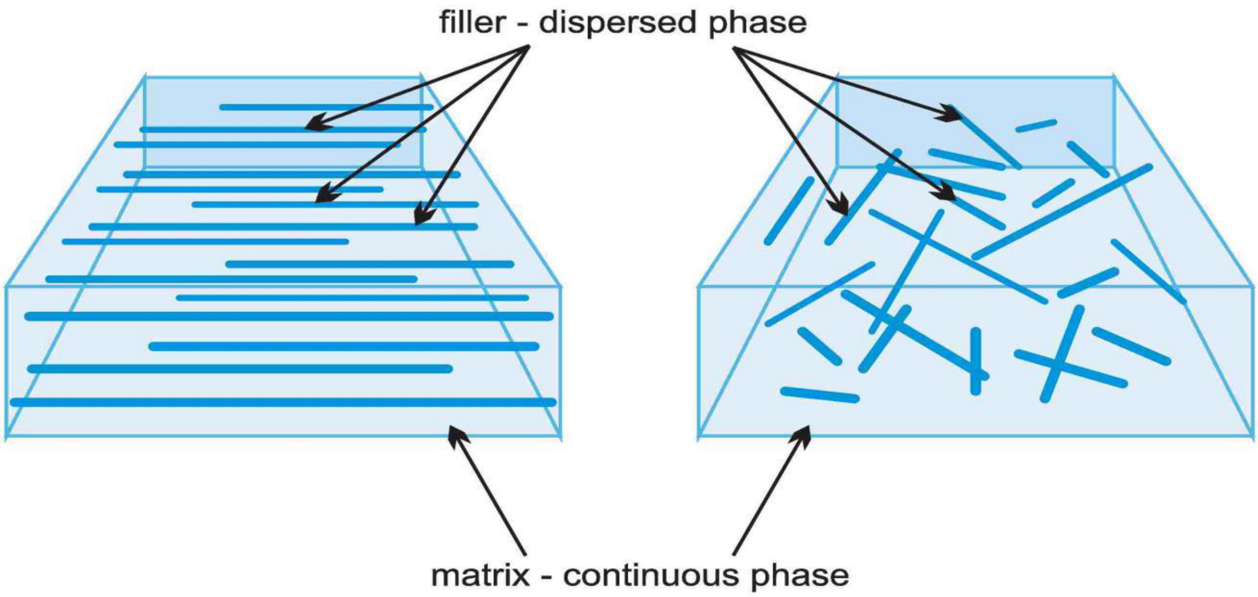

Figure. I.5 matrix surrounds fillers [13]

I.5.2. Role of the matrix

- Holds the fibers together
- Protects the fibers from environment
- Protects the fibers from abrasion (with each other)
- Helps to maintain the distribution of fibers
- Distributes the loads evenly between fibers

- Enhances some of the properties of the resulting material and structural component (that fiber alone is not able to impart). These properties are such as
- transverse strength of a lamina
- Impact resistance
- Provides better finish to final product. [8]

I.5.3. Types of matrices

Matrix divides into three principle types

Polymer matrix, ceramic matrix, metal matrix.

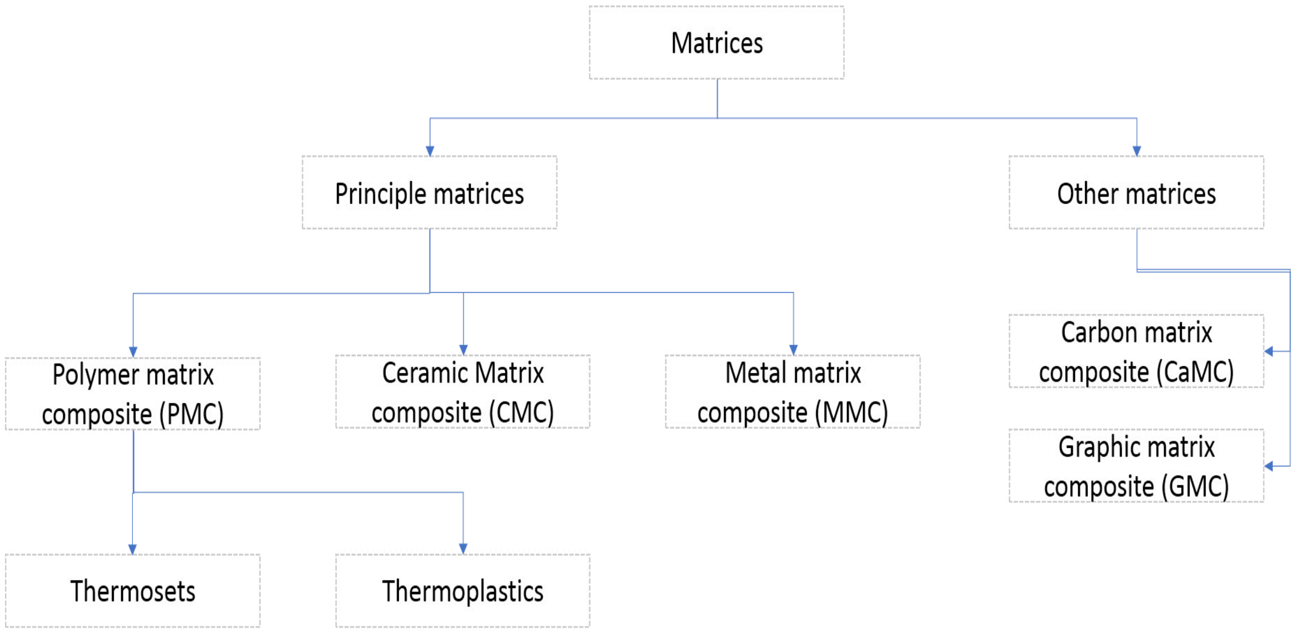

Figure. I.6 types of matrix

a) Polymer Matrix Composites

The most common advanced composites are polymer matrix composites (PMCs) consisting of a polymer (e.g., epoxy, polyester, urethane) reinforced by thin diameter fibers (e.g., graphite, aramids, boron). For example, graphite/ epoxy composites are approximately five times stronger than steel on a weight for-weight basis. The reasons why they are the most common composites include their low cost, high strength, and simple manufacturing principles.

The main drawbacks of PMCs include low operating temperatures, high coefficients of thermal and moisture expansion, and low elastic properties in certain directions.

These polymers include epoxy, phenolic, acrylic, urethane, and polyamide.[8]

Figure. I.7 sport equipment made of polymer composite material [14]

- Classification of polymers

Polymers are classified into thermosets and thermoplastics materials

Thermoset polymers are insoluble and infusible after cure because the chains are rigidly joined with strong covalent bonds; thermoplastics are formable at high temperatures and pressure because the bonds are weak and of the van der Waals type. Typical examples of thermoset include epoxies, polyesters, phenolic, and polyamide; typical examples of thermoplastics include polyethylene, polystyrene, polyether–ether–ketone (PEEK), and polyphenylene sulfide (PPS). The differences between thermosets and thermoplastics are given in the following table

Table. I.1 the difference between thermosets and thermoplastics

Thermoplastics	Thermoset
Soften on heating and pressure, and thus easy to repair	Decompose on heating
High strains to failure	Low strains to failure
Indefinite shelf life	Definite shelf life
Can be reprocessed	Cannot be reprocessed
Not tacky and easy to handle	Tacky
Short cure cycles	Long cure cycles
Higher fabrication temperature and viscosities have made it difficult to process	Lower fabrication temperature
Excellent solvent resistance	Fair solvent resistance

- Problems with using polymer matrix materials

• Limited temperature range.

• Susceptibility to environmental degradation due to moisture, radiation, atomic oxygen (in space).

• Low transverse strength.

• High residual stress due to large mismatch in coefficients of thermal expansion both fiber and matrix.

• Polymer matrix cannot be used near or above the glass transition temperature. [8]

b) Metal Matrix

Metal matrix composites (MMCs), as the name implies, have a metal matrix. Examples of matrices in such composites include aluminum, magnesium, and titanium. Typical fibers include carbon and silicon carbide.

Metals are mainly reinforced to increase or decrease their properties to suit the needs of design. For example, the elastic stiffness and strength of metals can be increased, and large coefficients of thermal expansion and thermal and electric conductivities of metals can be reduced, by the addition of fibers such as silicon carbide.

I.5.3.b.1. Advantages of metal matrix composites

Metal matrix composites are mainly used to provide advantages over monolithic metals such as steel and aluminum. These advantages include higher specific strength and modulus by reinforcing low-density metals, such as aluminum and titanium; lower coefficients of thermal expansion by reinforcing with fibers with low coefficients of thermal expansion, such as graphite; and maintaining properties such as strength at high temperatures.

MMCs have several advantages over polymer matrix composites. These include higher elastic properties; higher service temperature; insensitivity to moisture; higher electric and thermal conductivities; and better wear, fatigue, and flaw resistances. The drawbacks of MMCs over PMCs include higher processing temperatures and higher densities.

I.5.3.b.2. Limitation of metal matrix composites

- Heavier
- More susceptible to interface degradation at the fiber/matrix interface and to corrosion.

I.5.3.b.3. Applications of metal matrix composites

Metal matrix composites applications are

- Space The space shuttle uses boron/aluminum tubes to support its fuselage frame. In addition to decreasing the mass of the space shuttle by more than 145 kg, boron/aluminum also reduced the thermal insulation requirements because of its low thermal conductivity. The mast of the Hubble Telescope uses carbon-reinforced aluminum.
- Military Precision components of missile guidance systems demand dimensional stability that is, the geometries of the components cannot change during use.27 Metal matrix composites such as SiC/aluminum composites satisfy this requirement because they have high micro yield strength. * In addition, the volume fraction of SiC can be varied to have a coefficient of thermal expansion compatible with other parts of the system assembly.
- Transportation Metal matrix composites are finding use now in automotive engines that are lighter than their metal counterparts. Also, because of their high strength and low weight, metal matrix composites are the material of choice for gas turbine engines (Figure. I.9). [8]

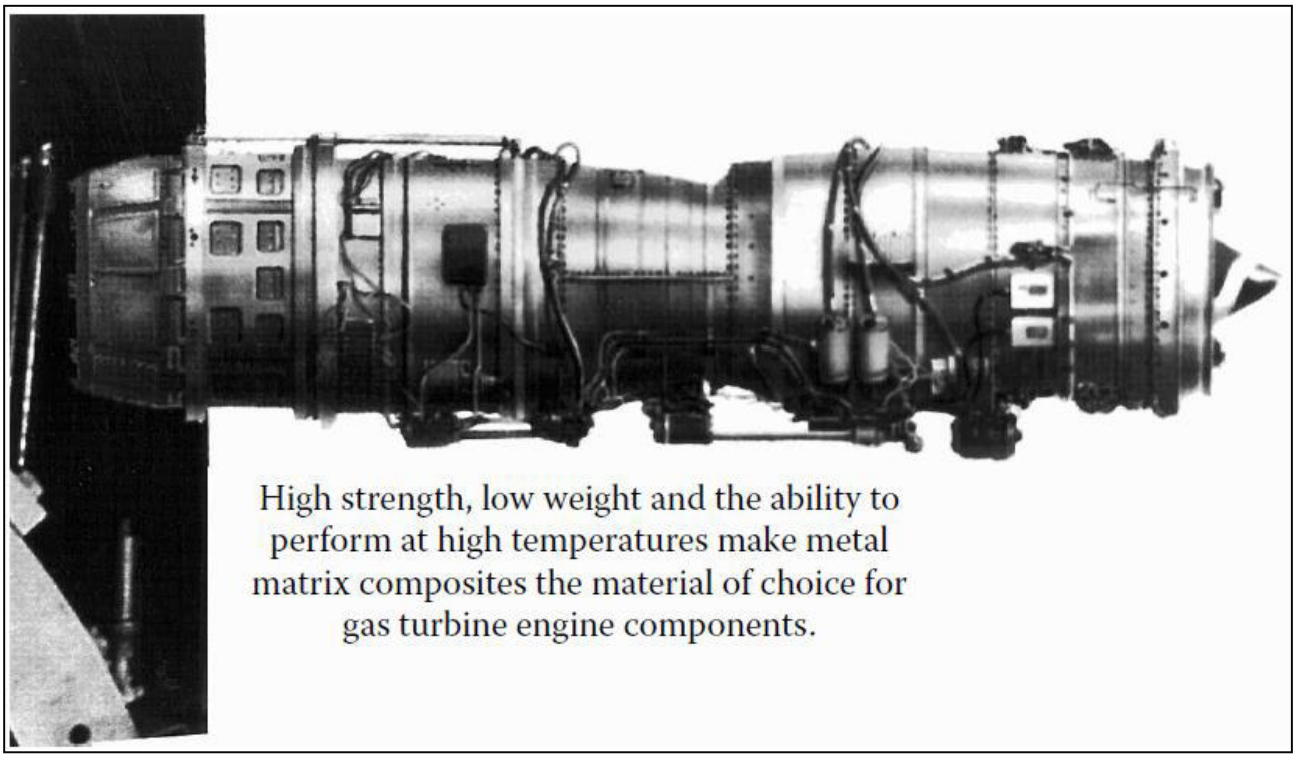

Figure. I.8 shows Gas turbine engine components made of metal matrix composites. (Photo courtesy of Specialty Materials, Inc., http://www.specmaterials.com.)

c) Ceramic Matrix Composites

I.5.3.c.1. Definition

Ceramic matrix composites (CMCs) have a ceramic matrix such as alumina calcium alumino-silicate reinforced by fibers such as carbon or silicon carbide.

I.5.3.c.2. Advantages of ceramic matrix composites

Advantages of CMCs include high strength, hardness, high service temperature limits* for ceramics, chemical inertness, and low density. However, ceramics by themselves have low fracture toughness. Under tensile or impact loading, they fail catastrophically. Reinforcing ceramics with fibers, such as silicon carbide or carbon, increases their fracture toughness (Table 1. 2)

because it causes gradual failure of the composite. This combination of a fiber and ceramic matrix makes CMCs more attractive for applications in which high mechanical properties and extreme service temperatures are desired.

Table. I.2 comparison of fracture toughness between different materials

Material	Fracture toughness (Mpa $m^{1/2}$)
Epoxy	3
Aluminum alloys	35
Silicon carbide	3
SiC/Al_2O_3	27
SiC/SiC	30

I.5.3.c.3. Disadvantages1/2

- brittleness
- Susceptible to flows

I.5.3.c.4. Applications of ceramic matrix composites

Ceramic matrix composites are finding increased application in high-temperature areas in which metal and polymer matrix composites cannot be used. This is not to say that CMCs are not attractive otherwise, especially considering their high strength and modulus, and low density. Typical applications include cutting tool inserts in oxidizing and high-temperature environments.

Textron Systems Corporation® has developed fiber-reinforced ceramics with SCS™ monofilaments for future aircraft engines. [8]

I.6. Reinforcement

I.6.1. Definition

Reinforcement materials usually add rigidity and greatly impede crack propagation. In particular, they enforce the mechanical properties of the matrix and, in most cases, are harder, stronger, and stiffer than the matrix. The reinforcement can be divided into four basic categories fibers, particulates, fillers, and flakes.

The role of the reinforcement in a composite material is fundamentally one of increasing the mechanical properties of the neat resin system.

I.6.2. Types of reinforcement

Reinforcements for the composites can be fibers, fabrics particles or whiskers. Fibers are essentially characterized by one very long axis with other two axes either often circular or near circular. Particles have no preferred orientation and so does their shape. Whiskers have a preferred shape but are small both in diameter and length as compared to fibers.

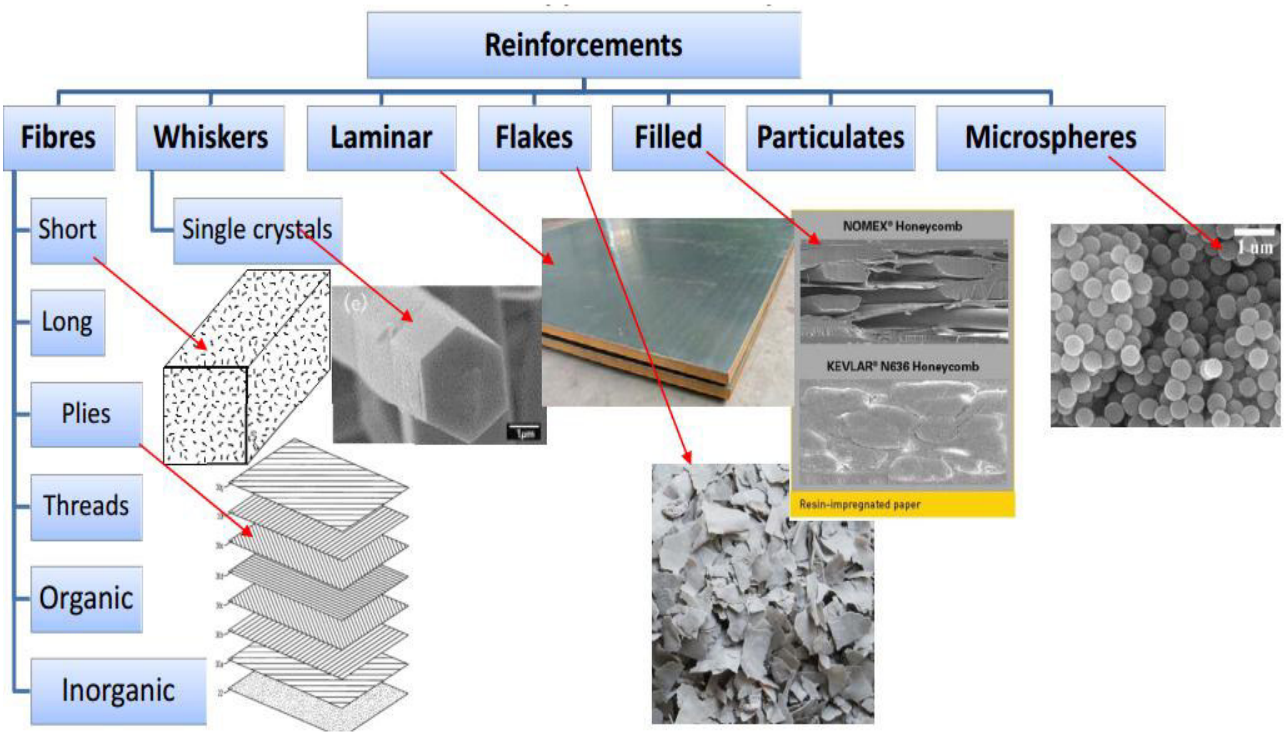

Figure. I.9 Reinforcements types

a) **Flakes**

are in flat platelet form and have a primarily two-dimensional geometry with strength and stiffness in two directions. They can form an effective composite material when suspended in a glass or plastic. Ordinarily, flakes are packed parallel to one another with a resulting higher density than fiber-packing concepts. Typical flake materials are mica, aluminum, and silver. Mica flakes embedded in a glassy matrix provide composites that can be machined easily and are used in electrical applications. Aluminum flakes are commonly used in paints and other coatings in which they orient themselves parallel to the surface of the coating. Silver flakes are used where good conductivity is required.

b) **Fillers**

are particles or powders added to material to change and improve the physical and mechanical properties of composites. They are also used to lower the consumption of a more expensive binder material. In particular, fillers are used to modify or enhance properties such as thermal conductivity, electrical resistivity, friction, wear resistance, and flame resistance. Typical fillers are calcium carbonate.

Toughening Mechanisms in Composite Materials aluminum oxide, lime (also known as calcium oxide), fumed silica, treated clays, and hollow glass beads.

c) **Particulates**

used in composites can be small particles (<0.25 mm), hollow spheres, cubes, platelets, or carbon nanotubes. In each case, the particulates provide desirable material properties, and the matrix acts as a binding medium necessary for structural applications. The arrangement of particulate materials may be random or with a preferred orientation. In general, particles are not very effective in improving strength and fracture resistance. Typical particle materials are lead, copper, tungsten, molybdenum, and chromium.

d) **Fiber**

is a rope or string used as a component of composite materials whose aspect ratio (length/diameter) is usually very large (>100). The cross-section can be circular, square, or hexagonal. Commonly used fibers in the composite include the following

- Glass fiber, which consists primarily of silicon dioxide and metallic oxide modifying elements and are generally produced by mechanical drawing of molten glass through a small orifice. They are widely used due to low cost and high corrosion resistance. Glass fibers can be used in fishing rods, storage tanks, and aircraft parts.
- Aramid fiber, which has higher specific strength and is lighter than glass, is more ductile than carbon. Examples of industrial application are armor, protective clothing, and sporting goods.
- Carbon fiber, which is often produced from an oxidized polyacrylonitrile or via pyrolysis carbonized polymers. The carbon fiber can have a modulus as high as 950 GPa with low density. Its diameter is usually between 5 and 8 um, smaller than a human hair (50 um).

- Boron fiber, which usually has high stiffness, good compressive strength, and large diameters (0.05–0.2 mm) compared to other types of fibers. Composites with boron fibers are widely used in aerospace structures where high stiffness is needed.
- Silicon carbide fiber, which is usually used in high-temperature metal and ceramic matrix composites (CMC)because of its excellent oxidation resistance, high modulus, and strength in high temperature atmosphere.

e) WHISKERS

Whiskers differ from fibers in that whiskers are shorter. Practically, fibers are usually considered to have a length of at least 5 mm. Below that length, the material is considered to be a whisker. (If the material does not have a high aspect ratio, that is, high length to radius ratio, it is called a particle. Particles are not usually considered reinforcements in the same sense as fibers and whiskers.)

Because whiskers are short, the probability of encountering a defect is much lower than with conventional fibers. Hence, on average, individual whiskers have higher tensile properties than individual fibers. However, in a composite, the higher properties are often not fully realized because of end effects (weakening of the composite because of problems at the ends of the fibers).

In addition, the whiskers are so much closer to the critical length that full transfer of force from the matrix to the reinforcement is not sustained for as long a time as with conventional fiber lengths.[4]

I.7. Classification of composite materials

Classification based on matrix materials, four commonly accepted composites are

- Metallic matrix composite
- Ceramic matrix composite
- Polymer matrix composite
- Carbon matrix composite

Classification based on the geometry of reinforcement

- Fiber reinforced composite
- Whiskers composites
- Flake composite
- Particulate composite

I.8. Application of composite materials

a) Aircraft/military commercial, pleasure and military aircrafts, including components for aerospace and related applications.

b) Appliance/business composite applications for the household and office including appliances, power tools, business equipment, etc.
c) Automotive/transportation the largest of the markets, products include parts for automobiles, trucks, rail and farm applications.
d) Civil infrastructure a relatively new market for composites, these applications include the repair and replacement of civil infrastructure including buildings, roads, bridges, piling, etc.
e) Construction includes materials for the building of homes, offices, and architectural components. Products include swimming pools, bathroom fixtures, wall panels, roofing, architectural cladding.
f) Consumer products include sports and recreational equipment such as golf clubs, tennis rackets, snowmobiles, mobile campers, furniture, microwave cookware.
g) Corrosion-resistant equipment products for chemical-resistant service such as tanks, ducts and hoods, pumps, fans, grating, chemical processing, pulp and paper, oil and gas, and water/wastewater treatment markets.
h) Electrical this encompassing market includes components for both electrical and electronic applications such as pole line hardware, substation equipment, microwave antennas, printed wiring boards, etc.
i) Marine products for commercial, pleasure and naval boats and ships.[6]

I.9. Lamina and Laminate

I.9.1. Laminae

The basic building block of a laminate is a lamina which is a flat (sometimes curved as in a shell) arrangement of unidirectional fibers or woven fibers in a matrix. Two typical flat laminae along with their principal material axes that are parallel and perpendicular to the fiber direction are shown in Figure. I.-11. The fibers are the principal reinforcing or load-carrying agent and are typically strong and stiff. The matrix can be organic, metallic, ceramic, or carbon. The function of the matrix is to support and protect the fibers and to provide a means of distributing load among, and transmitting load between, the fibers. The latter function is especially important if a fiber breaks as in Figure. I.-12. There, load from one portion of a broken fiber is transferred to the matrix and, subsequently, to the other portion of the broken fiber as well as to adjacent fibers. The mechanism for load transfer is the shearing stress developed in the matrix; the shearing stress resists the pulling out of the broken fiber. This load-transfer mechanism is the means by which whisker- reinforced composite materials carry any load at all above the inherent matrix strength.

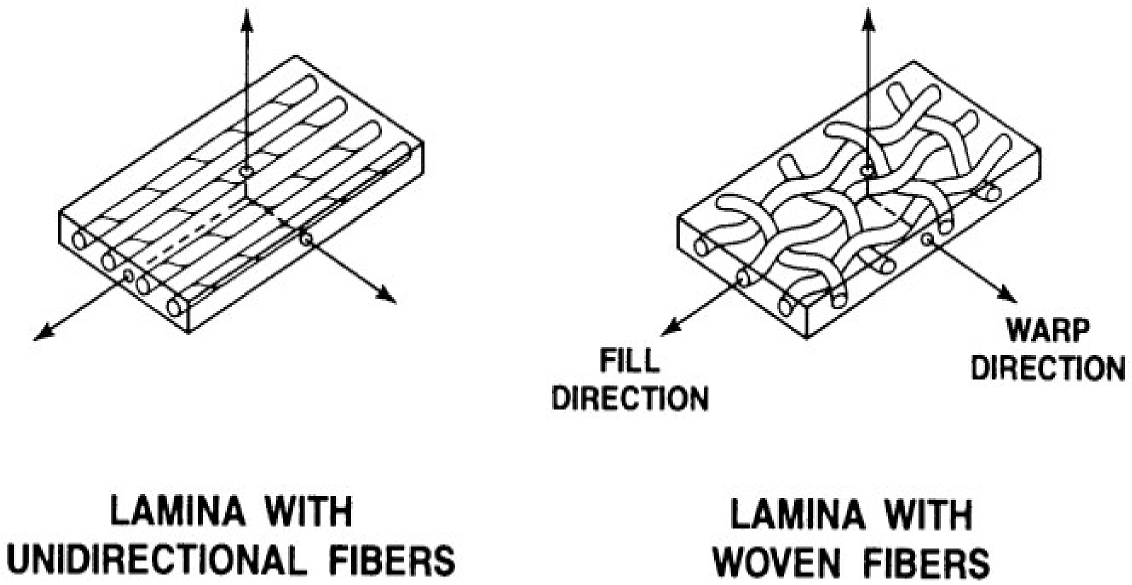

Figure. I.10 Two Principal Types of Laminae [Robert M. JONES Mechanics of composite materials second edition book's picture]

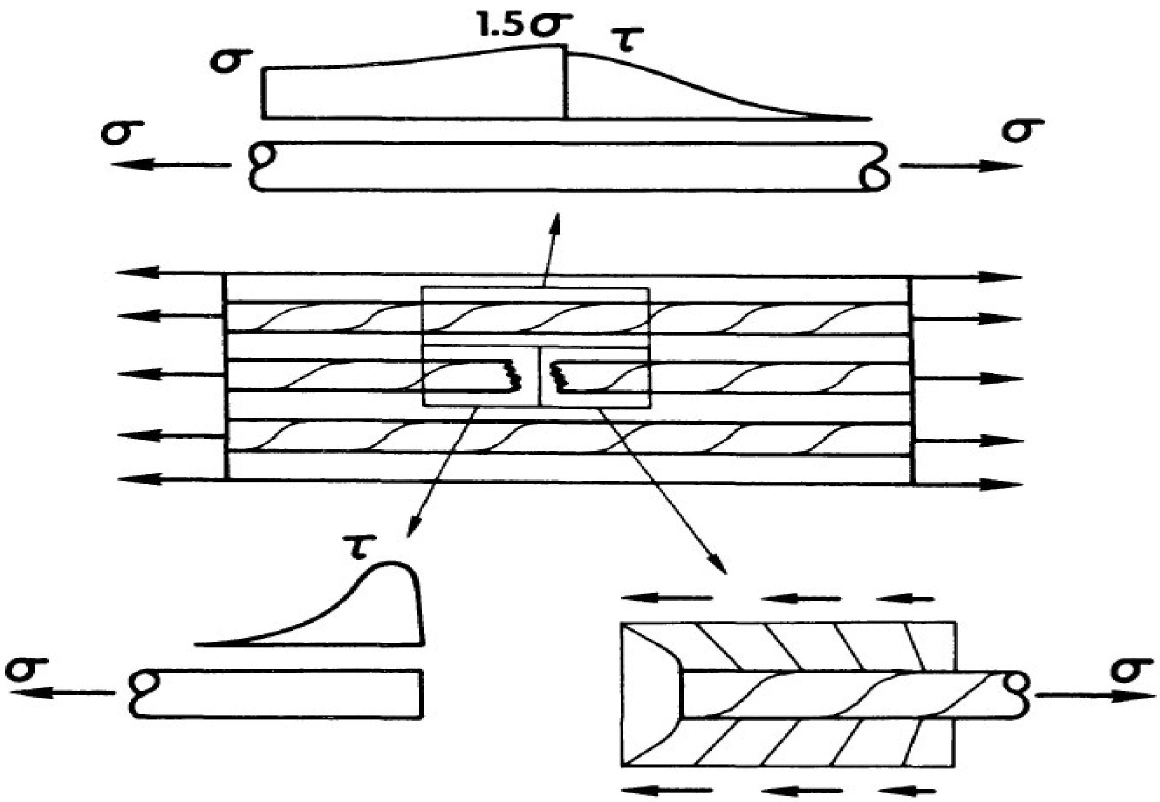

Figure. I.11 Effect of Broken Fiber on Matrix and Fiber. [Robert M. JONES Mechanics of composite materials second edition book's picture]

The properties of the lamina constituents, the fibers and the matrix, have been only briefly discussed so far. Their stress-strain behavior is typified as one of the four classes depicted in Figure. I.-13. Fibers generally exhibit linear elastic behavior, although reinforcing steel bars in concrete are more nearly elastic-perfectly plastic. Aluminum, as well as

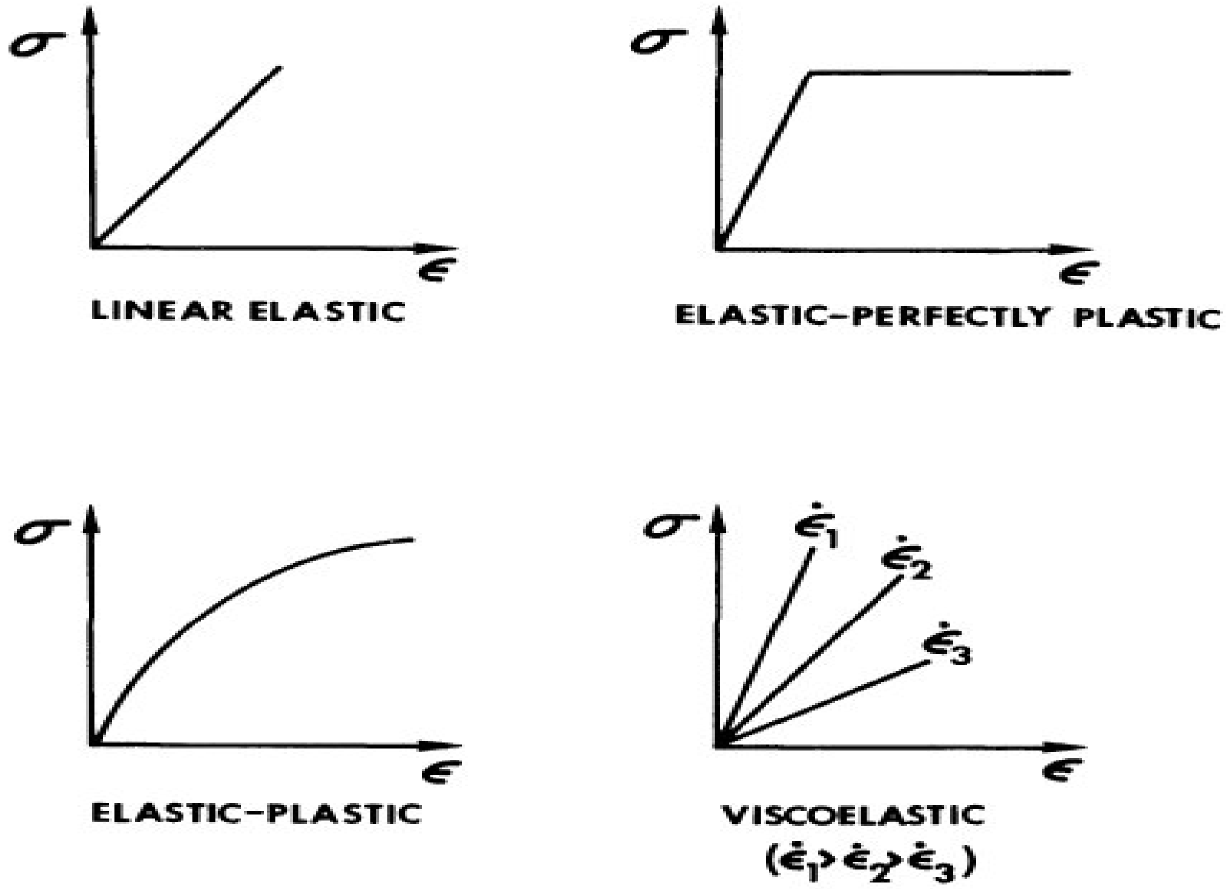

Figure. I.12 Various Stress-Strain Behaviors. [Robert M. JONES Mechanics of composite materials second edition book's picture]

many polymers, and some composite materials exhibit elastic-plastic behavior that is really nonlinear elastic behavior if there is no unloading. Commonly, resinous matrix materials are viscoelastic if not viscoplastic, i.e., have strain-rate dependence and linear or nonlinear stress-strain behavior. The various stress-strain relations are sometimes referred to as constitutive relations because they describe the mechanical constitution of the material.

Fiber-reinforced composite materials such as boron-epoxy and graphite-epoxy are usually treated as linear elastic materials because the essentially linear elastic fibers provide the majority of the strength and stiffness. Refinement of that approximation requires consideration of some form of plasticity, viscoelasticity, or both (viscoplasticity). Very little work has been done to implement those models or idealizations of composite material behavior in structural applications.

I.9.2. Laminates

A laminate is a bonded stack of laminae with various orientations of principal material directions in the laminae as in Figure. I.-14. Note that the fiber orientation of the layers in Figure. I.14 is not symmetric about the middle surface of the laminate. The layers of a laminate are usually bonded together by the same matrix material that is used in the individual laminae. That is, some of the matrix material in a lamina coats the surfaces of a lamina and is used to bond the lamina to its adjacent laminae without the addition of more matrix material. Laminates can be composed of plates of different materials or, in the present context, layers of fiber-reinforced laminae. A laminated circular cylindrical shell can be constructed by winding resin-coated fibers on a removable core structure called a mandrel first with one orientation to the shell axis, then another, and so on until the desired thickness is achieved.

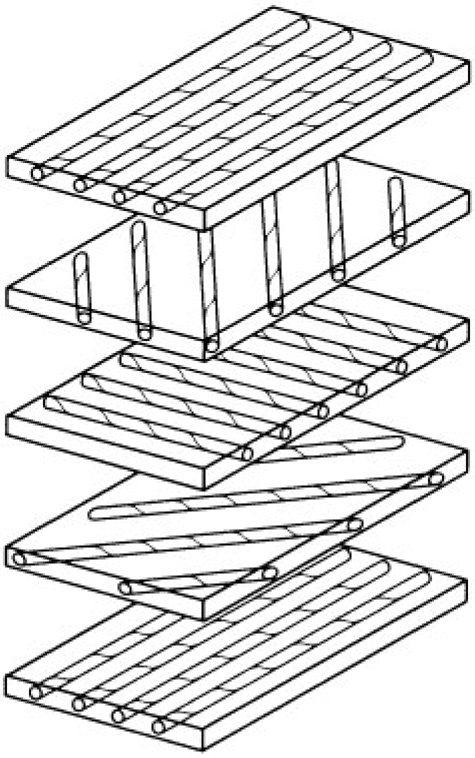

Figure. I.13 Unbounded View of Laminate Construction. [Robert M. JONES Mechanics of composite materials second edition book's picture]

A major purpose of lamination is to tailor the directional dependence of strength and stiffness of a composite material to match the loading environment of the structural element. Laminates are uniquely suited to this objective because the principal material directions of each layer can be oriented according to need. For example, six layers of a ten-layer laminate could be oriented in one direction and the other four at 90° to that direction; the resulting laminate then has a strength and extensional stiffness roughly 50% higher in one direction than the other.

The ratio of the extensional stiffnesses in the two directions is approximately 64, but the ratio of bending stiffnesses is unclear because the order of lamination is not specified in the example. Moreover, if the laminae are not arranged symmetrically about the middle surface of the laminate, the result is stiffnesses that represent coupling between bending and extension.[5]

I.10. Mechanical terminology

I.10.1. Introduction

A composite is composed of two or more separate materials. Each of the material components may have distinct material properties. It is important to determine the effective material properties if we replace the composite with a homogeneous material. In classical mechanics, at a macrolevel, the material properties are always assumed to be homogeneous on an average basis, whereas at a microlevel, i.e., inside the composite, the material properties are heterogeneous.

At a microlevel, the heterogeneous microstructure and physical laws are usually known. The task is to find homogeneous material properties at a macrolevel based on the information of microstructure. These properties are often called overall material properties or effective material properties, and the process is often known as homogenization.[1]

I.10.2. Historic

Recently, some investigations have been made into the composite array using methods such as the homogenization method (Qin and Yang, 2008). Grassi et al. (2002) numerically examined the effect of fiber volume fraction of the through thickness Young's modulus. Qin (2004a,b, 2005) and Yang and Qin (2004) presented several boundary elements–micromechanics models for predicting effective properties of materials with defects or inclusions. Antoniou et al. (2009) developed a FE model to predict mechanical behavior of glass/epoxy tubes under static loading. Xu et al. (2008) conducted an experiment on the plate size in determining the effective modulus. Yang and Qin (2001, 2003) used the finite element method (FEM) to predict effective elasto-plastic properties of composites. To determine the ranges of effective properties using various micromechanics models, the Voigt and Reuss rule (Gasik, 1998) presented a method to find the upper and lower bounds, respectively, of the stiffness for a composite material with arbitrary fiber-matrix geometry. Micromechanics models were also used to determine effective properties of piezoelectric materials with cracks (Qin et al., 1998; Yu and Qin, 1996; Qin and Yu, 1997), microvoids (Qin and Yu, 1998), and of human dentine materials (Wang and Qin, 2007, 2011; Qin and Swain, 2004). Several other research studies have used representative unit cell models to investigate the dependence of component

properties on composite materials (Tvergaard, 1990; Bao et al., 1991; Zahl and McMeeking, 1991; Levy and Papazian, 1990; Li et al., 1995; Feng et al., 2003). This section briefly
describes major micromechanics models commonly used to determine effective material properties and to analyze the corresponding mechanical behavior of composite materials. It includes the mechanics of materials approach (MMA), finite element modeling, direct and indirect homogenization, and boundary element approach.[1]

I.10.3. Mechanics of materials approach

MMA (mechanics of materials approach) provides an analytical technique to calculate effective material properties of the fiber-reinforced composites. These overall material properties can be used to predict the material behavior with various interfaces. MMA is used to determine the overall material properties due to their respective fiber and matrix volume fractions and constituent material properties. It assumes an average of stresses and strains to examine the global response.[1]

a) Determination of longitudinal modulus E_1

We begin with determining the Young's modulus E_1 (Young's modulus in the fiber direction) of a fiber reinforced composite. To this end, consider a representative volume element (RVE) in Figure. I.15. It is subjected to a longitudinal normal stress σ_1, as shown in Figure. I.15. Static equilibrium requires that the total resultant force F on the RVE must equal the sum of the forces acting on the fiber and matrix

$$F = \sigma_1 A = \bar{\sigma}_{m1} A_{m1} + \bar{\sigma}_{f1} A_f \qquad \text{(I.1)}$$

where subscripts "m" and "f" refer to matrix and fiber, A, A_m, and A_f stand for cross areas of composite, matrix, and fiber respectively, and

$$\bar{\sigma}_{m1} = \frac{1}{V}\int \sigma_{m1} dV = \frac{1}{A}\int \sigma_{m1} dA, \bar{\sigma}_{f1} = \frac{1}{V}\int \sigma_{m1} dV = \frac{1}{A}\int \sigma_{f1} dA \qquad \text{(I.2)}$$

Since the length of matrix and fiber are the same (Figure. I.15), area fractions are equal to the corresponding volume fractions. As such, Eq. (I.1) can be rearranged to give a "rule of mixtures" for longitudinal stress

$$\sigma_1 = \bar{\sigma}_{m1}\frac{A_m}{A} + \bar{\sigma}_{f1}\frac{A_f}{A} = \bar{\sigma}_{m1} v_m + \bar{\sigma}_{f1} v_f \qquad \text{(I.3)}$$

where v_m and v_f are area fraction of matrix and fiber, respectively. If both the matrix and fiber are linear elastic and isotropic, we have from Hooke's law

$$\sigma_1 = E_1 \bar{\varepsilon}_1, \sigma_{m1} = E_m \bar{\varepsilon}_{m1}, \sigma_{f1} = E_f \bar{\varepsilon}_{f1} \qquad \text{(I.4)}$$

Where

$$\bar{\varepsilon}_1 = \frac{1}{A}\int \varepsilon_1 dA, \bar{\varepsilon}_{m1} = \frac{1}{A}\int \varepsilon_{m1} dA, \bar{\varepsilon}_{f1} = \frac{1}{A}\int \varepsilon_{f1}\, dA \qquad (\text{I.5})$$

and Eq (I.3) becomes

$$E_1\bar{\varepsilon}_1 = E_m\bar{\varepsilon}_m v_m + E_f\bar{\varepsilon}_f v_f \qquad (\text{I.6})$$

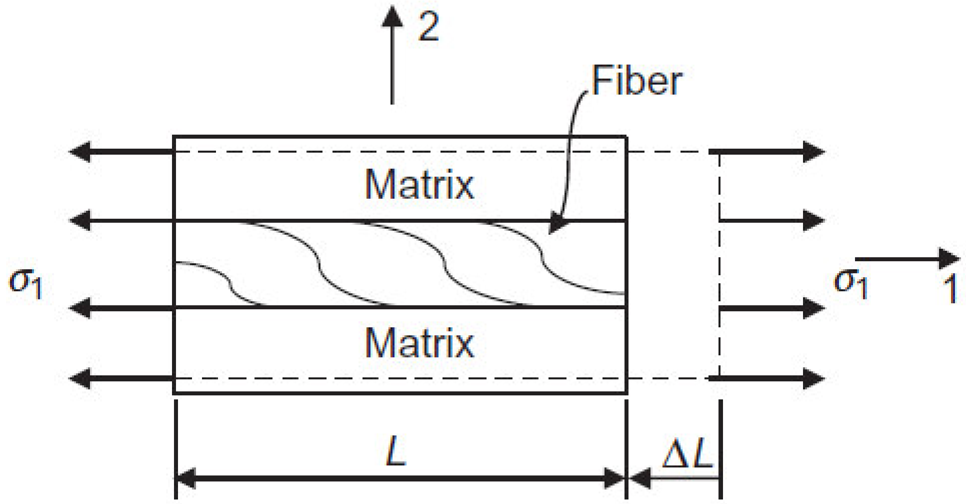

Figure. I.14 Composite loaded in fiber direction.

If the matrix and fiber are perfectly bonded, the average strains in the composite, matrix, and fiber along the one direction are all equal

$$\bar{\varepsilon}_1 = \bar{\varepsilon}_{m1} = \bar{\varepsilon}_{f1} \qquad (\text{I.7})$$

Combination of Eqs (I.6) and (I.7) yields the rule of mixtures for the longitudinal modulus

$$E_1 = E_m v_f + E_m v_m \qquad (\text{I.8})$$

b) Determination of transverse modulus E2

The Young's modulus of the composite material in the transverse direction can be determined by considering the loading case shown in Figure. I.16. With the loading case in Figure. I.16, the normal strains in the fiber and matrix are found to be

$$\varepsilon_{f2} = \frac{\sigma_2}{E_f}, \varepsilon_m = \frac{\sigma_2}{E_m} \qquad (\text{I.9})$$

The total elongation in the transverse direction is $\Delta W = \varepsilon_2 W$ on average. It should be equal to the sum of the corresponding transverse elongation in the fiber, $W_f\varepsilon_{f2}$, and the matrix, $W_m\varepsilon_{m2}$

$$\Delta W = \varepsilon_2 W = \frac{W}{E_2}\sigma_2 = \varepsilon_{f2}W_f + \varepsilon_{m2}W_m = (\frac{W_f}{E_f} + \frac{W_m}{E_m})\sigma_2 \qquad (\text{I.10})$$

where W, W_f, and Wm are, respectively, the width of composite, fiber, and matrix. Equation (I.10) can be reduced to the "inverse rule of mixtures" for E_2 by dividing W on both sides of the equation

$$\frac{1}{E_2} = \frac{v_f}{E_f} + \frac{v_m}{E_m} \qquad (\text{I.11})$$

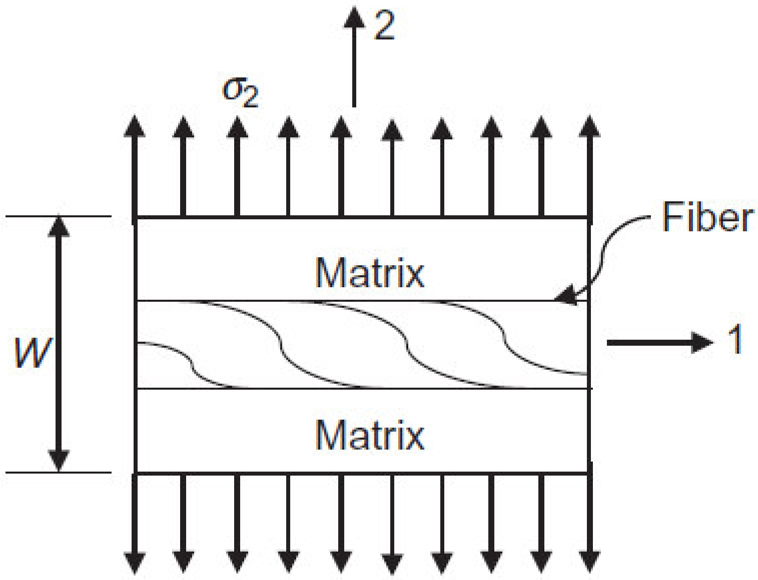

Figure. I.15 Composite loaded in transverse direction.

c) Determination of major Poisson's ratio

The major Poisson's ratio ν_{12}, is obtained by an approach similar to the derivation for E_1. For the loading case shown in Figure. I.15, the major Poisson's ratio is defined as

$$\nu_{12} = -\frac{\varepsilon_2}{\varepsilon_1} \tag{I.12}$$

The transverse deformation DW is then equal to $\varepsilon_2 W = -W\nu_{12}\varepsilon_1\varepsilon$. In a manner of the derivation for E_2, the transverse deformation in the fiber, ΔW_f, and the matrix, ΔW_m, are given as

$$\Delta W_m = W v_m \nu_m \varepsilon_1, \Delta W_f = W \nu_f v_f \varepsilon_1 \tag{I.13}$$

Since geometric compatibility requires that $\Delta W = \Delta W_f + \Delta W_m$, we have

$$\nu_{12} = v_m \nu_m + v_f \nu_f \tag{I.14}$$

This gives the rule of mixtures for the major Poisson's ratio.

d) Determination of in-plane shear modulus G_{12}

Consider the loading case shown in Figure. I.17a. The in-plane shear modulus of a lamina, G_{12}, is determined in the mechanics of materials method by assuming that the shearing stresses on the fiber and on the matrix, are the same. From this assumption, we obtain

$$\gamma = \frac{\tau}{G_{12}}, \gamma_m = \frac{\tau}{G_m}, \gamma_f = \frac{\tau}{G_f} \tag{I.15}$$

The shear deformations in matrix and fiber are then given as (Figure. I.17b)

$$\Delta_m = \gamma_m W_m = \gamma_m v_m W, \Delta_f = \gamma_f W_f = \gamma_f v_f W \tag{I.16}$$

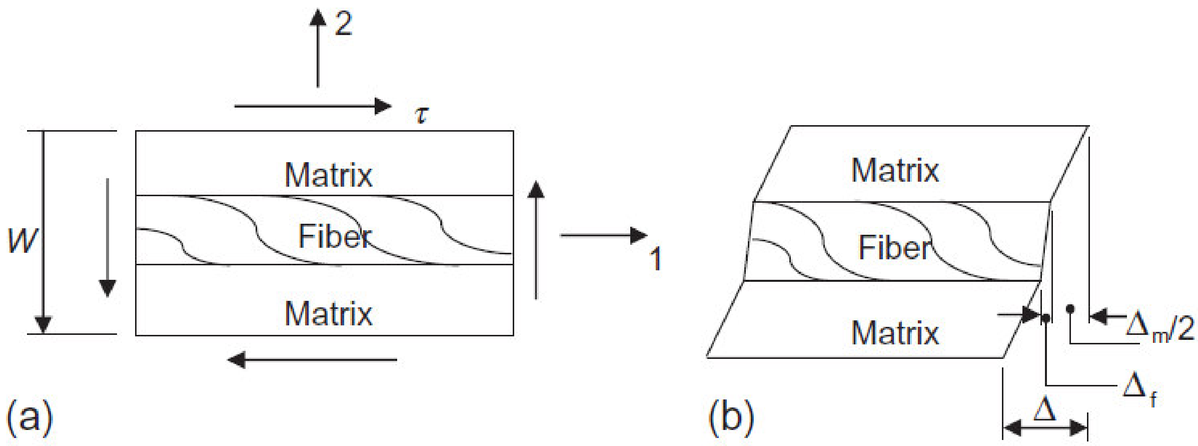

Figure. I.16 Composite loaded with shear stress.

The total shear deformation is $\Delta = \varepsilon W$, which is made up of approximate microscopic deformations (Figure. I.3). Again, geometric compatibility requires that $\Delta = \Delta_f + \Delta_m$ (Figure. I.3b), which yields by dividing W

$$\gamma = \gamma_m v_m + \gamma_f v_f \tag{I.17}$$

Substituting Eq. (I.15) into Eq. (I.17), we have

$$\frac{1}{G_{12}} = \frac{v_m}{G_m} + \frac{v_f}{G_f} \tag{I.18}$$

e) 2D stiffness and compliance matrix for unidirectional lamina in terms of constants matrix

$$\begin{bmatrix} \varepsilon_1 \\ \varepsilon_2 \\ \gamma_{12} \end{bmatrix} = \begin{bmatrix} \frac{1}{E_2} & \frac{\nu_{12}}{E_1} & 0 \\ \frac{\nu_{12}}{E_1} & \frac{1}{E_1} & 0 \\ 0 & 0 & \frac{1}{G_{12}} \end{bmatrix} * \begin{bmatrix} \sigma_1 \\ \sigma_2 \\ \tau_{12} \end{bmatrix} \tag{I.19}$$

f) Coefficients of stiffness matrix

$$\begin{bmatrix} \boldsymbol{\sigma_1} \\ \boldsymbol{\sigma_2} \\ \boldsymbol{\tau_{12}} \end{bmatrix} = \begin{bmatrix} \frac{E_1}{1-\nu_{21}\nu_{12}} & \frac{\nu_{12}E_2}{1-\nu_{21}\nu_{12}} & \mathbf{0} \\ \frac{\nu_{12}E_2}{1-\nu_{21}\nu_{12}} & \frac{E_2}{1-\nu_{21}\nu_{12}} & \mathbf{0} \\ \mathbf{0} & \mathbf{0} & G_{12} \end{bmatrix} * \begin{bmatrix} \boldsymbol{\varepsilon_1} \\ \boldsymbol{\varepsilon_2} \\ \boldsymbol{\gamma_{12}} \end{bmatrix} \tag{I.20}$$

g) Coordinates transformation stress and strain transformation are required

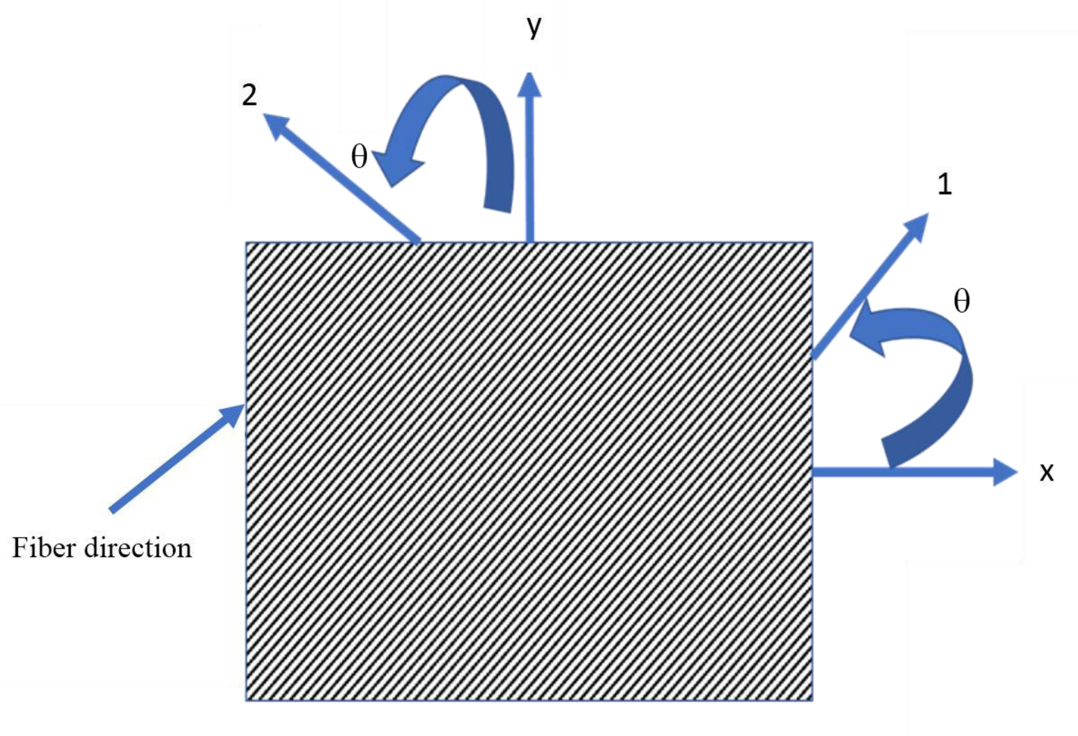

Figure. I.17 Transformation of coordinate

If we define the coordinate transformation matrix is

$$[T] = \begin{bmatrix} cos^2\theta & sin^2\theta & 2\ sin\ \theta\ cos\ \theta \\ sin^2\theta & cos^2\theta & -2\ sin\ \theta\ cos\ \theta \\ -sin\ \theta\ cos\ \theta & sin\ \theta\ cos\ \theta & sin^2\theta - cos^2\theta \end{bmatrix} \qquad (\text{I.21})$$

I.10.4. Finite element approach

In order to obtain values for the material properties of fiber-reinforced composites using an FEM, (finite element method) the basic formulations are briefly described in this section.

These differ to MMA in that they relate to the basic understanding of stress/strain relations and are not directly related to the volume fractions.

a) Calculation of E_1 and ν_{12}

E_1 and m12 can be determined by considering the loading case shown in Figure. I.15, where a stress σ_1 is applied in the fiber direction of the composite. The effective Young's modulus and major Poisson ratio are, then, evaluated by

$$E_1 = \frac{\bar{\sigma}_1}{\bar{\varepsilon}_1} = \frac{\int_V \sigma_1 {dV}/{V}}{\int_V \varepsilon_1 {dV}/{V}} = \frac{\int_V \sigma_1\, dV}{\int_V \varepsilon_1 dV}, \nu_{12} = \frac{\bar{\varepsilon}_2}{\bar{\varepsilon}_1} = \frac{\int_V \varepsilon_2 {dV}/{V}}{\int_V \varepsilon_1 {dV}/{V}} = \frac{\int_V \varepsilon_2 dV}{\int_V \varepsilon_1 dV} \qquad (\text{I.22})$$

If the left end is fixed and $\Delta \bar{L}$ represents the average displacement at the right end, the average strain can be defined as

$$\bar{\varepsilon} = \frac{\Delta L}{L} \qquad (\text{I.23})$$

Therefore, the major task for FE calculation is to determine $\Delta \bar{L}$ and the average stress $\bar{\sigma}_1$. Further, the calculation of major Poisson ratio requires the information $\varepsilon_2 = \Delta W/W$. As a result, the major issue for FE calculation is to calculate average transverse displacement ΔW. This has been implemented into our FE program.

10 Toughening Mechanisms in Composite Materials

b) Calculation of E2

Considering the loading case as shown in Figure. I.16, the effective transverse Young's modulus E_2 is defined as

$$E_2 = \frac{\bar{\sigma}_2}{\bar{\varepsilon}_2} = \frac{\int_V \sigma_2 {dV}/_{V}}{\int_V \varepsilon_2 {dV}/_{V}} = \frac{\int_V \sigma_2 \, dV}{\int_V \varepsilon_2 dV} \qquad (\text{I.24})$$

Where$\bar{\varepsilon}_2 = \Delta\bar{W}/W$. The major task for FE calculation is, then, to determine $\Delta\bar{W}$ and the average stress $\bar{\sigma}_2$.

c) Calculation of G12

The in-plane shear modulus of a fiber-reinforced composite can be determined by considering the loading case shown in Figure. I.17, a shear stress is applied over the boundary of the composite.

$$G_{12} = \frac{\bar{\tau}}{\bar{\gamma}} = \frac{\int_V \tau {dV}/_{V}}{\int_V \gamma {dV}/_{V}} = \frac{\int_V \tau \, dV}{\int_V \gamma dV} \qquad (\text{I.25})$$

Considering the fact that the shear strain can be defined as u/y, where u is displacement in fiber direction and y stands for the vertical coordinate originated at the bottom of the composite, the task of FE calculation, in this case, is to evaluate shear stress and the displacement u.

From these equations, we can determine $E_1,\ E_2\ and\ G_{12}$, noting that all other stresses and strains are taken as zero except for the stress and strain along the direction for the material property being determined.[1]

I.11. Conclusion

We have seen in this chapter a concept on composite materials and its existence from long years ago, its benefits and limits in several fields of use also we have touched its components from reinforcement and matrix and their types, define mechanical proprieties of the composite material and have an idea about the laminae and the laminate.

What we are going to see in the next chapter is that how do this composite material acts when it's subjected to a force that can damage it.

CHAPTER II

FRACTURE IN COMPOSITE MATERIALS

II.1. Introduction

The strength of any material is inherently related to the flaws that are always present. Specifically, the strengths of composite materials are governed by their flaw-initiated characteristics. Thus, the mechanics of fracture including crack propagation or extension are of extreme im- portance in the design analysis of composite structures. Fracture me- chanics criteria are now a part of every metal airplane design. This step was made by the Air Force as a result of fracture and fatigue problems on F-111, C5-A, Electra, etc. The prospect for composite materials ap- plications in the near future is that they, too, will have fracture mechanics design criteria imposed.

The fracture process generally takes place in three stages. First, a microcrack is initiated (or a preexisting flaw or imperfection can be present). Second, the microcrack grows in a stable fashion and might link with other microcracks to attain macrocrack size. Third, the macro-crack propagates in an unstable fashion at a critical stress level. These three stages are found and clearly defined only in ductile materials. Some of the stages, for example, stage two, are not found in brittle ma- terials. A prominent characteristic of composite materials is their high resistance to crack propagation

Fracture is caused by higher stresses around flaws or cracks than in the surrounding ma-terial. However, fracture mechanics is much more than the study of stress concentration factors. Such factors are useful in determining the influence of relatively large holes in bodies, but are not particularly helpful when the body has sharp notches or crack-like flaws. For composite materials, fracture has a new dimension as opposed to homogeneous isotropic materials be-cause of the presence of two or more constituents. Fracture can be a fracture of the individual constituents or a separation of the interface between the constituents.

The discussion of fracture mechanics will be divided in two parts. First, basic principles of fracture mechanics will be described. Second, the application of fracture mechanics concepts to composite materials will be discussed. In both parts, the basic approach is that of Wu

II.2. Definition

A fracture is the separation of an object or material into two or more pieces under the action of stress. The fracture of a solid usually occurs due to the development of certain dis-placement discontinuity surfaces within the solid. If a displacement develops perpendicular to the surface of displacement, it is called a normal tensile crack or simply a crack; if a displacement develops tangentially to the surface of displacement, it is called a shear crack, slip band, or dislocation.

Fracture strength or breaking strength is the stress when a specimen fails or fractures.

The word fracture is often applied to bones of living creatures (i.e. a bone fracture), or to crystalline materials, such as gemstones or metal. Sometimes, individual crystals fracture without the structure actually separating into two or more pieces. Depending on the substance, a fracture reduces strength (most substances) or inhibits transmission of waves, such as light (optical crystals). A detailed understanding of how fracture occurs in materials may be assisted by the study of fracture mechanics. [7]

II.3. Historical perspective

Designing structures to avoid fracture is not a new idea. The fact that many structures commissioned by the Pharaohs of ancient Egypt and the Caesars of Rome are still standing is a testimony to the ability of early architects and engineers. In Europe, numerous buildings and bridges constructed during the Renaissance Period are still used for their intended purpose.

The ancient structures that are still standing today obviously represent successful designs. There were undoubtedly many more unsuccessful designs with much shorter life spans. Because knowledge of mechanics was limited prior to the time of Isaac Newton, workable designs were probably achieved largely by trial and error. The Romans supposedly tested each new bridge by requiring the design engineer to stand underneath while chariots drove over it. Such a practice would not only provide an incentive for developing good designs, but would also result in the social equivalent of Darwinian natural selection, where the worst engineers were removed from the profession.

The durability of ancient structures is particularly amazing when one considers that the choice of building materials prior to the Industrial Revolution was rather limited. Metals could not be produced in sufficient quantity to be formed into load-bearing members for buildings and bridges. The primary construction materials prior to the 19th century were timber, brick, and mortar; only the latter two materials were usually practical for large structures such as cathedrals, because trees of sufficient size for support beams were rare.

Brick and mortar are relatively brittle and are unreliable for carrying tensile loads. Consequently, pre-Industrial Revolution structures were usually designed to be loaded in compression. Schematically illustrates a Roman bridge design. The arch shape causes compressive rather than tensile stresses to be transmitted through the structure.

The arch is the predominant shape in pre-Industrial Revolution architecture. Windows and roof spans were arched in order to maintain compressive loading. For example, Figure. II.2 shows two windows and a portion of the ceiling in King's College Chapel in Cambridge, England. Although these shapes are aesthetically pleasing, their primary purpose is more pragmatic.

Compressively loaded structures are obviously stable, since some have lasted for many centuries; the pyramids in Egypt are the epitome of a stable design.

With the Industrial Revolution came mass production of iron and steel. (Or, conversely, one might argue that mass production of iron and steel fueled the Industrial Revolution.)

The availability of relatively ductile construction materials removed the earlier restrictions on design. It was finally feasible to build structures that carried tensile stresses. Note the difference between the design of the Tower Bridge in London and the earlier bridge design.

The change from brick and mortar structures loaded in compression to steel structures in tension brought problems, however. Occasionally, a steel structure would fail unexpectedly at stresses well below the anticipated tensile strength. One of the most famous of these failures

Was the rupture of a molasses tank in Boston in January 1919. Over 2 million gallons of molasses were spilled, resulting in 12 deaths, 40 injuries, massive property damage, and several drowned horses.

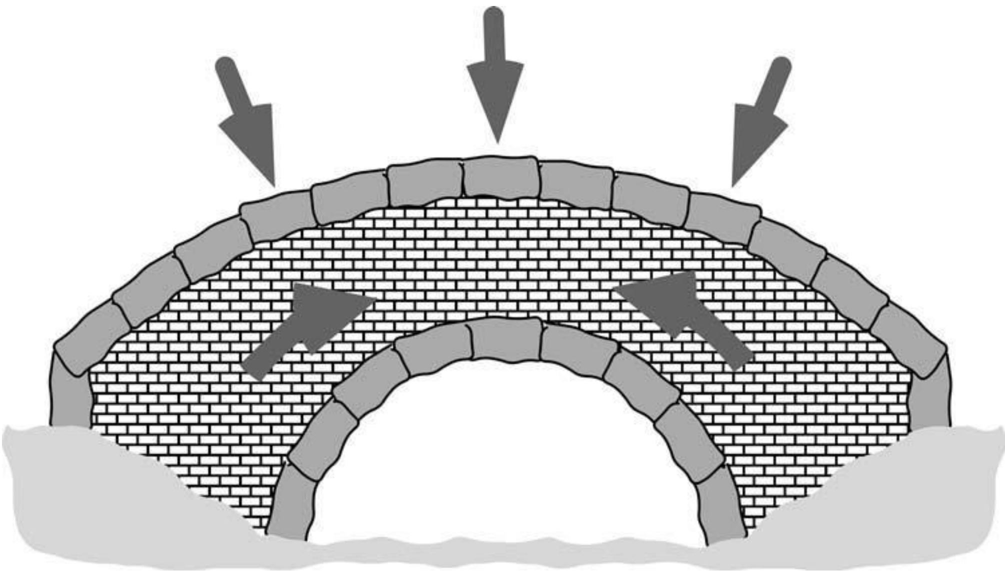

Figure. II.1 Schematic Roman bridge design. The arch shape of the bridge causes loads to be transmitted through the structure as compressive stresses. [15]

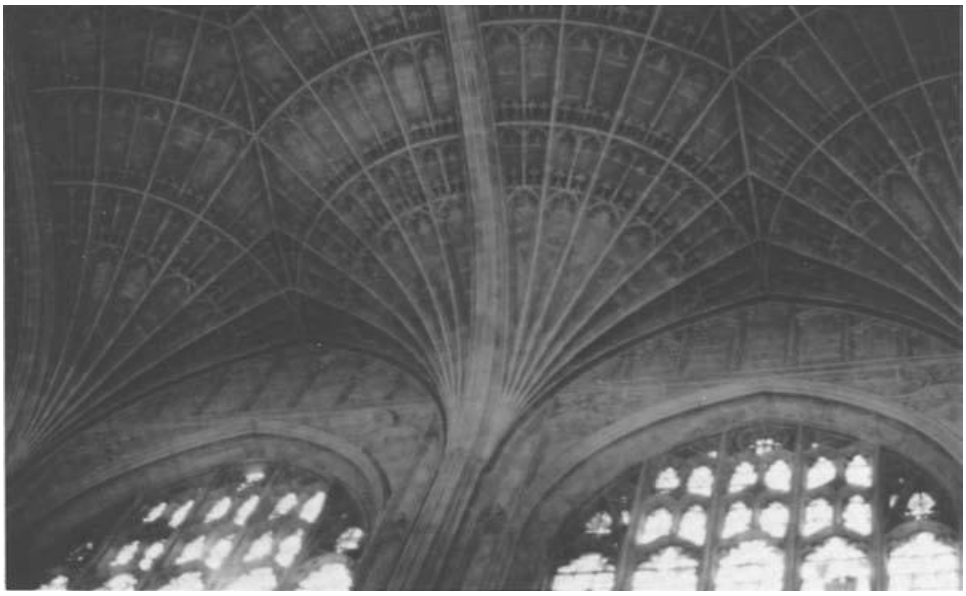

FIGURE. II.2 Kings College Chapel in Cambridge, England. This structure was completed in 1515. [16]

The cause of the failure of the molasses tank was largely a mystery at the time. In the first edition of his elasticity text published in 1892, Love [6] remarked that "the conditions of rupture are but vaguely understood." Designers typically applied safety factors of 10 or more (based on the tensile strength) in an effort to avoid these seemingly random failures. [5]

II.4. The reason of the failure of structures

The cause of most structural failures generally falls into one of the following categories:

1. Negligence during design, construction, or operation of the structure.
2. Application of a new design or material, which produces an unexpected (and undesirable) result.

In the first instance, existing procedures are sufficient to avoid failure, but are not followed by one or more of the parties involved, due to human error, ignorance, or willful misconduct. Poor workmanship, inappropriate or substandard materials, errors in stress analysis, and operator error are examples of where the appropriate technology and experience are available, but not applied.

The second type of failure is much more difficult to prevent. When an ''improved" design is introduced, invariably, there are factors that the designer does not anticipate. New materials can offer tremendous advantages, but also potential problems. Consequently, a new design or material should be placed into service only after extensive testing and analysis.

Such an approach will reduce the frequency of failures, but not eliminate them entirely; there may be important factors that are overlooked during testing and analysis. [2]

II.5. Relevance of fracture mechanics for damage analysis

Fracture mechanics developed and matured well before damage mechanics emerged. For both fields, the impetus came from the need to analyze failure of metals. Fracture mechanics initially addressed brittle failure from sharp defects based on idealized stress analysis of cracks. In contrast, damage mechanics was concerned with the effect of distributed voids and cracks on the average response of a solid. For composite materials, the complexity of failure processes involving a multitude of cracks gave rise to further development of damage mechanics. Today, damage mechanics of composite materials stands on its own as a mature field solidly founded in thermodynamics and having a variety of analytical and computational methodologies associated with it. Fracture mechanics has aided the development of damage mechanics of composite materials in providing energy-based concepts for addressing evolution of failure states. However, the stress analysis of cracks, characterized by stress intensity factors, is less relevant to composite damage analysis. Other than a few cases where single crack growth is a dominant failure mechanism, such as delamination emanating from free edges in laminates, crack front singularities are of little interest. Indeed, individual cracks constituting damage modes are usually arrested at interfaces. Therefore, their growth is of little interest. Instead, energy dissipation occurs due to crack multiplication. Therefore, an appropriate energy-based analysis, needed to treat this type of situation, does not resort to stress intensity factors, as is the case in brittle fracture of metals. [3]

II.6.Basic Principles of Fracture Mechanics

The acknowledged father of fracture mechanics is A. A. Griffith. His principal contribution is an analysis of crack stability based on energy equilibrium. If a crack is in equilibrium, the decrease of strain energy U must be equal to the increase of surface energy S due to crack extension, that is:

$$\frac{\partial U}{\partial a} = \frac{\partial S}{\partial a} \tag{II.1}$$

where a is the crack length. The strain-energy-release rate, $\partial U/\partial a$, is actually the crack-extension force. Prior to Griffith's approach, the application of classical elasticity concepts led to infinite stresses at the crack tip.

Irwin extended Griffith's theory to elastic-plastic materials and pointed out the three kinematically admissible crack-extension modes shown in Figure. II.3 These modes, opening, forward-shear, and parallel-shear, can be summed to obtain any crack.

Attention will be restricted to the strain-energy-release rate for the opening mode. This mode occurs for the plate with a centrally located crack of iength 2a under load P in Figure. II.4. [5]

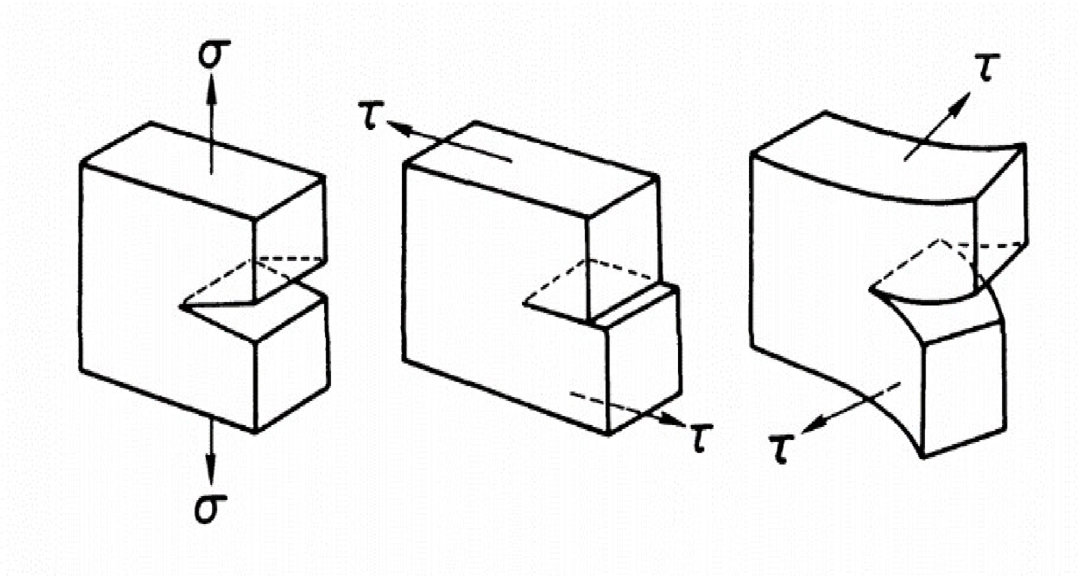

a) Opening Mode b) Forward-Shear Mode c) Parallel-Shear Mode

Figure. II.3 Crack-Extension Modes

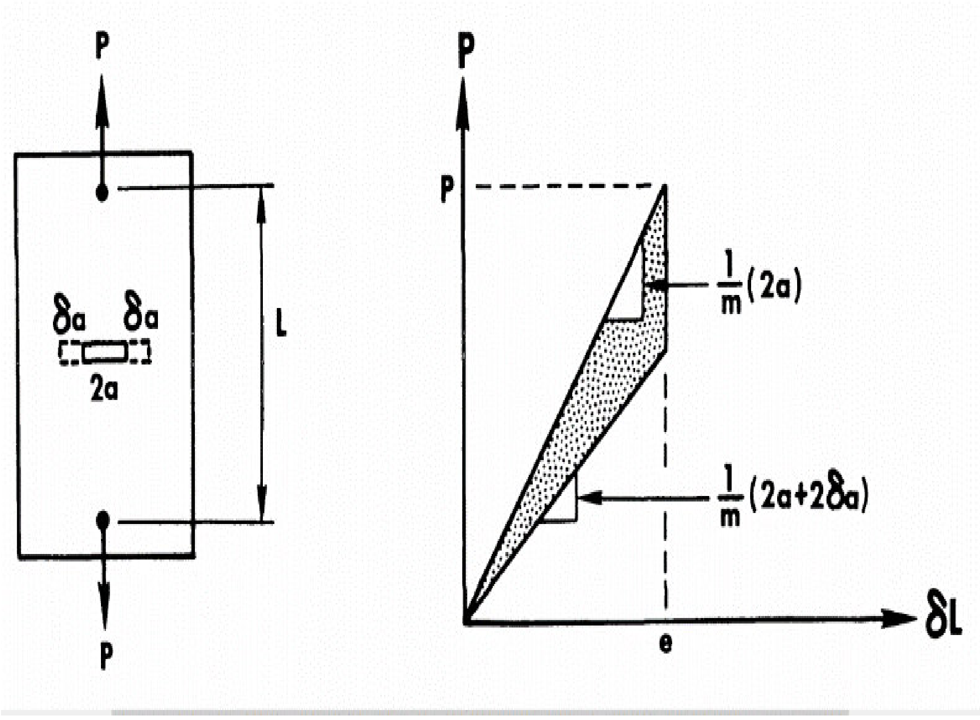

Figure. II.4 Cracked Plate and Load-Deformation Diagram

II.7. Application of Fracture Mechanics to Composite Materials

Composite materials have many distinctive characteristics relative to isotropic materials that render application of linear elastic fracture mechanics difficult. The anisotropy and heterogeneity, both from the standpoint of the fibers versus the matrix, and from the standpoint of multiple laminae of different orientations, are the principal problems. The extension to homogeneous anisotropic materials should be straightfor- ward because none of the basic prmciples used in fracture mechanics is then changed. Thus, the approximation of composite materials by ho- mogeneous anisotropic materials is often made. Then, stress-intensity factors for anisotropic materials are calculated by use of complex variable mapping techniques.

Wu derives the stress distribution around a crack tip in an anisotropic material. He finds the intensities of the stresses σ_x , σ_y , and T τ_{xy} are controlled not only by the parameters $\sigma^{\infty}\sqrt{a}$ and $\tau^{\infty}\sqrt{a}$ but also by functions of the anisotropic material properties and the orientation of the crack relative to the principal material directions. A simplification occurs when the crack maintains a constant orientation relative to the principal material directions (a likely circumstance if the flaws or possible paths of crack extension are, for example, all parallel to the fibers in a unidirectional lamina). However, unless the material is orthotropic and the crack is parallel to a principal material direction. the opening mode has both symmetric and skew-symmetric stresses in the stress distrib- ution around the crack tip.

Wu performed a series of experiments to determine the ap- plicability of linear elastic fracture mechanics to composite materials. He subjected unidirectionally reinforced fiberglass-epoxy plates with centrally located cracks in the fiber direction to tension, pure shear, and combined tension and shear as in Figure. II.5 He recorded the critical load and crack length at incipient rapid crack extension and noted that the cracks propagated colinear with the original crack. Moreover, the symmetric loads led to the crack-opening mode, and the skew-symmetric loads led to the forward-shear or sliding mode. This distinction is clearer than for isotropic materials! For load path 1, the stress-intensity factors are:

$$\begin{aligned} k_1 &= \sigma^{\infty}\sqrt{a} \\ k_2 &= 0 \end{aligned} \tag{II.2}$$

And the critical stress-intensity factors are:

$$\begin{aligned} k_{1_c} &= \sigma_c^{\infty}\sqrt{a_c} \\ k_{2_c} &= 0 \end{aligned} \tag{II.3}$$

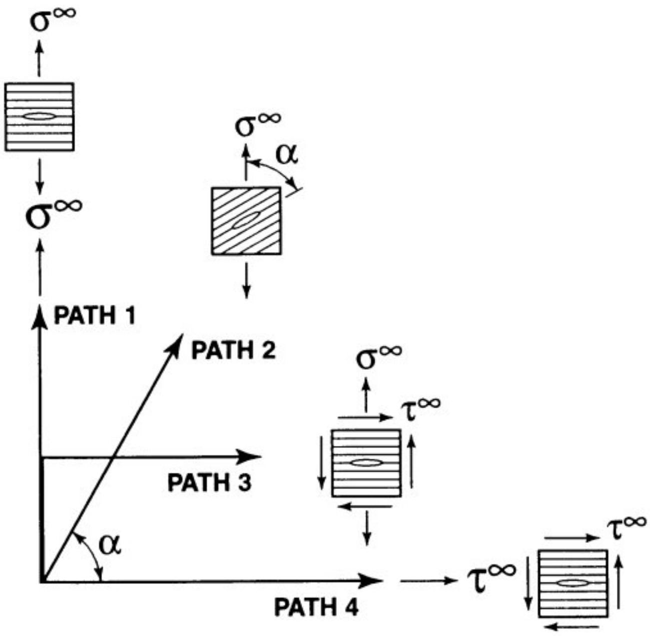

Figure. II.5 Wu's Load Paths and Crack Orientations

Where σ_c^∞ is the critical stress and a_c the critical crack length at incipient rapid crack propagation. If k_{1_c} is truly a material constant, as we would hope it is, then the experimental data on a plot of log σ_c^∞ versus log a_c should be a straight line with slope -1/2 because Equation (II.3)can be written as:

$$\log k_{1_c} = \log \sigma_c^\infty + \frac{1}{2} \log a_c \quad \text{(II.4)}$$

Indeed, the slope of Figure. II.6 is actually -.49, so the theory is apparently applicable to an orthotropic lamina with cracks in the fiber direction. The contention is further substantiated by tests for the other loading paths shown in Figure. II.5.

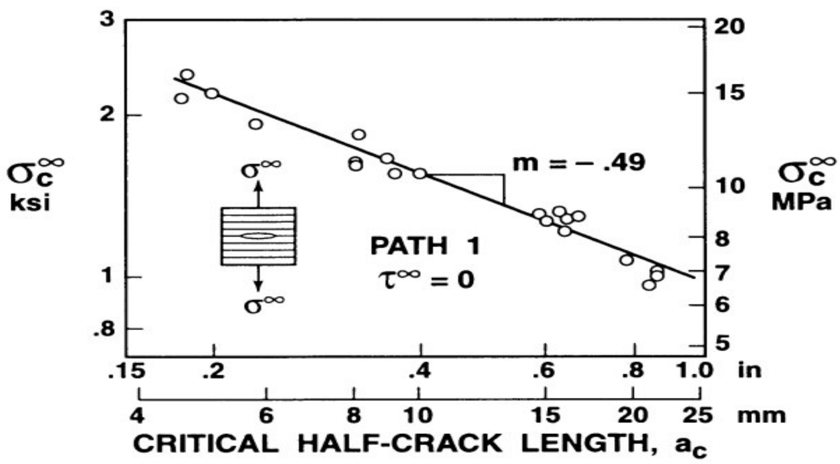

Figure. II.6 Cracked Unidirectionally Reinforced Plate under Tension Perpendicular to fibers

Other researchers have substantially advanced the state of the art of fracture mechanics applied to composite materials. Tetelman and Corten discuss fracture mechanics from the point of view of micromechanics. Sih and Chen treat the mixed-mode fracture problem for noncollinear crack propagation. Waddoups, Eisenmann, and Kaminski and Konish, Swedlow, and Cruse extend the concepts of fracture mechanics to laminates. Impact resistance of unidirectional composites is discussed by Chamis, Hanson, and Serafini .They use strain energy and fracture strength concepts along with micromechanics to assess impact resistance in longitudinal, transverse, and shear modes.

All efforts to predict crack growth and fatigue in a composite lami- nate are affected by the unique and complex manner in which cracks can grow in a laminate. Cracks tend to grow in the matrix parallel to the fi- bers. Thus, if a crack is cut parallel to the fibers, as in Figure. II.7a, it will grow in a direction parallel to itself, i.e., in a *self-similar* manner. However, if a crack is cut at some angle to the fibers, then the crack will still grow parallel to the fibers and not parallel to itself, i.e., *non-self- similar* crack growth as in Figure. II.7 b. Then, because a composite laminate has many layers at various orientations, a crack cut in a lami- nate results in crack growth that is locally sometimes self-similar and sometimes not. Globally, crack growth is non-self-similar, so predicting the effects of many kinds of damage growth is very difficult, if not im- possible. [5]

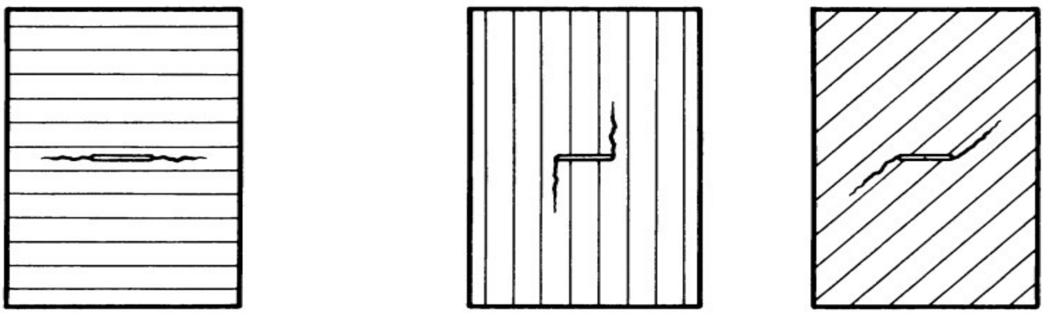

a)Self-Similar Crack Growth b)Non-Self-Similar Crack Growth

Figure. II.7 Composite Laminate Crack Growth

II.8.Other Analysis and Behavior Topics

$$U = \frac{1}{2} Pe \tag{II.5}$$

Where e is the elongation between loading points separated by distance L. The spring constant of the plate is :

$$\frac{1}{m} = \frac{P}{e} \tag{II.6}$$

The strain-energy-release rate due to crack extension $2\delta a$ is the shaded area in Figure. II.-4 if the loading-frame head does not move during crack extension, that is:

$$\frac{\partial e}{\partial a}=0 \tag{II.7}$$

From Equation (II.5):

$$\frac{\partial U}{\partial a}=\frac{1}{2}e\frac{\partial P}{\partial a}+\frac{1}{2}P\frac{\partial e}{\partial a} \tag{II.8}$$

But, because of Equation (II.6):

$$\frac{\partial U}{\partial a}=\frac{1}{2}e\frac{\partial P}{\partial a} \tag{II.9}$$

Then, from Equation (II.6):

$$\frac{\partial P}{\partial a}=\frac{1}{m}\frac{\partial e}{\partial a}+e\frac{\partial}{\partial a}\left[\frac{1}{m}\right]=-\frac{P}{m}\frac{\partial m}{\partial} \tag{II.10}$$

so that:

$$\frac{\partial U}{\partial a}=-\frac{P^2}{m}\frac{\partial m}{\partial a} \tag{II.11}$$

lnwin calls the strain-energy-release rate G, so

$$G=\frac{P^2}{m}\frac{\partial m}{\partial a} \tag{II.12}$$

Which can be measured because P and m can be measured. The same value of G results if the load is held constant during crack extension.

The strain-energy-release rate was expressed in terms of stresses around a crack tip by lrwin. He considered a crack under a plane stress loading of σ^{∞}, a symmetric stress relative to the crack, and τ^{∞} a skewsymmetric stress relative to the crack in Figure. II.5. The stresses have a superscript $^{\infty}$ because they are applied an infinite distance from the crack. The stress distribution very near the crack can be shown by use of classical elasticity theory to be, for example:

$$\sigma_X=\frac{\sigma^{\infty}\sqrt{a}}{\sqrt{2r}}\cos\frac{\theta}{2}\left[1-\sin\frac{\theta}{2}\sin\frac{3\theta}{2}\right]-\frac{\tau^{\infty}\sqrt{a}}{\sqrt{2r}}\sin\frac{\theta}{2}\left[2+\cos\frac{\theta}{2}\cos\frac{3\theta}{2}\right] \tag{II.13}$$

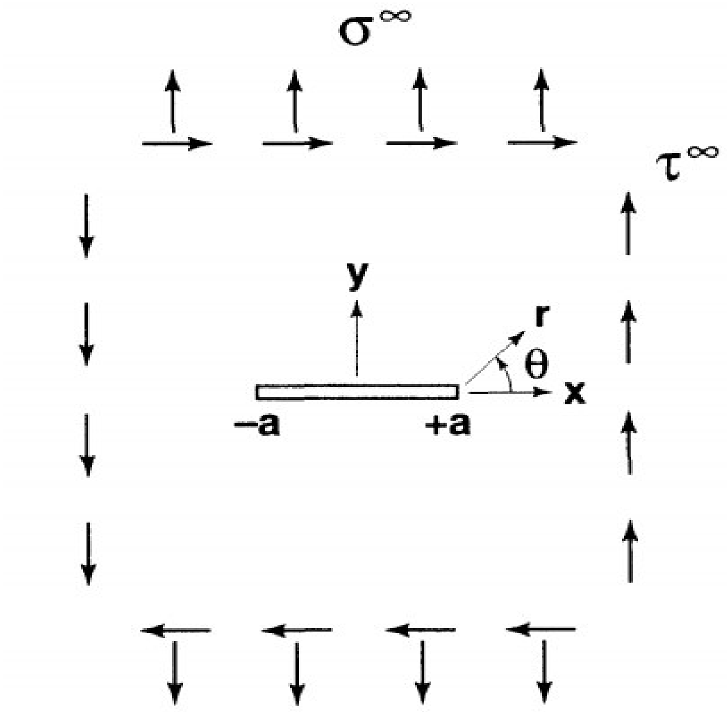

Figure. II.8 Cracked Plate with Symmetric and Skew-Symmetric Stresses at Infinity

The stress singularity for this and the other stress components σ_y and τ_{xy} is of order $1/\sqrt{r}$ Moreover, the terms $\sigma^{\infty}\sqrt{r}$ and $\tau^{\infty}\sqrt{r}$ are calied symmetric and skewsymmetric stress-intensity factors:

$$k_1 = \sigma^{\infty}\sqrt{a}$$
$$k_2 = \tau^{\infty}\sqrt{a} \tag{II.14}$$

The symmetric stress-intensity factor is associated with the opening mode of crack extension in Figure. II.3 The skew-symmetric stress- intensity factor k_2 is associated with the forward-shear mode. These plane-stress-intensity factors must be supplemented by another stress-intensity factor to describe the parallel-shear mode. The stress-intensity factors depend on the applied loads, body geometry, and crack geom- etry. For plane loads, the stress distribution around the crack tip can always be separated into symmetric and skew-symmetric distributions. The stress-intensity factors are quite different from stress concen- tration factors. For the same circular hole, the stress concentration factor is 3 under uniaxial tension, 2 under biaxial tension, and 4 under pure shear. Thus, the stress concentration factor, which is a single scalar parameter, cannot characterize the stress state, a second-order tensor. However, the stress-intensity factor exists in all stress components, so is a useful concept in stress-type fracture processes. For example:

$$G = \frac{\pi k_1^2}{E} \tag{II.15}$$

For an opening-mode crack that extends parallel to itself. Other such re- lations can be obtained for plane strain and the other crack modes. The point is that the stress-intensity factors appear in the strain-energy- release rate. [5]

II.9. Fracture criteria

The traditional strength of the materials approach to structural design and material selection is based on the notion of yield or failure stress (strength) of a given material. The fracture mechanics approach instead recognizes the presence of material flaws whose unstable growth could cause catastrophic failure. To determine conditions for this type of failure the local tress field in the vicinity of flaws (modeled as cracks) is analyzed. The singularity of this stress field is characterized by the so-called stress intensity factor and its critical value is associated with unstable crack growth. Alternatively, energy balance considerations are used to find the so-called energy release rate, per unit increment in the crack surface, and its critical value is associated with the condition of unstable crack growth. For linear elastic materials undergoing brittle failure the two approaches produce the same failure criteria. [3]

II.10. The stress intensity criterion

Consider an infinite plate with a through thickness edge crack of size a subjected to a remote tensile stress as shown in Figure. II.9. For a linear elastic plate material, the stress field in close vicinity of the crack tip is given by:

$$\begin{aligned}
\sigma_{xx} &= \frac{K_I}{\sqrt{2\pi r}}\cos\left(\frac{\theta}{2}\right)\left[1-\sin\left(\frac{\theta}{2}\right)\sin\left(\frac{3\theta}{2}\right)\right] \\
\sigma_{yy} &= \frac{K_I}{\sqrt{2\pi r}}\cos\left(\frac{\theta}{2}\right)\left[1+\sin\left(\frac{\theta}{2}\right)\sin\left(\frac{3\theta}{2}\right)\right] \\
\tau_{xy} &= \frac{K_I}{\sqrt{2\pi r}}\cos\left(\frac{\theta}{2}\right)\sin\left(\frac{\theta}{2}\right)\cos\left(\frac{3\theta}{2}\right)
\end{aligned} \tag{II.16}$$

Where r and θ are as shown in the Figure. II.8 and K_I, known as the stress intensity factor, is given by:

$$K_I = \sigma\sqrt{\pi a} \tag{II.17}$$

Where the subscript I denotes the opening mode (mode I). It can be noted that the stress field is singular at the crack tip with a $r^{1/2}$ singularity. The condition of failure, i.e., unstable crack growth, is assumed when:

$$K_I \geq K_{IC} \tag{II.18}$$

K_{IC}, known as the critical stress intensity factor, or fracture toughness, is a parameter representing the material resistance to fracture, and can be obtained experimentally. [3]

II.11. The energy criterion

In the energy-based approach, one considers a cracked body and examines the changes brought about by an incremental crack growth in the potential energy of applied forces

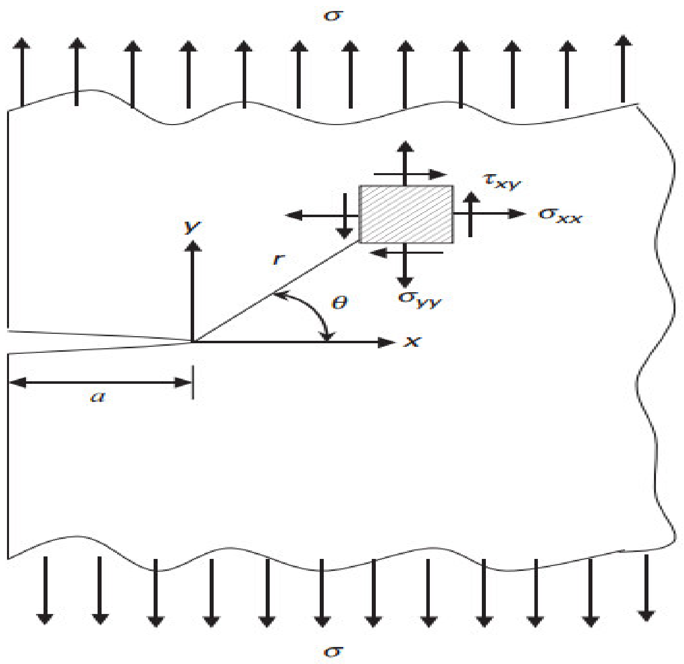

Figure. II.9 Edge crack in a plate in tension.

The stored elastic strain energy and the crack surface energy. The condition for unstable crack growth is then expressed as:

$$G \geq G_C \tag{II.19}$$

Where G is the energy available for crack growth per unit of crack surface area, called the energy release rate, and G_C is its critical value, which depends on the material in which the crack is advancing. G_C is viewed as the resistance to crack growth induced by the material. For a linear elastic material undergoing small-scale yielding at the crack front, the energy release rate is found to be related to the stress intensity factor, described above, as:

$$G = \frac{K_I^2}{E'} \tag{II.20}$$

Where $E' = E$ for plane stress condition, and $E' = \frac{E}{1-\upsilon^2}$ for plane strain condition. [3]

II.12. Crack separation modes

A crack is activated, i.e., it produces stresses at its front, when the two crack surfaces separate. The separation can take place in combination of three

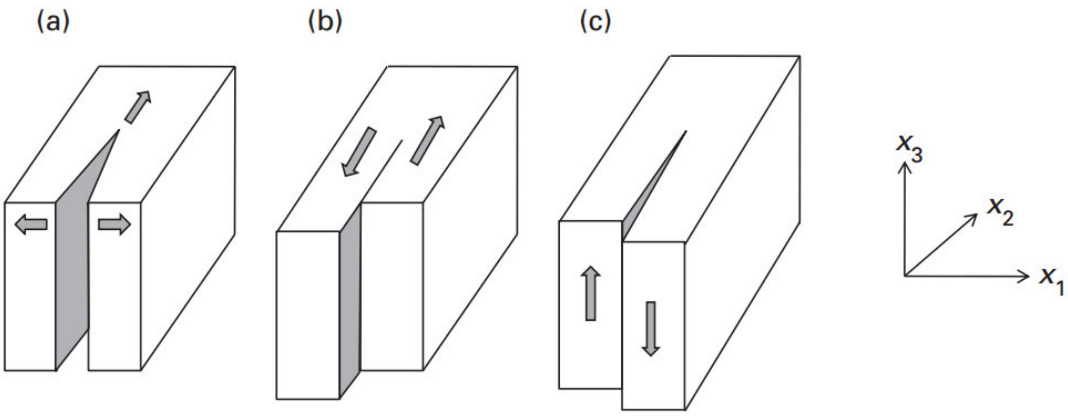

Figure. II.10 Crack separation modes: (a) opening; (b) sliding; and (c) tearing.

Independent modes, denoted as modes I, II, and III, illustrated in Figure. II.10. In mode I, also called the crack opening mode, the two crack surfaces separate symmetrically about the crack plane. Mode II is a sliding mode, in which the two crack surfaces remain in contact and slide past each other in the crack plane. Finally, mode III, described as the tearing mode, is driven by out-of-plane shear, resulting in displacement of the two crack surfaces in the x3-direction. Any displacement of the crack surfaces for a general loading can be viewed as a superposition of these three modes. Denoting the stress intensity factors in individual modes as KI, KII, and KIII, the energy release rate for mixed-mode is given by:

$$G = \frac{K_I^2}{E'} + \frac{K_{II}^2}{E'} + \frac{1+\upsilon}{E} K_{III}^2 \qquad \text{(II.21)}$$

Where:

$$K_I = \sigma_{11}\sqrt{\pi a} \quad , K_{II} = \sigma_{12}\sqrt{\pi a}\ ,\ K_{III} = \sigma_{13}\sqrt{\pi a} \qquad \text{(II.22)}$$

Where the stresses s11, etc. refer to the axes shown in Figure. II.9. [3]

II.13. Crack surface displacements

The displacement jump across the two crack surfaces, expressed as:

$$\Delta u_i = u_i^+ - u_i^- \qquad \text{(II.23)}$$

Where u_i^+ and u_i^- represent the displacements of the upper and lower crack surfaces, respectively, is a quantity of interest in fracture analysis. For the opening mode of crack separation, mode I, illustrated in Figure. II.10, i = 2, this quantity is described as crack opening displacement (COD). For an infinite isotropic homogeneous medium, the COD value is given by:

$$\Delta u_2 = k\sqrt{1-\left(\frac{x_1}{a}\right)^2}$$

(II.24)

Which describes an elliptical crack opening profile. [3]

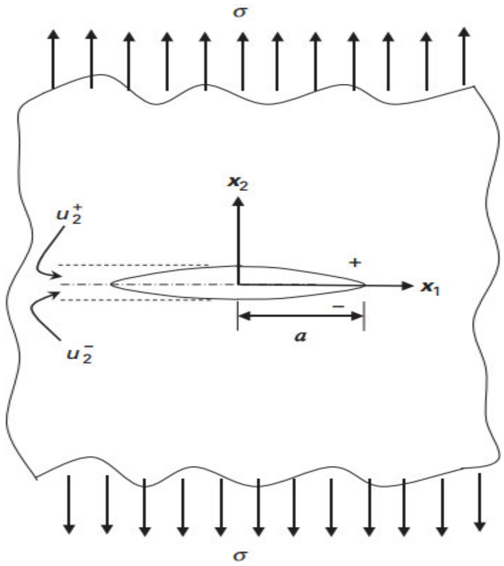

Figure. II.11 Crack opening displacement for a crack of size “2a.”

II.14. Fracture Mechanics Analyses of Through-Thickness Cracks

Much of the early work on fracture.in composites involved investigations of the applicability of linear elastic fracture mechanics, which had been originally. Consider the through-thickness crack in the uniaxially loaded homogeneous, isotropic, linear elastic plate of infinite width shown in. Figure. II.12 Griffith reasoned that the strain energy of the cracked plate would be less than the corresponding strain energy of the uncracked plate, and from a stress analysis, he estimated that the strain energy released by the creation of the crack under plane stress conditions would be:

$$U_r = \frac{\pi\sigma^2 a^2 t}{E} \tag{II.25}$$

Where:

U_r = strain energy released

σ = applied stress

a = half-crack length

t = plate thickness

E = modulus of elasticity of the plate

The corresponding expression in Griffith's original paper was later found to be in error, and Equation (II.12) is consistent with the corrected expression in more recent publications In addition, Griffith's energy terms were given on a per unit thickness basis Equation (II.12) is also consistent with the strain energy released by relaxation of an elliptical zone having major and minor axes of lengths 4a and 2a, respectively, where the minor axis is coincident.

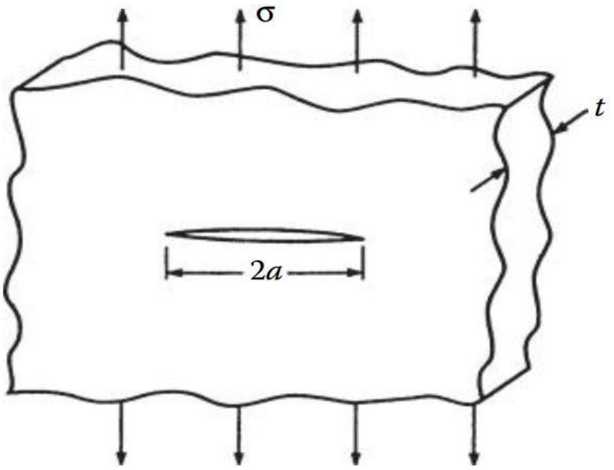

Figure. II.12 The Griffith crack: A through-thickness crack in a uniaxially stressed plate of infinite width

With the crack and the major axis is perpendicular to the crack the volume of such an ellipse is:

$$V = \pi(2a)(a) = 2\pi a^2 t \quad \text{(II.26)}$$

Since the plate was assumed to be uniformly stressed before the introduction of the crack, the strain energy released due to relaxation of the elliptical volume around the crack is:

$$U_r = \frac{1}{2}\frac{\sigma^2}{E}V = \frac{\pi\sigma^2 a^2 t}{E} \quad \text{(II.27)}$$

Griffith also assumed that the creation of new crack surfaces required the absorption of an amount of energy given by:

$$U_s = 4at\gamma_s \quad \text{(II.28)}$$

Where:

U_s = energy absorbed by creation of new crack surfaces

γ_s = surface energy per unit area

As the crack grows, if the rate at which energy is absorbed by creating new surfaces is greater than the rate at which strain energy is released, then

$$\frac{\partial U_s}{\partial a} > \frac{\partial U_r}{\partial a} \tag{II.29}$$

And crack growth is stable if the strain energy is released at a greater rate than it can be absorbed, then

$$\frac{\partial U_r}{\partial a} > \frac{\partial U_s}{\partial a} \tag{II.30}$$

And crack growth is unstable the threshold of stability, or the condition of neutral equilibrium, is therefore given by:

$$\frac{\partial U_r}{\partial a} = \frac{\partial U_s}{\partial a} \tag{II.31}$$

Or

$$\frac{\pi\sigma^2 a}{E} = 2\gamma_s \tag{II.32}$$

Thus, the critical stress, σ_c for self-sustaining extension of the crack in plane stress is:

$$\sigma_c = \sqrt{\frac{2E\gamma_s}{\pi a}} \tag{II.33}$$

Alternatively, the critical flaw size for plane stress at stress level σ is:

$$a_c = \frac{2E\gamma_s}{\pi\sigma^2} \tag{II.34}$$

It is interesting to note that when we rearrange Equation II.32 as:

$$\sigma\sqrt{\pi a} = \sqrt{2E\gamma_s} \tag{II.35}$$

The terms on the left-hand side depend only on loading and geometry, whereas the terms on the right-hand side depend only on material properties Thus, when the stress reaches the critical fracture stress, σ_c, the left-hand side becomes $\sigma_c\sqrt{\pi a}$ The term $\sigma_c\sqrt{\pi a}$ is now referred to as the fracture toughness, K_c This is a very important concept, which we will return to later

The application of the Griffith-type analysis to composites presents some difficulties, but, fortunately, many of these problems have been solved over the years since Griffith's work For example, for metals and many polymers the energy absorbed in crack extension is actually greater than the surface energy Recognizing this, both Irwin and Orowan modified the Griffith analysis to include energy absorption due to plastic deformation at the crack tip In this analysis the factor $2\gamma_s$ on the right-hand side of Equation II.32 and in all subsequent equations is replaced by the factor $2(2\gamma_s + \gamma_p)$, where γ_p is the energy of plastic deformation The solutions of several other problems encountered in the development of composite fracture mechanics have been made possible by the use of several different analytical techniques Two of these techniques, now referred to as the “stress intensity factor” approach and the “strain energy release rate” approach, will be discussed in the following sections. [3]

II.15. Stress Intensity Factor Approach

The Griffith analysis was originally developed for homogeneous, isotropic materials using effective modulus theory, we can replace the heterogeneous, anisotropic composite with an equivalent homogeneous, anisotropic material it turns out that by considering the stress distribution around the crack tip, we can develop another interpretation of the Griffith analysis

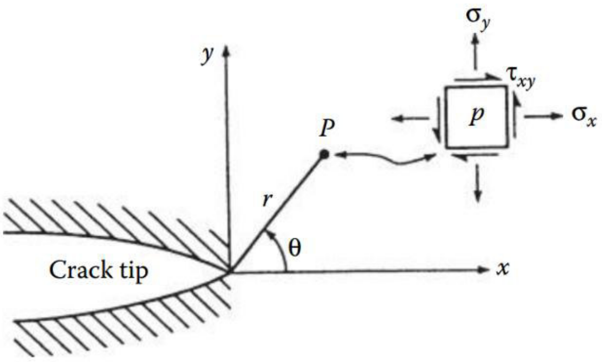

Figure. II.13 stresses at the tip of a crack under plane stress.

Which can be applied equally well to homogeneous isotropic or anisotropic materials and to states of stress other than the simple uniaxial stress that Griffith used Referring to the plane stress condition in the vicinity of the uniaxially loaded crack in Figure. II.13, Westergaard used a complex stress function approach to show that the stresses for the isotropic case at a point P defined by polar coordinates (r , θ) can be expressed as:

$$\sigma_x = \frac{K_I}{\sqrt{2\pi r}} f_1(\theta) \tag{II.36}$$

$$\sigma_y = \frac{K_I}{\sqrt{2\pi r}} f_2(\theta) \tag{II.37}$$

$$\tau_{xy} = \frac{K_I}{\sqrt{2\pi r}} f_3(\theta) \tag{II.38}$$

Where K_I is the stress intensity factor for the crack opening mode, as defined by:

$$K_1 = \sigma\sqrt{\pi a} \tag{II.39}$$

And $f_i(\theta)$ are trigonometric functions of the angle Irwin recognized that the term $\sigma\sqrt{\pi a}$ controls the magnitudes of the stresses at a point (r , θ) near the crack tip Returning to the discussion following Equation II.35, we see that the critical value of the stress intensity factor, K_{IC} corresponding to the critical stress, σ_C, is the fracture toughness That is:

$$K_{IC} = \sigma_c\sqrt{\pi a} \tag{II.40}$$

The fracture toughness, K_{IC}, is a material property that can be determined experimentally, as shown later Thus, if the fracture toughness of the material is known, the fracture mechanics analysis can be used in two ways, depending on whether the applied stress or the crack size is known If the applied stress, σ, is known, equations such as Equation II.39can be used to find the critical crack size, ac, which will lead to unstable and catastrophic crack growth Knowing the critical crack size, we can specify inspection of the component in question to make sure that there are no cracks of that size On the other hand, if the crack size, a, is known, then equations such as Equation II.39 can be used to find the critical stress, σ_C, which will lead to unstable and catastrophic crack growth loading on the component in question would then be specified so as not to exceed this stress.

The reader is cautioned that the stress intensity factor is defined as $k_1 = \sigma\sqrt{a}$ in some publications .This definition corresponds to the cancellation of $\sqrt{\pi}$ in both the numerator and the denominator of Equations II.36 through II.38, so that the denominator corresponding to k_1 would be $\sqrt{2r}$ instead of $\sqrt{2\pi r}$, and thus $K_I = k_1\sqrt{\pi}$.

Expressions for stress distributions for other types of loading and crack geometries in isotropic materials lead to expressions that are similar to Equations II.36 through II.38, and the corresponding stress intensity factors can be found in the same way Other important results such as finite width correction factors (recall that the Griffith analysis is for a crack in an infinite width plate) have been tabulated in Ref The three basic modes of crack deformation are shown in Figure. II.10 Thus, for the crack opening mode in the above example (mode I), we have the stress intensity factor K_I For the in-plane shear mode (mode II) we have the stress intensity factor K_{II} , and for the antiplane shear mode (mode III) we have K_{III} For example, for the cases of pure shear loading in modes II and III we have

$$K_{II} = \tau\sqrt{\pi a} \quad \text{And} \quad K_{III} = \tau\sqrt{\pi a} \tag{II.41}$$

Respectively, where the shear stress, τ, is different for modes II and III, as shown in Figure. II.10

Although the stress analyses for the corresponding anisotropic material cases are more difficult and the expressions are more complicated, the stress intensity factors for certain loading conditions and crack geometries are the same as those for the isotropic case For example, Lekhnitskii has used a stress function approach to show that if the crack shown in Figures 2.12 and 2.13 lies in an anisotropic material for which the xy-plane is a plane of material property symmetry, then the stresses are given by:

$$\sigma_x = \frac{K_1}{\sqrt{2\pi r}} F_{1(\theta, s_1, s_2)} \quad \text{(II.42)}$$

$$\sigma_y = \frac{K_1}{\sqrt{2\pi r}} F_{2(\theta, s_1, s_2)} \quad \text{(II.43)}$$

And:

$$\tau_{xy} = \frac{K_1}{\sqrt{2\pi r}} F_{3(\theta, s_1, s_2)} \quad \text{(II.44)}$$

where the functions $f_{i(\theta, s_1, s_2)}$ include not only trigonometric functions of the angle, θ, but also s_1 and s_2, which are complex roots of the characteristic equation corresponding to a differential equation in the stress function as pointed out by Wu the magnitudes of the stresses at point (r, θ) in an isotropic material (Equations II.36 through II.38) are completely determined by the stress intensity factors, but in the anisotropic case (Equations II.42 through II.44), these magnitudes also depend on s1 and s2 Wu has also shown, however, that if the crack lies along a principal material direction in the anisotropic material, then the stress intensity factors given by Equations II.39 and II.41 are still valid for their respective loading conditions shown in Figure. II.13

Several experimental investigations have shown that the concept of a critical stress intensity factor can be used to describe the fracture behavior of through-thickness cracked unidirectional composites and laminates Wu reasoned that if the fracture toughness, K_{IC}, is a material constant, then by considering the logarithm of Equation II.40, the slope of the log σ_C versus log ac plot must be –0 5 Wu's experimental results for unidirectional E-glass/epoxy showed good agreement with this prediction Konish et al showed that the critical stress intensity factors for 0°, 90°, 60°, 45° s, and [0°/45°/60°/90°]s carbon/epoxy laminates could be determined by using the same fracture toughness test method that had been developed for metals Parhizgar et al showed both analytically and experimentally that the fracture toughness of unidirectional E-glass–epoxy composites is a constant material property that does not depend on crack length but that does depend on fiber orientation.

The fracture toughness, K_{IC}, has been found to be an essentially constant material property for a variety of randomly oriented short fiber composites, as shown in papers by Alexander et al and Sun and Sierakowski. Although the random fiber orientation in such materials allows one to use the numerous tabulated solutions for stress intensity factors of isotropic materials, it appears that the simple crack growth assumed in the Griffith type analysis does not always occur in these materials as an alternative to crack growth, the concept of a damage zone ahead of the crack tip in short fiber composites has been proposed by Gagger and Broutman. [3]

II.16. Conclusion

As every material on this planet, the composite material submit fracture that can damage it.

Each composite material can handle a maximum stress that it depends on the characteristics of each material.

Cracks decreases the materials characteristics, strength and performance.

In the next chapter, we are about to prove that the increase in the crack size decreases the characteristics of the material.

CHAPTER III

EXPERIMENTAL STUDY

III.1. The aim of this work

The aim of our work in this chapter is to calculate and compare experimentally the behavior results of the specimen of cracked glass/epoxy and cracked carbon/epoxy by tensile test then study the impact of those different crack sizes and angles in glass/epoxy and carbon/epoxy.

This result obtained by tensile machine (ZWICK ROELL 250 KN).

So, in our experiences we have cases to calculate

- Without crack in (glass/epoxy) (carbon/epoxy)
- With crack a=2.5mm, a=5mm, a=7.5, a=10mm, a=12.5mm, a=15 mm.
- With crack a=15mm & θ=30°, θ=45°, θ=60°, θ=90°.

III.2. The machine of test

it is made by Zwick-Roell Group see figure. III.1, This machine of traction electro mechanic is equipped of a training by ball screw and it is static machine and for testing: tensile tests, compression and cyclic...etc. this version is 250 KN

This machine use software program ***testXpert*® II** for give us results and can read it.

Figure. III.1 ZWICK ROELL 250 KN machine

III.3. Materials tested by Z250 machine

- ✓ Thermoplastic and thermosetting materials.
- ✓ Rubbers and elastomers.
- ✓ Rubbers and elastomers.
- ✓ Fiber reinforced composites.
- ✓ Flexible cellular plastics.
- ✓ Thin sheeting and plastic film.
- ✓ Adhesives and sealing.

III.4. Tensile test

The tensile test is the experimental test method most widely employed to characterize the mechanical properties of materials. From any complete test record, one can obtain important information concerning the material's elastic properties, the character and extent of plastic deformation, yield and tensile strengths, and toughness. That so much information can be obtained from one test justifies its extensive use in engineering materials research.

We use the tensile test because we evaluate the crack in a laminar composite have a problem with crack in our structure of plan and this crack propagate by traction force on the plan.

III.5. Material and geometry of Specimen used

Specimens that are used in this test are plates of glass/epoxy and carbon/epoxy with specific geometry

With length l= 150mm, width w= 30mm and depth b= 2mm.

Glass/epoxy and carbon/epoxy specimens produced by glass fiber and carbon fiber eight layups with orientation angle [0/90^{o}].

The materials that are used in this experience and the specimens are obtained from the Algeria airlines company.

III.6. Process of fabrication of CFRP & GFRP

III.6.1. Tools of work

- Carbon fiber & glass fiber tissues
- Clean plan
- Epoxy and hardener boxes
- Vacuum bag
- Pumping felt
- Peeling film
- Vacuum Bache


Figure. III. 2 carbon fiber tissue


Figure. III. 3 glass fiber tissue

Figure. III. 4 epoxy box

Figure. III.5 hardener box


Figure. III.6 vacuum bag


Figure. III. 7 pumping felt


Figure. III.8 peeling film


Figure. III. 9 vacuum bache

III.6.2. The process

Step 01

Prepare tissues of both carbon and glass fibers, measure and cut as apparent in figure below

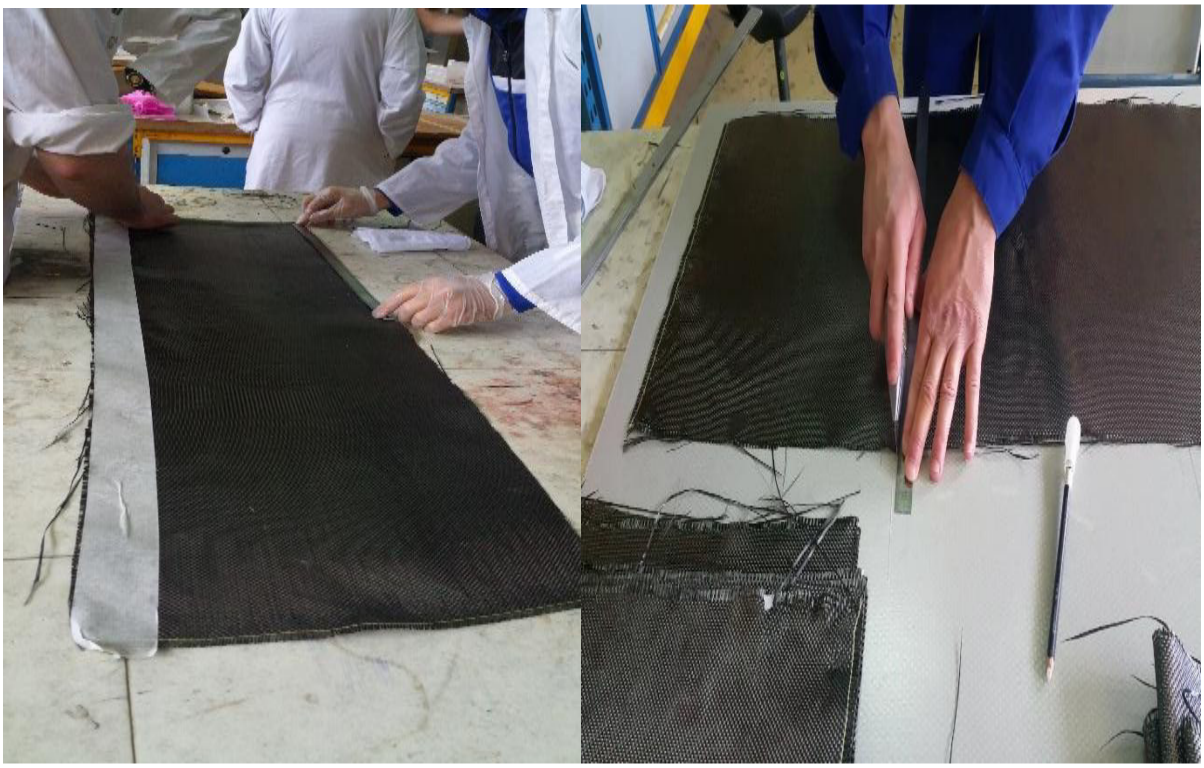
Figure. III.10 measure and cut the carbon fiber tissue

Step 02

We cover a sufficient surface from that clean plan using Vacuum Bache Then we put the resin after been mixed with hardener (hardener must be 15% of the amount of the epoxy) as apparent in figure. III.11

Figure. III.11 preparing the space of work

Step 03

We put the first ply on that resin then we mold resin on that ply using the roller to distribute the resin on the whole ply surface and forth for the other plies as apparent in figure below

Figure. III.12 molding resin on plies

step 04

Cover that after finishing using the peeling film to absorb the rejected resin as in figure. III.13

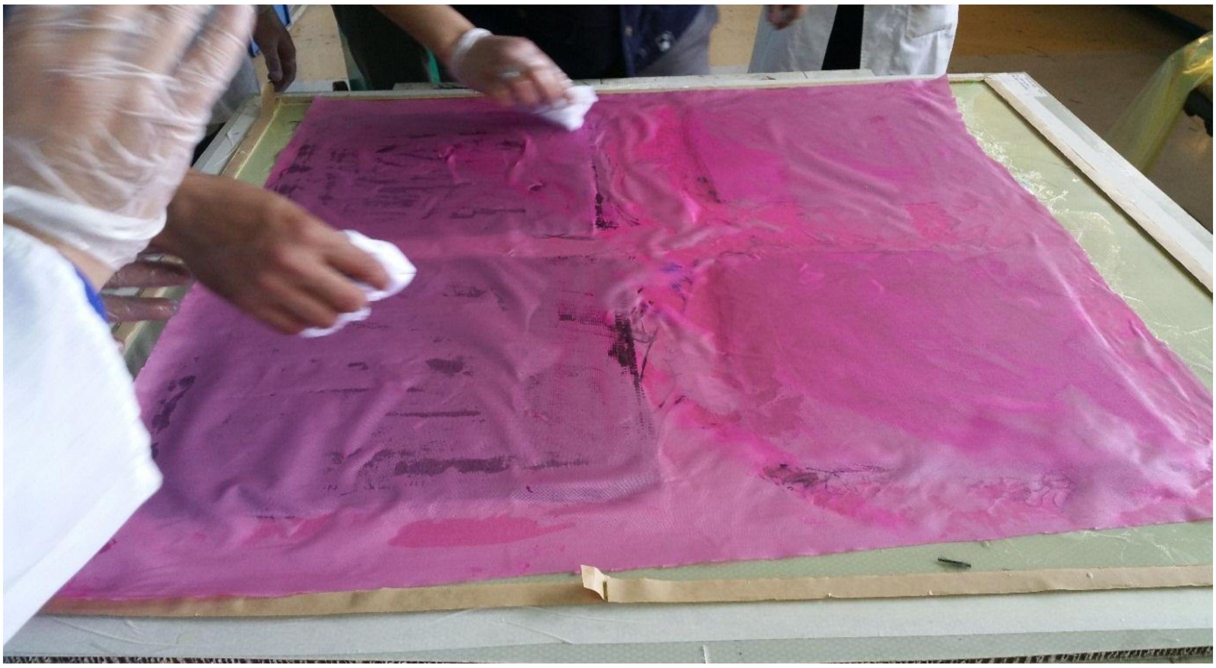

Figure. III.13 use peeling film to absorb resin

Step 05

Use the pumping felt to help to increase the inside heat and evenly distribute the pressure on each part of that flat's surface as apparent in figure below

Figure. III.14 use the pumping felt to increase heat and pressure

Step 06

Cover the flat by another ply of vacuum bache and steak all that together to that plan by adhesive as apparent in figure. III.15

Figure. III.15 use vacuum bache as a final rug

Step 07

Inject a tube that is connected with the vacuum bag under that plastic to absorb air inside that material to provoke pressure on it to make that resin and plies steak together as apparent in figure. III.16 and leave to dry for 7 to 8 hours

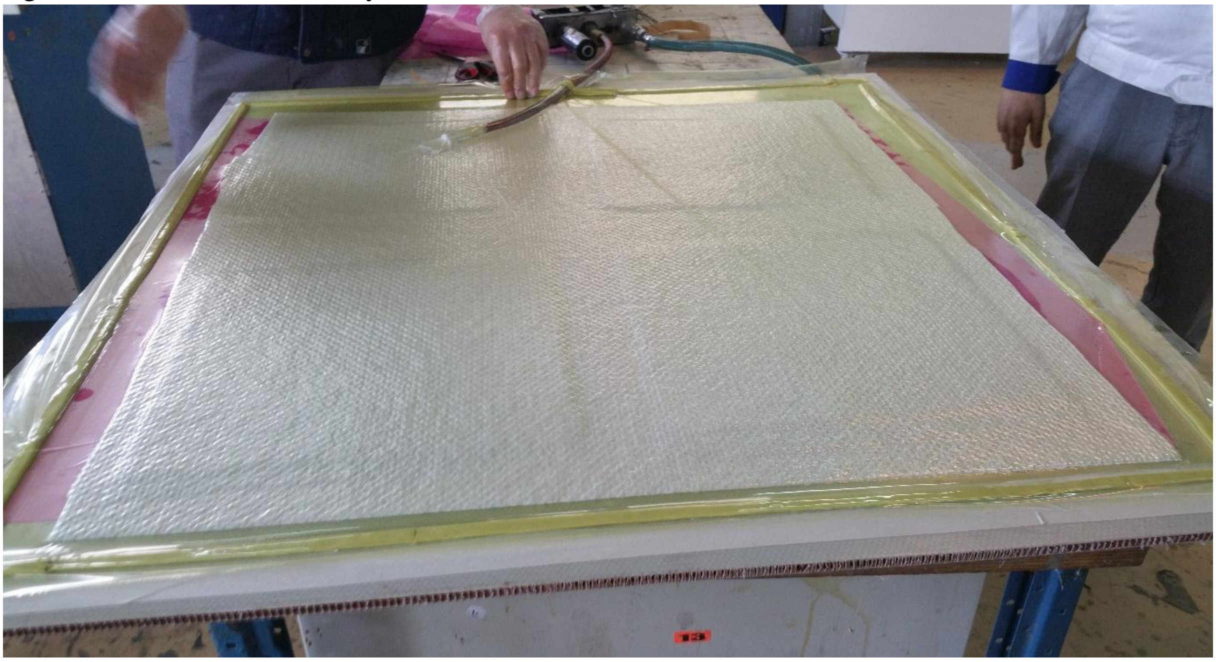

Figure. III.16 use vacuum bag to throwaway air and provoke pressure

Step 08

Trace and cut the obtained material to measured specimens

Figure. III.17 tracing and cutting the obtained composite material

Figure. III.18 carbon fiber and glass fiber specimen

The obtained specimens before tensile test and after been cracked to different sizes and angles

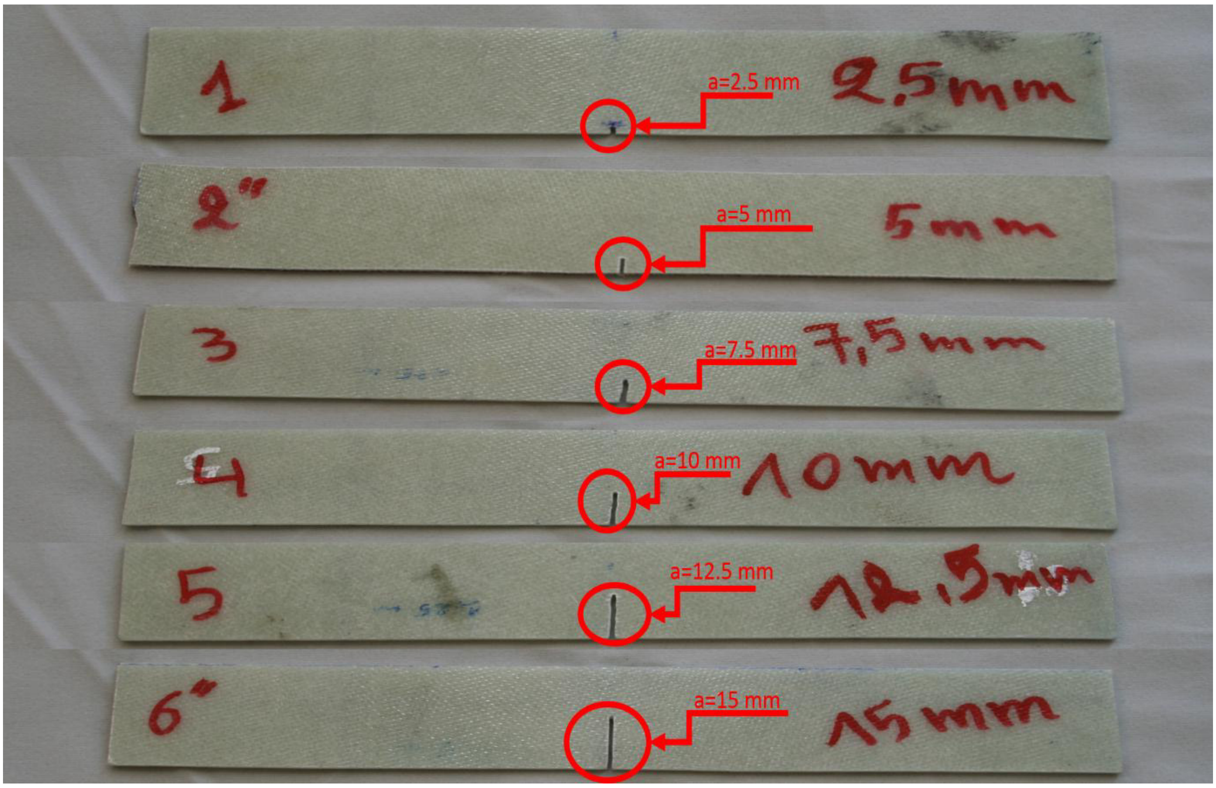

Figure. III.19 glass/epoxy specimens with different crack sizes

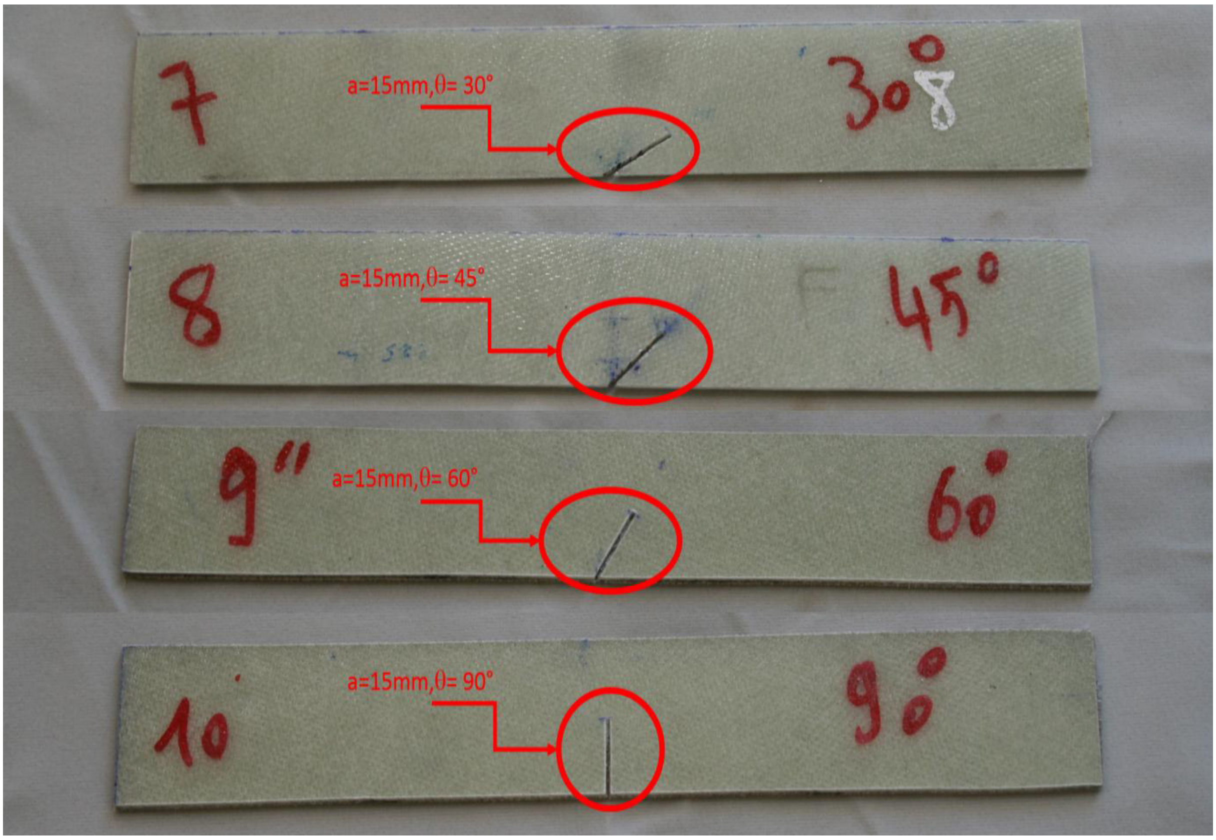

Figure. III.20 glass/epoxy specimens with different crack angles

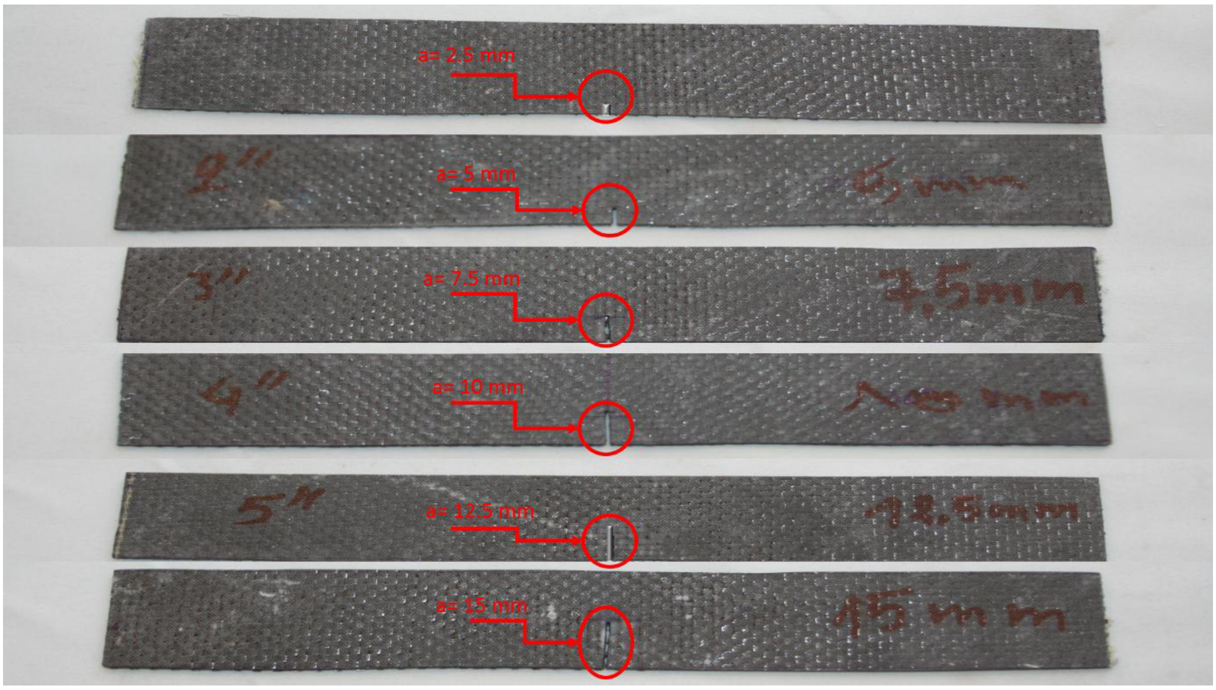

Figure. III.21 carbon/epoxy specimens with different crack sizes

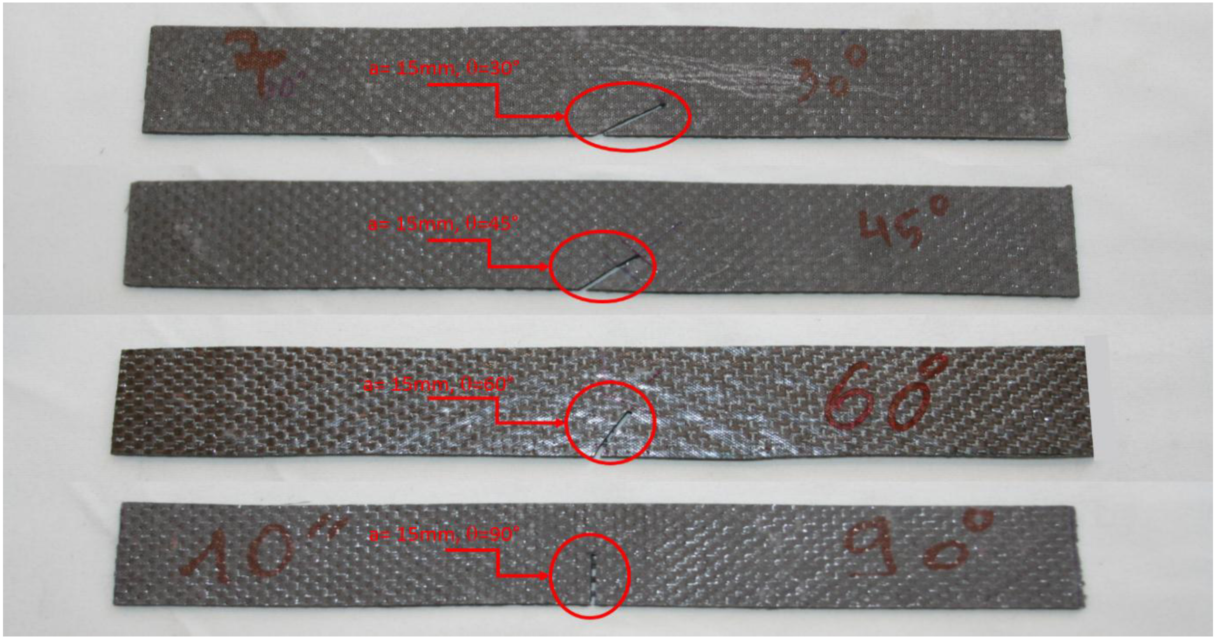

Figure. III.22 carbon/ epoxy specimens with different crack angles

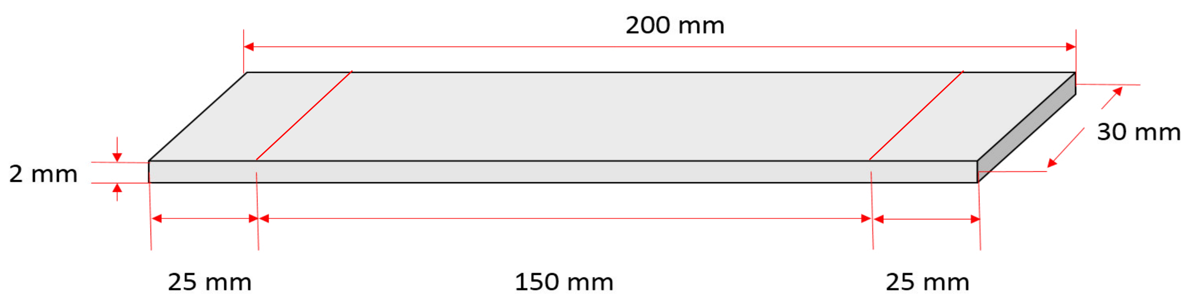

Figure. III.23 the dimension of specimens

The obtained carbon/epoxy and glass/epoxy composite material specimens after tensile test

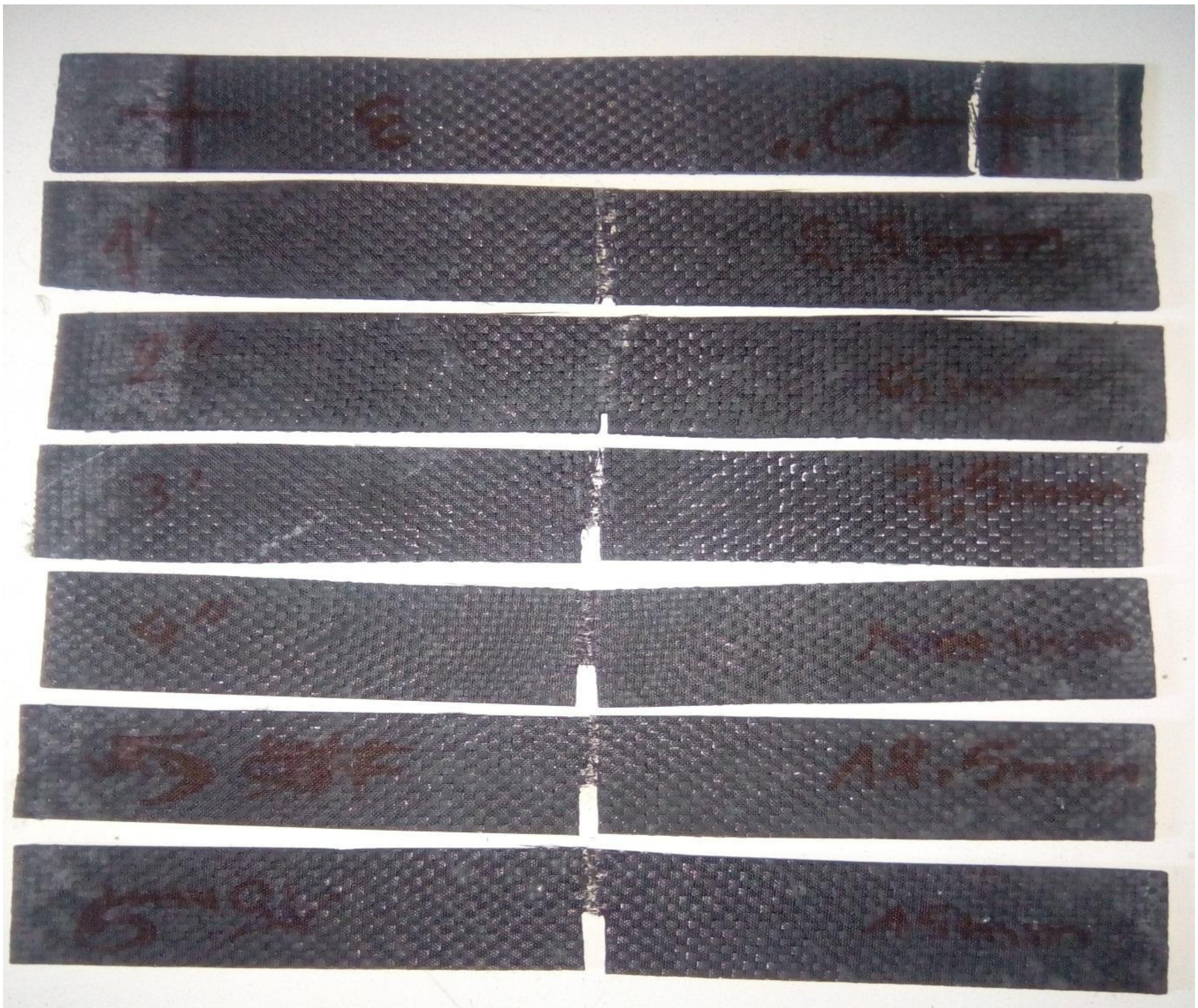

Figure. III.24 different carbon/epoxy crack seizes specimens after tensile test

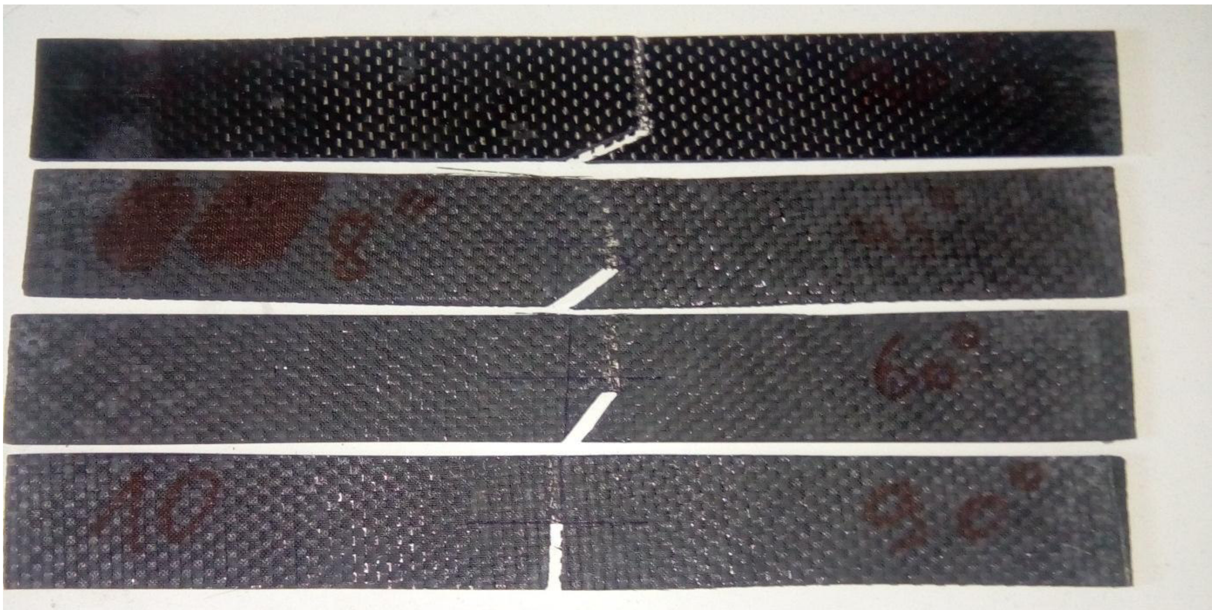

Figure. III.25 different carbon/epoxy crack angles after tensile test

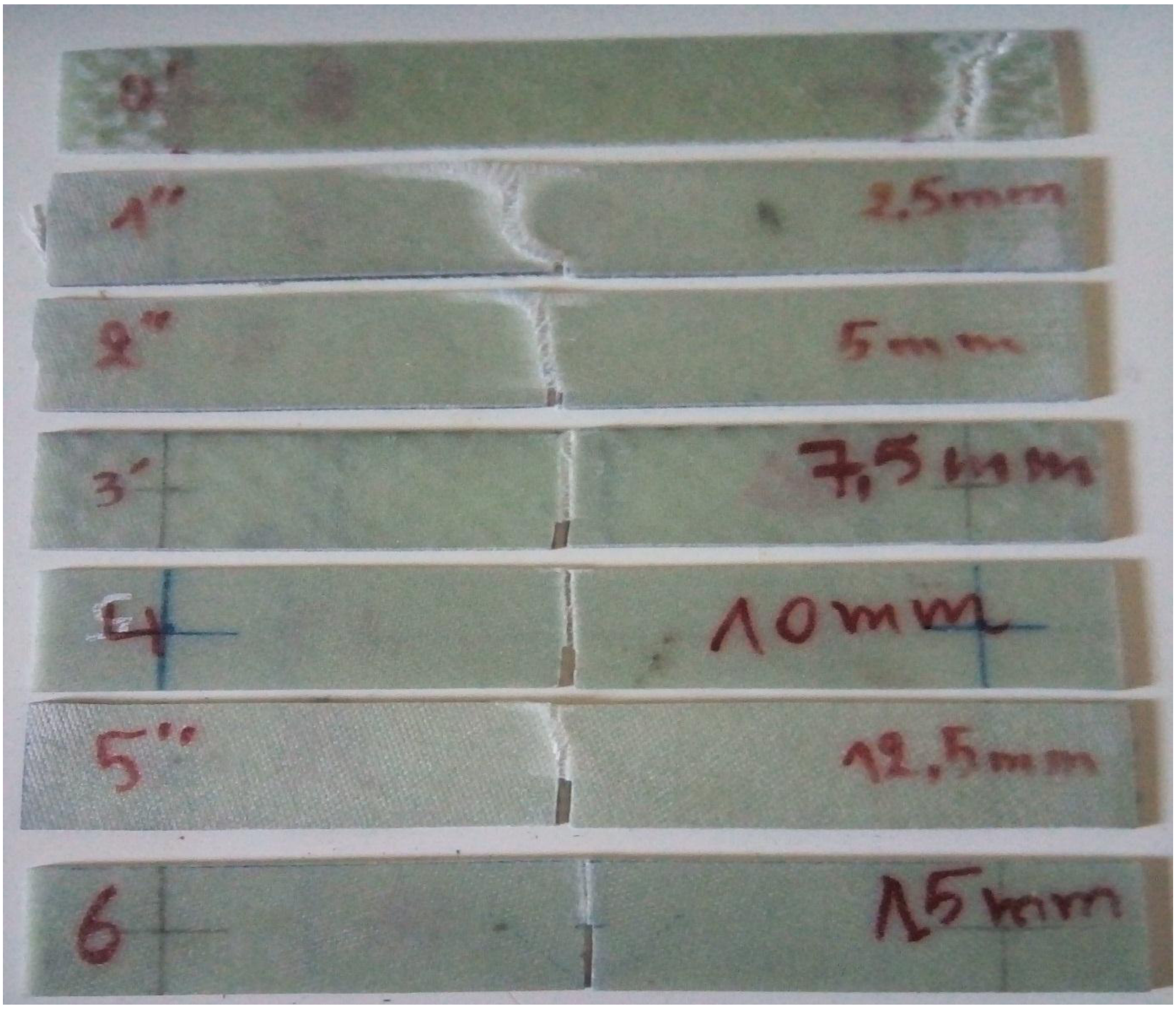

Figure. III.26 different glass/epoxy crack sizes after tensile test

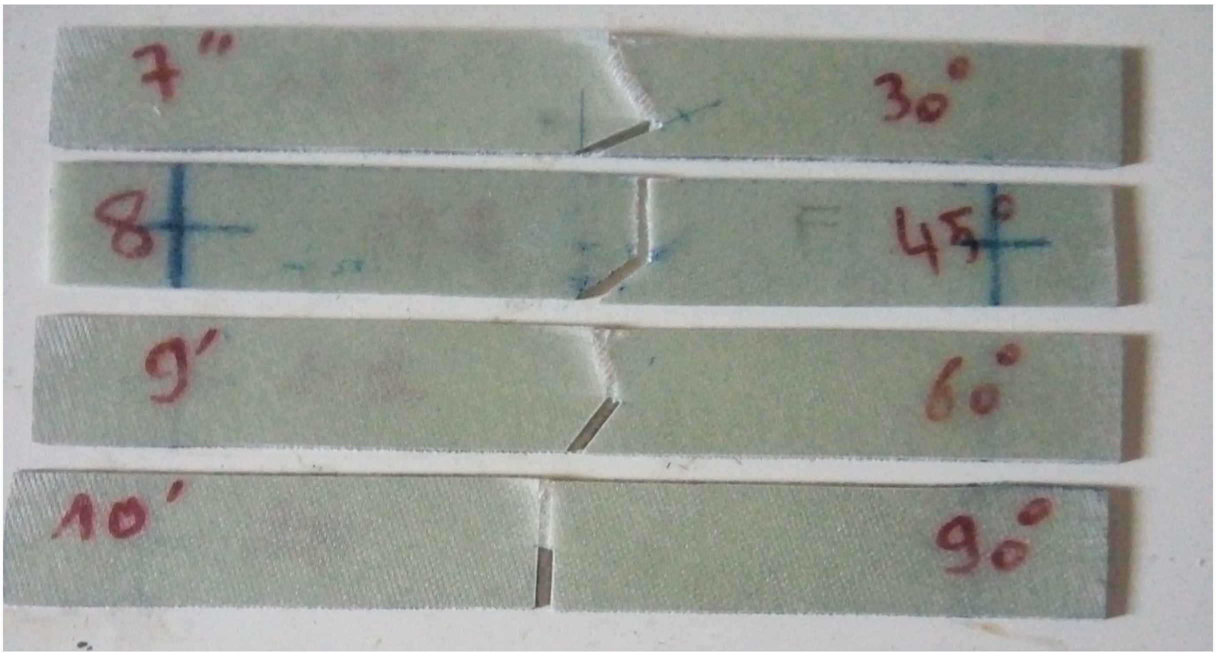

Figure. III.27 different glass/epoxy crack angles tensile test

- Materials proprieties

the specimens plate is isoperimetric on the length and width plan, so we are interested on the values that can be obtained from two dimensions (x,y) by tensile test.

Table. III.1 carbon/epoxy and Glass/epoxy mechanical proprieties

The material	Density $\rho\ (\frac{kg}{m^3})$	*young modulus* E_1(GPa)	Young modulus E_2 (GPa)	ν_{12}	G_{12} (GPa)	Volume fraction V_f/V_m
Carbon/epoxy	1750	116.5	116.5	0.3	44.71	73.5/26.5
Glass/epoxy	2500	44.5	44.5	0.25	34.4	67.5/32.5

III.7. Result and discussion

III.7.1. Glass/epoxy result graphs (different crack sizes)

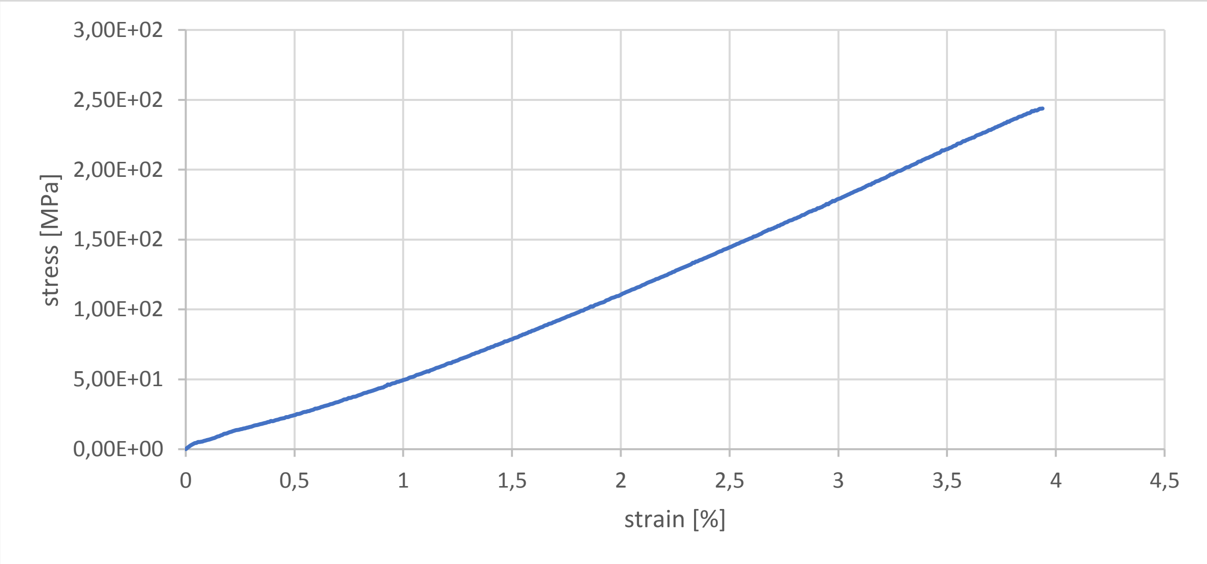

Figure. III.28 tensile test's graph on glass/epoxy specimen without crack

We observe from this graph that the stress increased proportionally with strain until the value of rupture, this point of rupture has a peak value of stress which is $\sigma_{rup} = 244$ MPa and the strain attained a maximum value $\varepsilon_{max} = 3.94$ %.

The variation of the stress with strain is approximately on the form $F(x) = 59.104x$

We can so clearly note that the variation of the stress with strain isn't a linear form that's the effect of composite material, defaults of production and defaults of cutting the specimens

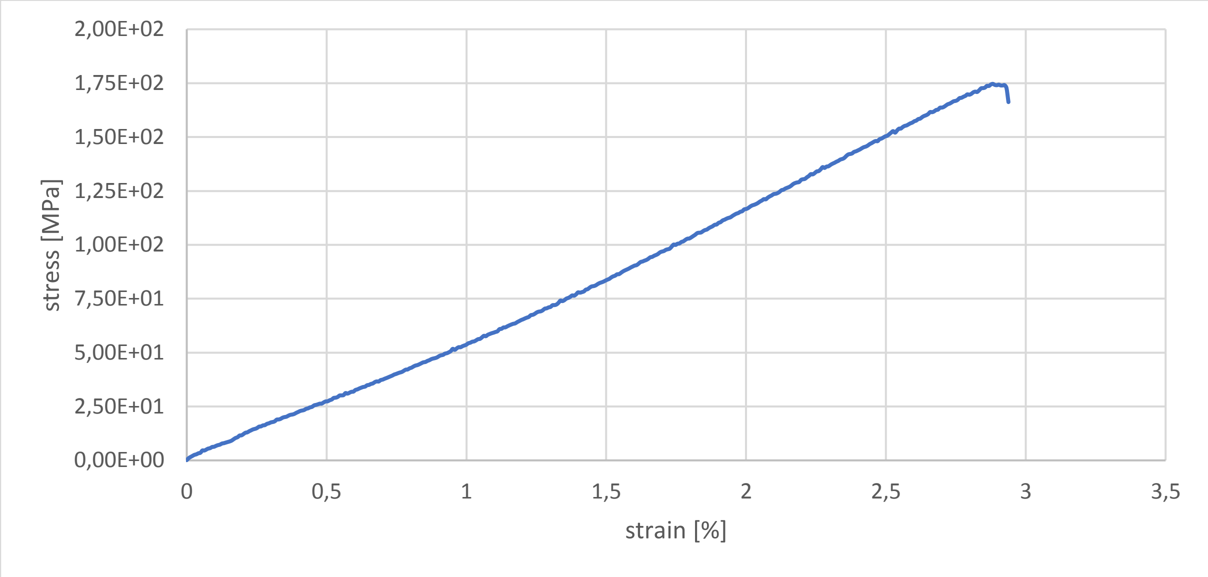

Figure. III.29 tensile test's graph on glass/epoxy specimen with crack a=2.5mm

We observe from this graph that the stress increased proportionally with strain until it reaches the peak value of the stress $\sigma_{max} = 175\ MPa$ then it decreased with increase of strain till the rupture.

The rupture of the whole material occurred at the point where $\sigma_{repture} = 166\ MPa$ and strain $\varepsilon_{max} = 2.94\ \%$

It's clear that the region between the x axis values [0;2.90] doesn't variate linearly, it progresses plastically because of the effect of the composite material and the other defaults that we mentioned previously.

The curve progresses approximately following the polynomial equation

$F(x) = -1{,}5491x^6 + 13{,}39x^5 - 45{,}702x^4 + 76{,}968x^3 - 59{,}286x^2 + 69{,}816x$

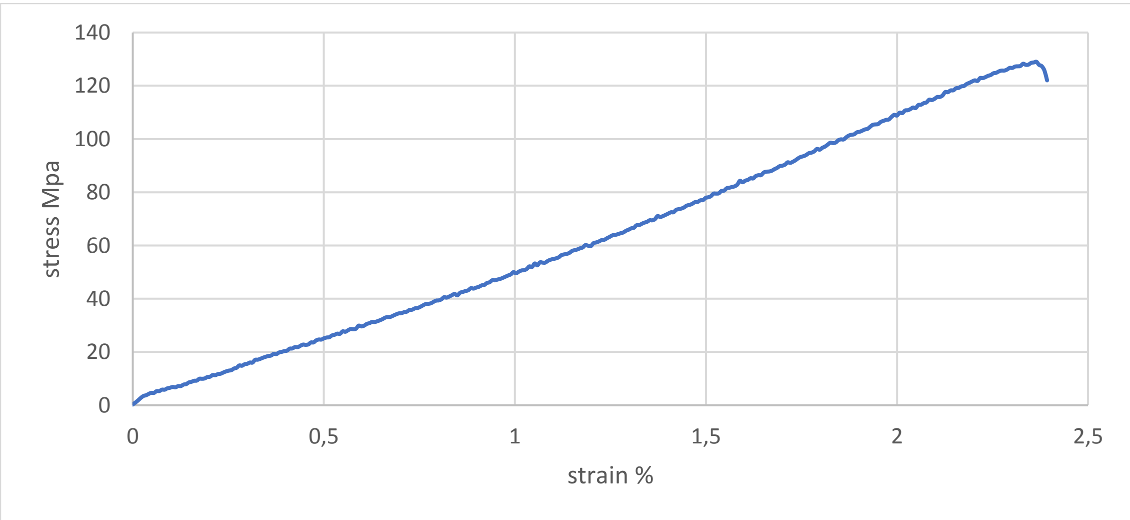

Figure. III.30 tensile test's graph of glass/epoxy specimen with crack a=5mm

We observe from this graph that the stress increased proportionally with strain until it reached the value of the stress max $\sigma_{max} = 129\ MPa$ then it decreases with increase of strain till the rupture.

The rupture of the whole material occurred at the point where $\sigma_{repture} = 122\ MPa$ and strain $\varepsilon_{max} = 2.39\ \%$

The curve progresses approximately following the polynomial equation

$F(x) = -4.5588x^6 + 29.472x^5 - 73.605x^4 + 90.1x^3 - 50.399x^2 + 57.76x$

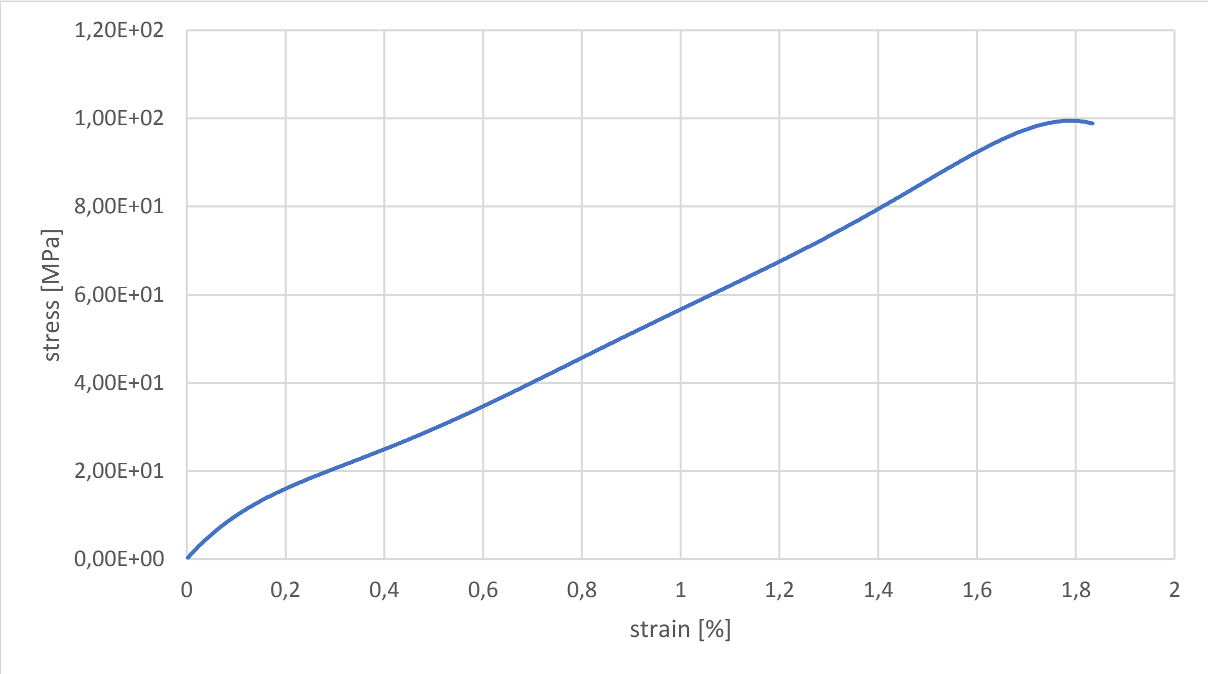

Figure. III.31 tensile test's graph of glass/epoxy specimen with crack a=7.5mm

We observe from this graph that the stress increased proportionally with strain until it reached the value of the stress max $\sigma_{max} = 101\ MPa$ then it decreased with increase of strain till the rupture.

The rupture of the whole material occurred at the point where $\sigma_{repture} = 94.2\ MPa$ and strain $\varepsilon_{max} = 1.83\ \%$

The curve progresses approximately following the polynomial equation

$F(x) = -33.148x^6 + 168.32x^5 - 326.22x^4 + 302.32x^3 - 131.92x^2 + 72.886x.$

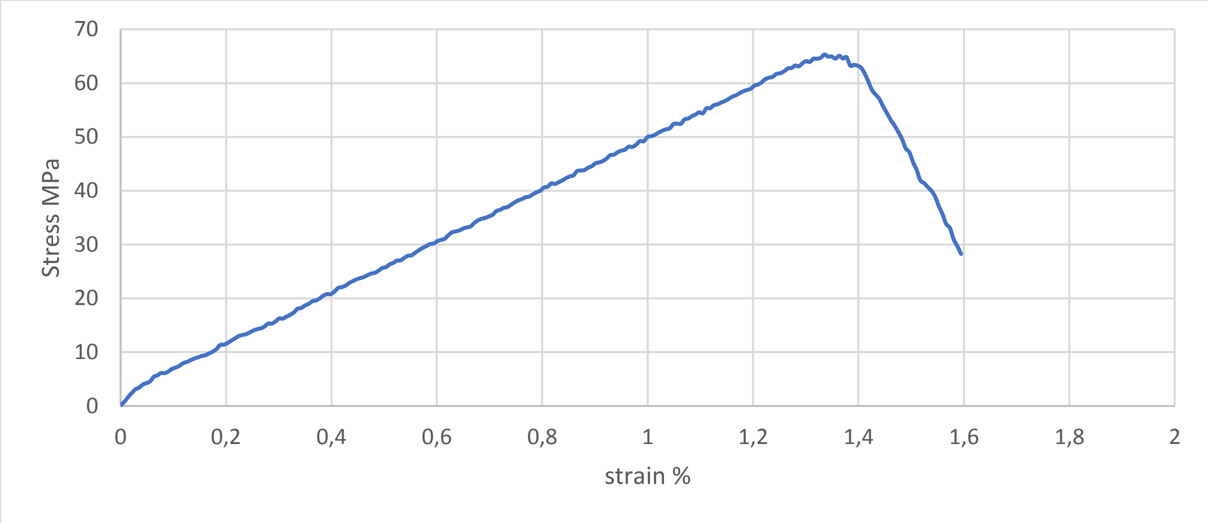

Figure. III.32 tensile test's graph of glass/epoxy specimen with crack a=10mm

We observe from this graph that the stress increased proportionally with strain until it reached the value of the stress max $\sigma_{max} = 65.3\ MPa$ and strain $\varepsilon = 1.34\%$ then it decreased with increase of strain till the rupture.

The rupture of the whole material occurred at the point where $\sigma_{repture} = 28.3\ MPa$ and strain $\varepsilon_{max} = 1.59\%$

We note that the curve's wiggles and that due to the weak adhesion of fiber matrix and that causes matrix break in the first region that is contained in the interval [0,1.38] then it's due to the break of both fibers (one after one or group after group) and matrix in the second region till the whole break of the specimen.

The curve progresses approximately following the polynomial equation

$F(x) = -89.623x^6 + 302.86x^5 - 382.17x^4 + 229.74x^3 - 71.352x^2 + 59.328x$

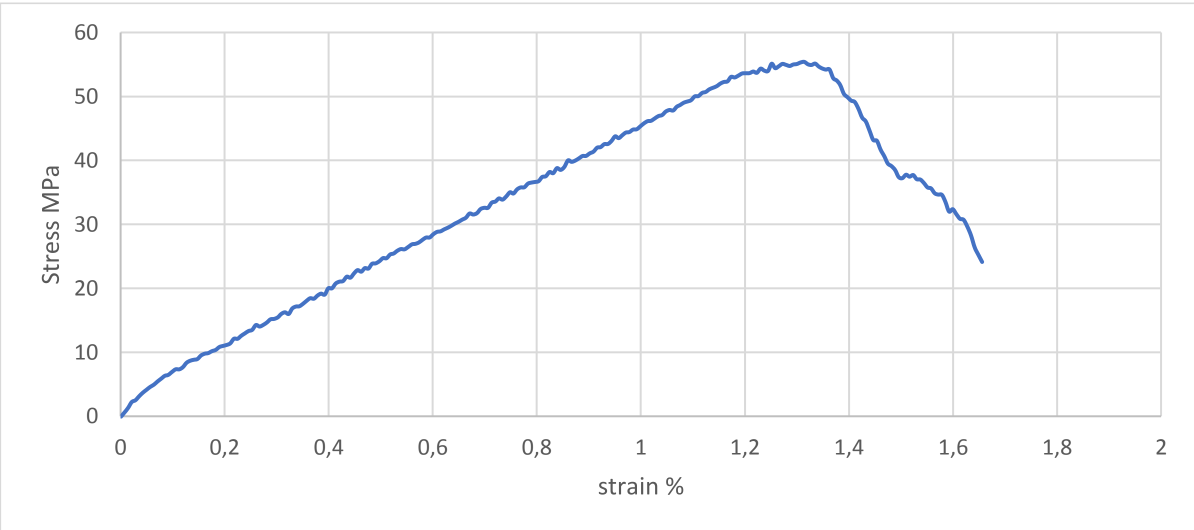

Figure. III.33 tensile test's graph of glass/epoxy specimen with crack a=12.5mm

We observe from this graph that the stress increased proportionally with strain until it reached the value of the stress max $\sigma_{max} = 55.1\ MPa$ then it decreases with increase of strain till the rupture.

The rupture of the whole material occurred at the point where $\sigma_{repture} = 24.1MPa$ and strain $\varepsilon_{max} = 1.66\%$

We note that the decrease region of the stress doesn't occurs linearly but we note that there is wiggle on the curves line and it increased its value at the point (1.5, 37.2) and that due to the weak adhesion fiber-matrix and the break of fibers one after one or group after group, that means that the whole material doesn't break together at one time.

The curve progresses approximately following the polynomial equation

$F(x) = 128.74x^6 - 619.81x^5 + 1066.4x^4 - 810.42x^3 + 262.2x^2 + 17.37x$

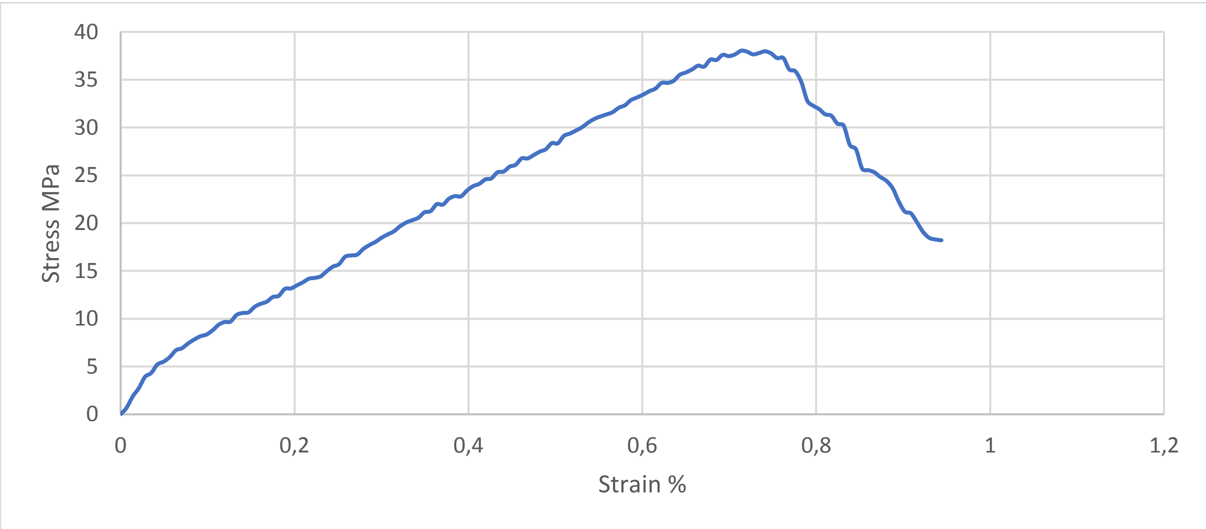

Figure. III.34 tensile test's graph of glass/epoxy specimen with crack a=15mm

We observe from this graph that the stress increased proportionally with strain until it reached the value of the stress max $\sigma_{max} = 38\ MPa$ then it decreasd with increase of strain till the rupture.

This point of rupture has a pick value of stress which is $\sigma_{repture} = 18.2\ MPa$ and strain $\varepsilon_{max} = 0.944\%$

We note a quick growth in stress-strain curve in the interval [0,0.00423] and that due to a sliding made by the tensile test machine between the specimen and the specimen's handles

We note that the curve's wiggles and that due to the weak adhesion of fiber matrix and that causes matrix break in the first region that is contained in the interval [0,0.72] then it's due to the break of both fibers (one after one or group after group) and matrix in the second region till the whole break of the specimen.

The curve progresses approximately following the equation below

$F(x)= 2133.8x^6 - 5569.5x^5 + 5007.7x^4 - 1837.5x^3 + 213.49x^2 + 62.806x$

Table III.2 results of tensile test on specimens of glass fiber with different crack sizes

Glass fiber reinforcement polymer composite material					
Crack size [mm]	Crack angle [degrees °]	Max stress [MPa]	Stress of rupture [MPa]	Max stress strain [%]	Max strain [%]
0	90	244	244	3.94	3.94
2.5	90	175	166	2.88	2.94
5	90	129	122	2.37	2.39
7.5	90	101	94.2	1.79	1.83
10	90	65.3	28.3	1.34	1.59
12.5	90	55.1	24.1	1.31	1.66
15	90	38	18.2	0.74	0.94

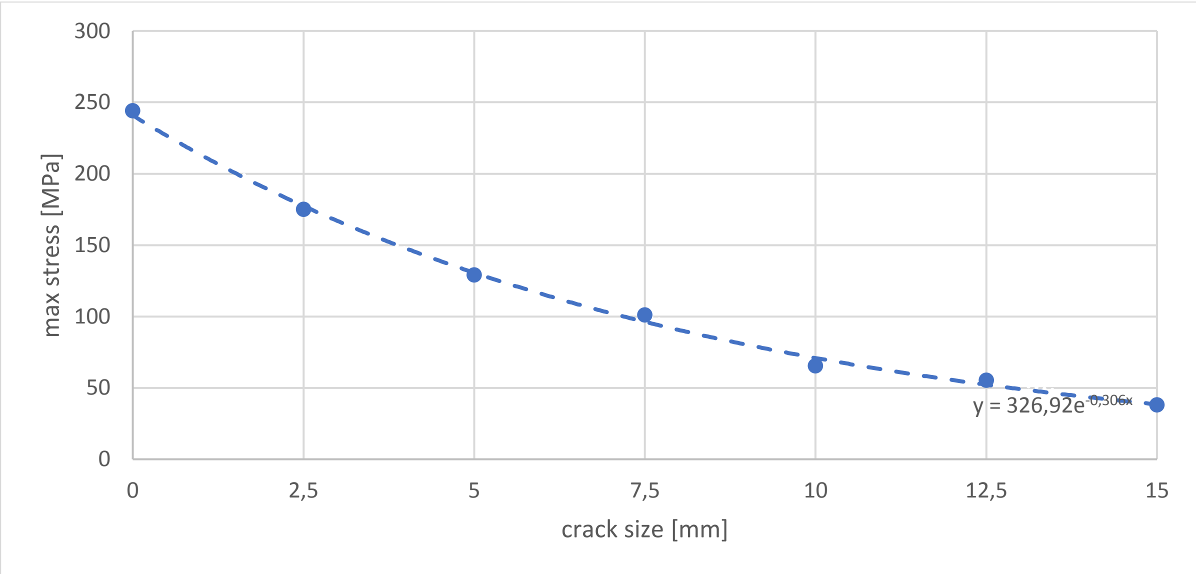

Figure. III.35 the effect of glass /epoxy material's different crack sizes on the maximum stress

We observe from this graph that the maximum stress decreases appositively with the increase of crack sizes from 244MPa to reach 38MPa at the highest crack size which is 15 mm

The curve is technically the right form of which the stress reacts with the strain and it is on the form $F(x)= 326.92e^{-0.306x}$, the points that are out of the curve, are the errors that are caused by the material's defaults.

The max stress has been reduced more than six times from the 0 mm crack size to the biggest crack size which is 15 mm.

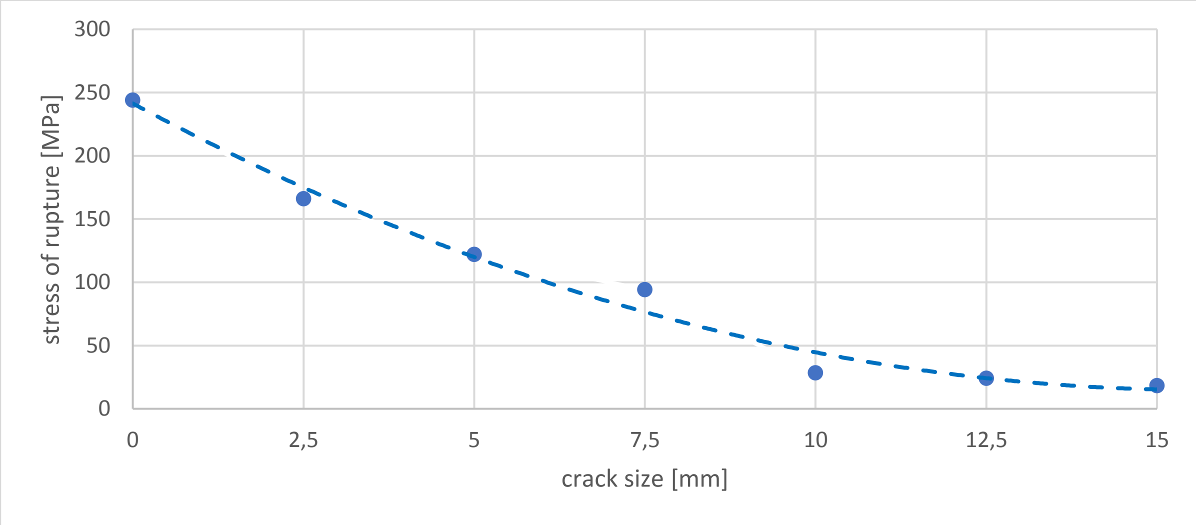

Figure. III.36 the effect of glass/epoxy different crack sizes on the stress of rupture by tensile test

We observe from this graph that the stress of rupture decreased appositively with the increase of crack sizes from 244MPa to 18.2MPa at the biggest crack size which is 15 mm

The curve is technically the right form of which the stress reacts with the strain and it is on the form $F(x) = 5.7536x^2 - 83.704x + 244$, the points that are out of curve, are practically the errors that are caused by the material's defaults.

The stress of rupture has been reduced more than thirteen times from the 0 mm crack size to the biggest crack size which is 15 mm.

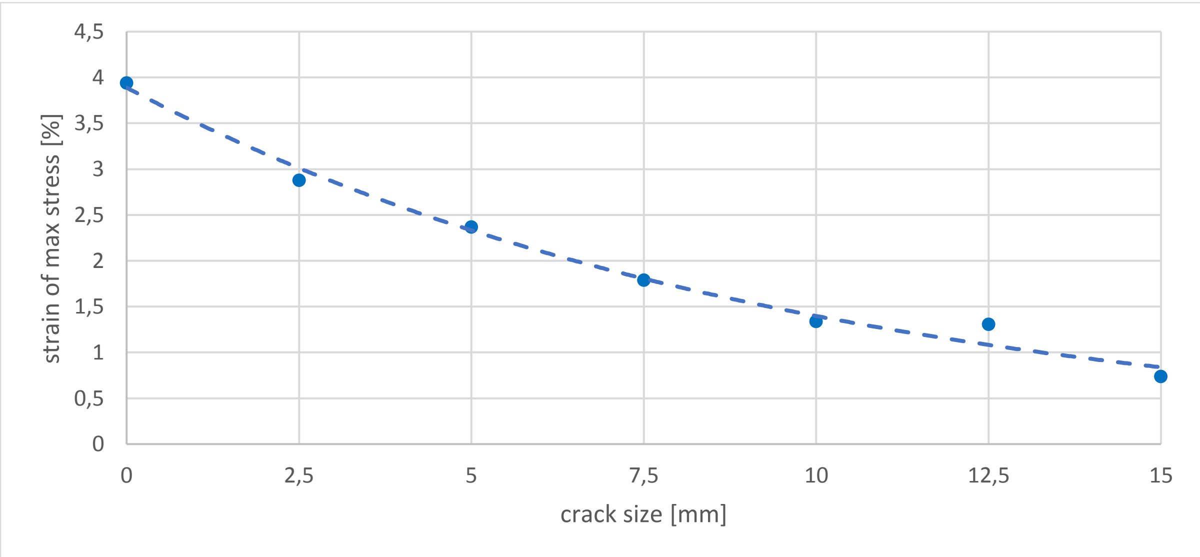

Figure. III.37 the effect of glass/epoxy different crack sizes on the strain of max stress of specimens by tensile test

We observe from this graph that the strain of max stress decreased appositively with the increase of crack sizes from 3.94 % to 0.74 % at the biggest crack size which is 15 mm

The curve is technically the right form of which the strain reacts with the crack size and it is on the form $F(x)= 3.8893e^{-0.102x}$, the points that are out of the curve, are practically the errors that are caused by the material's defaults.

The stress of strain has been reduced more than five times from the 0 mm crack size to the biggest crack size which is 15 mm.

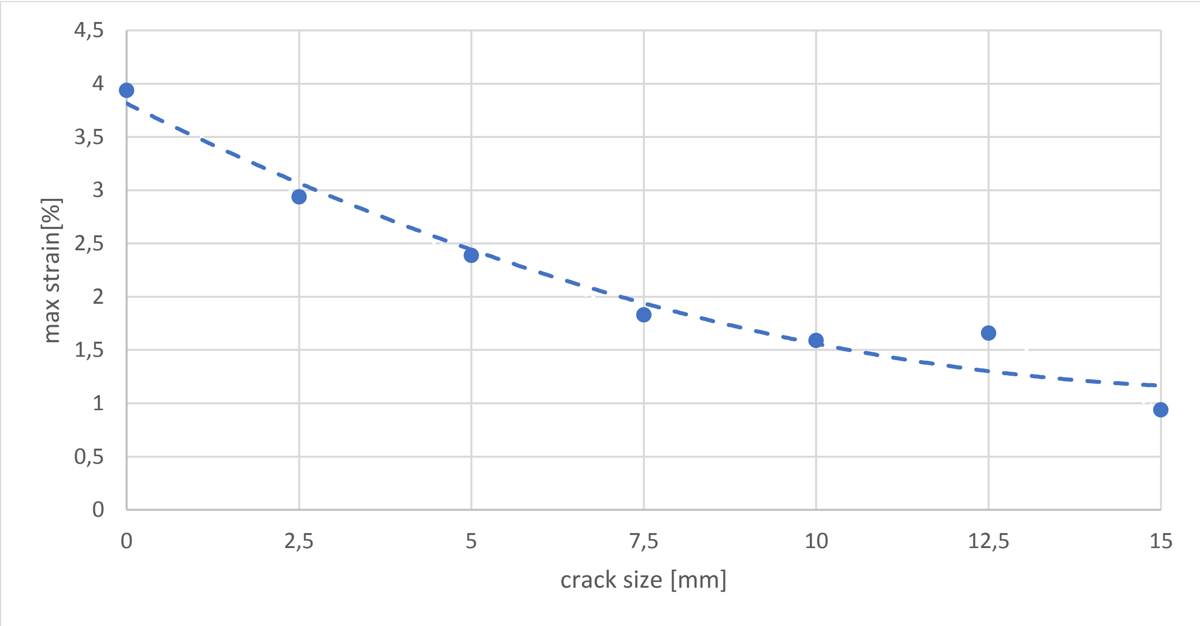

Figure. III.38 the effect of glass/epoxy different crack sizes on the strain of rupture of specimens by tensile test

We observe from this graph that the stress of rupture decreased appositively with the increase of crack sizes from 3.94 % to 0.94 % at the biggest crack size which is 15 mm

The curve is technically the right curve of which the strain reacts with the crack size and it is on the form $F(x)= 0.0098x^2 - 0.3234x + 3.8145$. the points that are out of the curve, are practically the errors that are caused by the material's defaults.

The max strain has been reduced more than four times from the 0 mm crack size to the biggest crack size which is 15 mm.

III.7.2. Glass/epoxy result graphs (different crack angles)

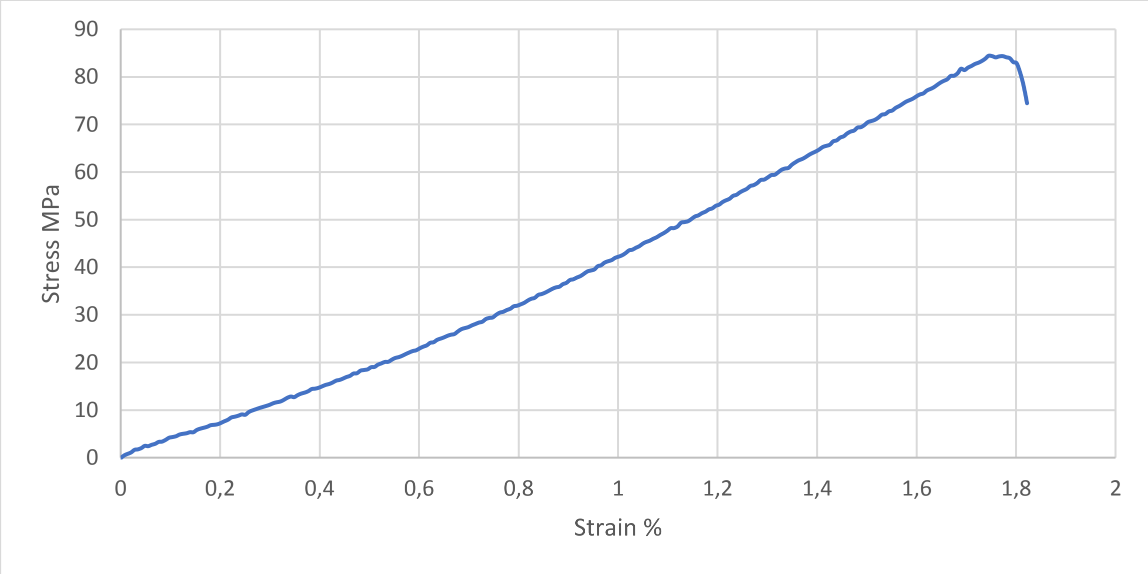

Figure. III.39 tensile test's graph of glass/epoxy specimen with crack a=15mm, θ=30°

We observe from this graph that the stress increases proportionally with strain until it reaches the value of the stress max which is $\sigma_{max} = 84.4\ MPa$ then it decreases with increase of strain till the rupture.

the rupture of the whole material occurs at the point where $\sigma_{rup} = 74.5\ MPa$ and

$\varepsilon_{max} = 1.82\%$

We observe that the curve progressed parabolically in the interval [0,1.76] instead of a linear form and submitting some wiggles and that's due to the effect of the composite material proprieties and its defaults, also it refers to the weak adhesion fiber-matrix that caused microcrack in the matrix which is the reason of the curve's wiggles.

The curve progresses approximately following the equation below

$F(x)= -37.251x^6 + 187.82x^5 - 361x^4 + 328.12x^3 - 130.7x^2 + 55.543x$

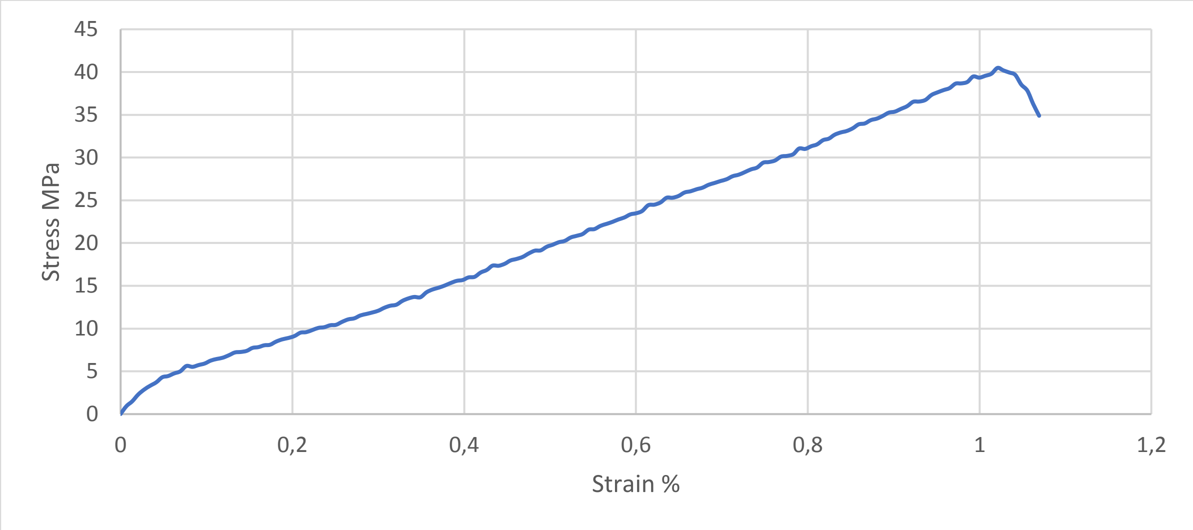

Figure. III.40 tensile test's graph of glass/epoxy specimen with crack a=15mm, θ=45°

We observe from this graph that the stress increases proportionally with strain until it reaches the value of the stress max $\sigma_{max} = 40\ MPa$ then it decreases with increase of strain till the rupture.

the rupture of the whole material occurs at the point where $\sigma_{rup} = 34.9\ MPa$ and

$\varepsilon_{max} = 1.07\%$

We observe that the curve progressed in a quick manner in the interval [0, 0.0485] and that due to a sliding between the specimen and the specimen's holders in the machine, then we note that the curve progressed linearly till it reaches to the point (1.02; 40.5) submitting some wiggles that are a result of a weak fiber-matrix adhesion and occurred because of a microcrack in the matrix

The curve progressed following the equation below

$F(x) = -1052.9x^6 + 3296.1x^5 - 3953x^4 + 2263.5x^3 - 618.7x^2 + 103.95x$

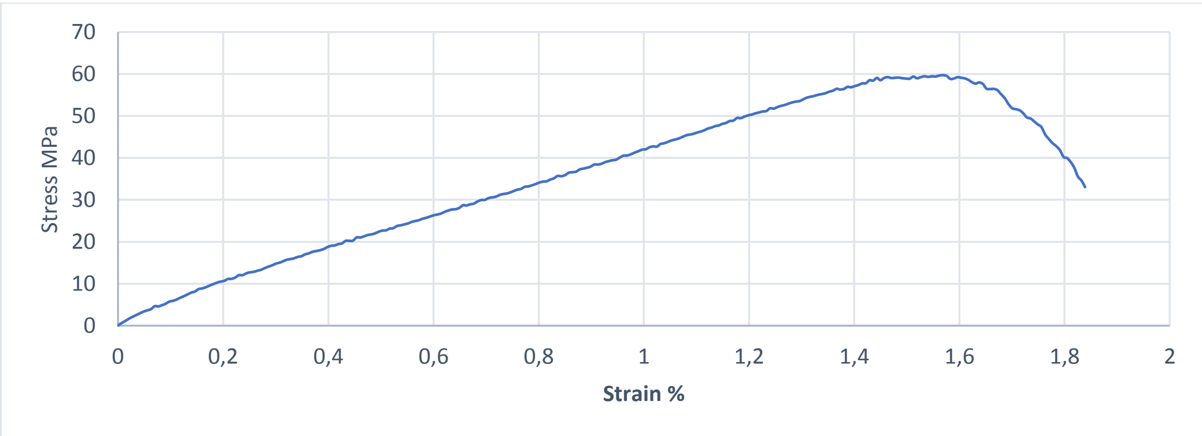

Figure. III.41 tensile test's graph of glass/epoxy specimen with crack a=15mm, θ=60°

We observe from this graph that the stress increases proportionally with strain until it reaches the value of the stress max $\sigma_{max} = 59.7\ MPa$ then it decreases with increase of strain till the rupture.

the rupture of the whole material occurs at the point where $\sigma_{rup} = 33\ MPa$ and

$\varepsilon_{max} = 1.84\%$

We note that the curve progressed approximately with a linear form except in the beginning to the point 0.223 where we can see that it progressed with a quick manner resulting of the slid between the specimen and its holders in the tensile test machine.

We can see also wiggles on it as result of a weak adhesion of fiber-matrix that caused mini and microcrack in the matrix, then we note that the curve stabilized a little bit so the stress almost took a constant value when the strain was increasing till it reached to the value 1.58 % then the stress decreased and the curve submitted to some wiggles which are the result of the rupture of fibers group by group that means that the fibers didn't break at once for all and that occurred till the rupture of the whole material.

The curve proceeded following the equation below

F(x)= $-29.704x^6 + 127.06x^5 - 218.85x^4 + 197.8x^3 - 100.16x^2 + 65.549x$

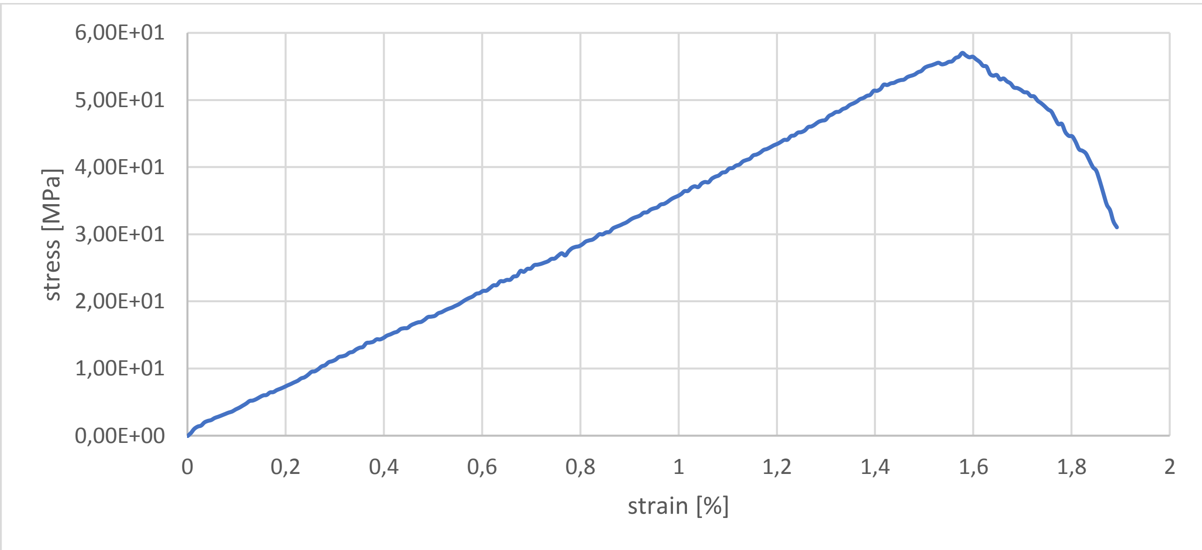

Figure. III.42 tensile test's graph of glass/epoxy specimen with crack a=15mm, θ=90°

We observe from this graph that the stress increases proportionally with strain until it reaches the value of the stress max $\sigma_{max} = 57\ MPa$ then it decreases with increase of strain till the rupture.

The rupture of the whole material occurred at the point where $\sigma_{rep} = 31MPa$ and

$\varepsilon_{max} = 1.98\%$

We note that the curve progressed linearly and submitted some wiggles till it reached the point (1.58;56.6), those wiggles are a result of a weak adhesion of fiber-matrix which made a mini and micro crack in the matrix, then we can see when the stress decreased, the curved submitted another time to wiggles and that are a result of both rupture of fibers and matrix.
The curve progressed following the equation below
$F(x)= -10.982x^6 + 29.685x^5 - 17.502x^4 - 7.8115x^3 + 7.6555x^2 + 34.05x$

Table. III.3 results of tensile test on specimens of glass fiber with different crack angles

Glass fiber Reinforcement					
Crack size [mm]	Crack angle [degrees°]	Max stress [MPa]	Stress of rupture [MPa]	Strain of max stress [%]	Max strain [%]
0	0	244	244	3.94	3.94
15	30	84.4	74.5	1.77	1.82
15	45	40.5	34.9	1.02	1.07
15	60	59.7	33	1.57	1.84
15	90	57	31	1.58	1.89

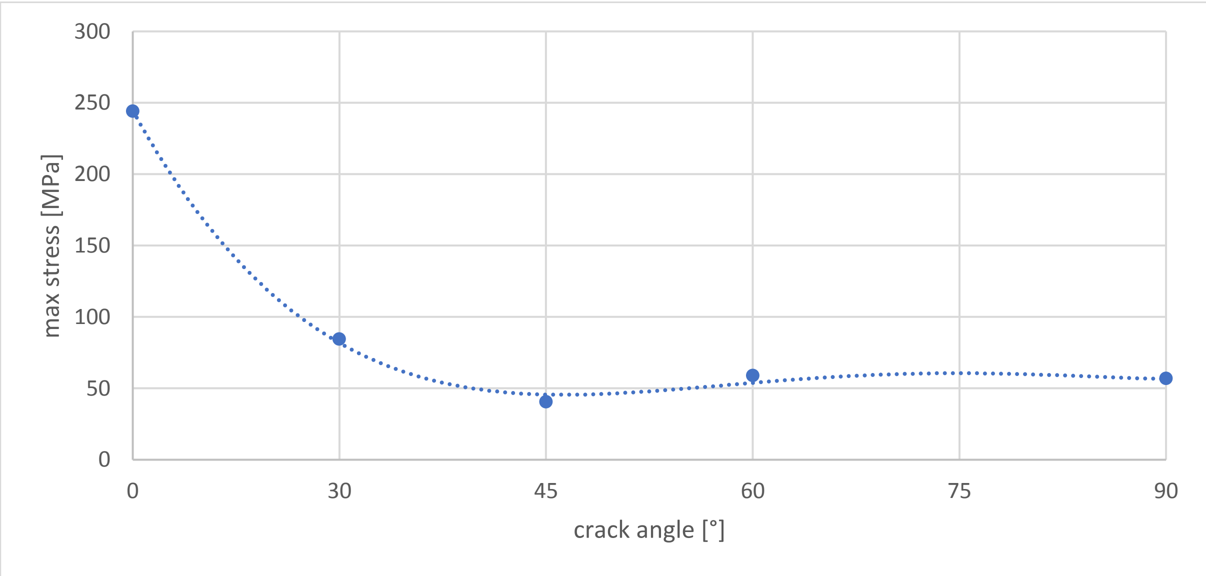

Figure. III.43 the effect of glass/epoxy different crack angles on the maximum stress

We observe from this graph that the stress decreases appositively with the increasing of crack angle till the angle 45° then it increases till the angle 60° then it decreases another time to the end of the graph
The curve is approximately the right form of which the stress reacts with the strain and it is on the form $F(x)= 1.5167x^4 - 28.865x^3 + 198.54x^2 - 579.01x +244$, the points that are out of the curve, are the errors that are caused by the material's defaults.

The max stress has been reduced more than four times from the0 mm crack size to the biggest crack angle which is 90°.

We note that the curve is almost stable from 45 to 90 it means that the stress takes approximately the same value

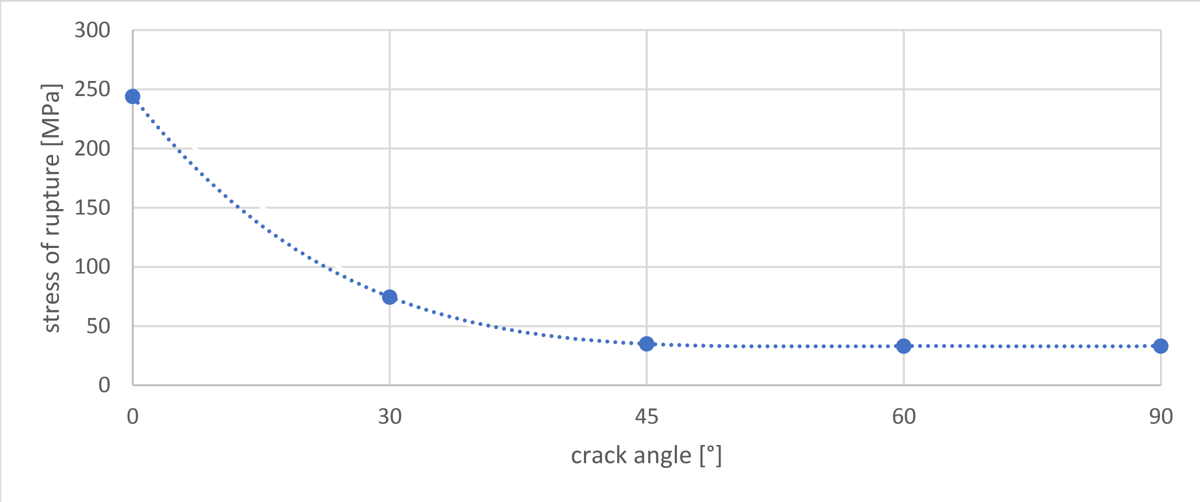

Figure. III.44 the effect of glass/epoxy different crack angles on the stress of rupture

Interpretation of the graph

We observe from this graph that the stress of rupture decreases appositively with the increasing of crack angles

The curve progressed on the following equation

F(x)= 2.3583x4 - 38.95x3 + 239.69x2 - 651.3x +244

The stress of rupture has been reduced more than seven times from the 0 mm crack size to the biggest crack angle which is 90°.

We note that the curve is almost stable from 45 to 90 it means that the stress takes approximately the same value.

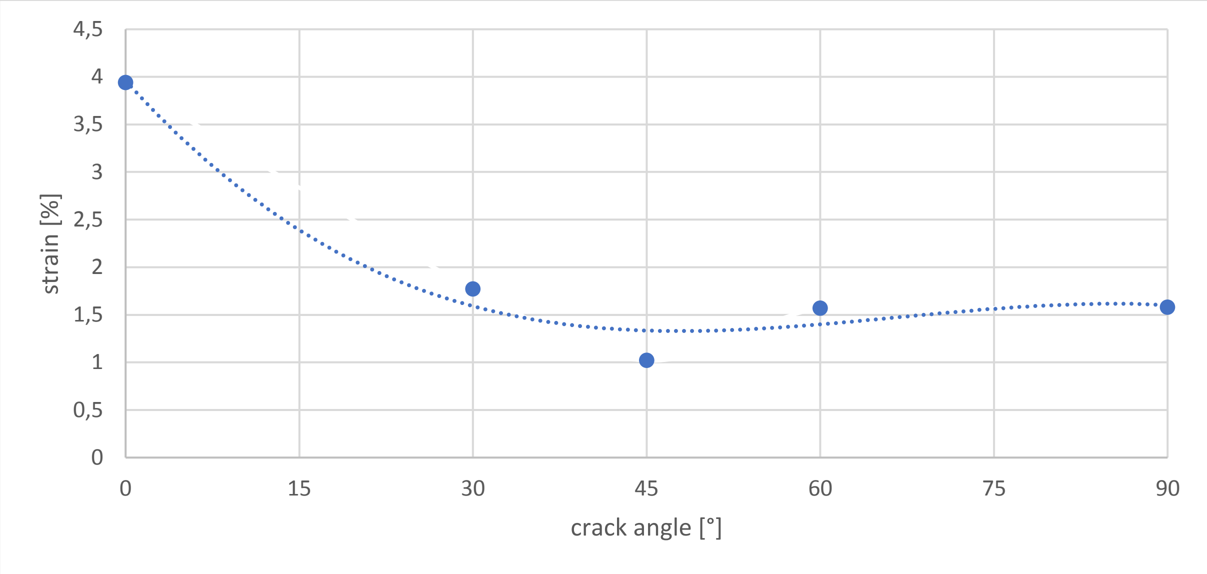

Figure. III.45 the effect of glass/epoxy different crack angles on the strain of max stress of specimens by tensile test

We observe from this graph that the strain of max stress decreased appositively with the increase of crack angles from 3.94 % to 1.02 % then it increased a little bit till it reached the biggest angle size which is 90° to attain 1.58%.

The curve approximately proceeded following the equation below

$F(x) = -1E\text{-}05x^3 + 0.0022x^2 - 0.1351x + 3.9601$, the points that are out of the curve, are practically the errors that are caused by the material's defaults.

The strain of max stress has been reduced more two times from the 0° crack angle to the biggest crack size which is 90° and more than 3 time at the angle 45°.

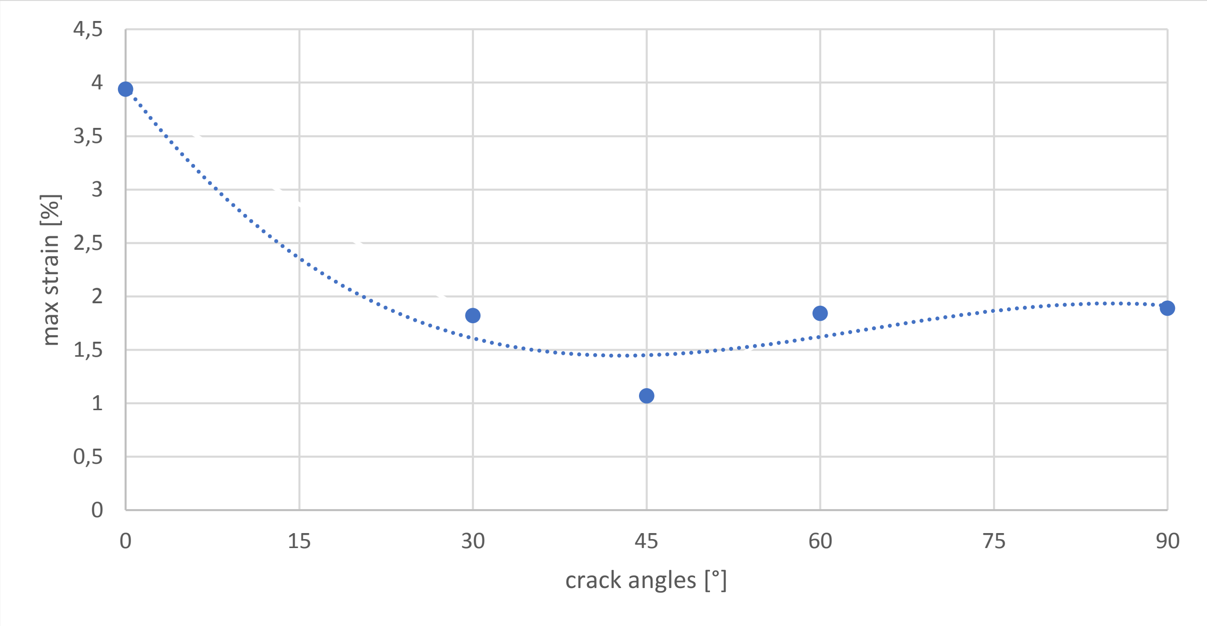

Figure. III.46 the effect of glass/epoxy different crack angles on the strain of rupture of specimens by tensile test

We observe from this graph that the strain of max stress decreased appositively with the increase of crack angles from 3.94 % to 1.07 % then it increased a little bit till it reached the biggest angle size which is 90° to attain 1.89%.

The curve approximately proceeded following the equation below

F(x)= -1E-05x3 + 0.0025x2 - 0.1413x + 3.9635, the points that are out of the curve, are practically the errors that are caused by the material's defaults.

The max strain has been reduced more two times from the 0° crack angle to the biggest crack size which is 90° and more than 3 time at the angle 45°.

III.7.3. Carbon/epoxy result graphs (different crack sizes)

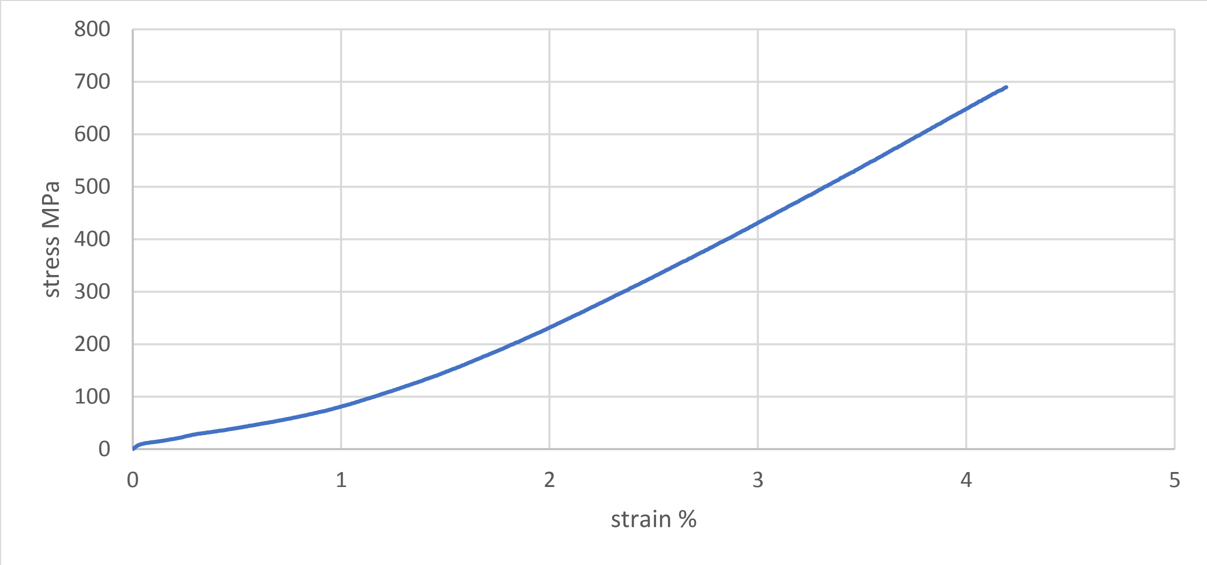

Figure. III.47 tensile test's graph of carbon/epoxy specimen without crack

We observe from this graph that the stress increased proportionally with strain until it reached the value of the maximum stress $\sigma_{max} = 690MPa$ then the rupture of the whole material occurred.

We can see that the curve in the interval [0;1.82] progressed parabolically then it progressed linearly till the end of the graph and that because of the proprieties of composite materials and its defaults of production, measure and cut.

The linear region of this curve progressed following the equation F(x)= 169.99x - 72.667 but the whole curve approximately proceeded following the equation below

F(x)= $-5.1788x^3 + 55.887x^2 + 17.861x$

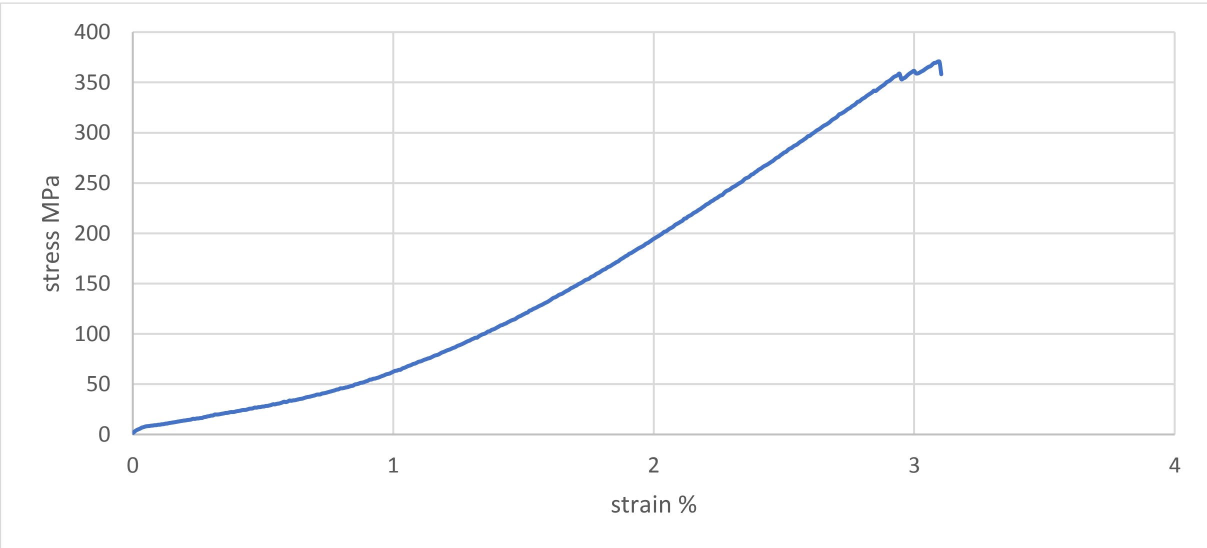

Figure. III.48 tensile test's graph of carbon/epoxy specimen with crack a=2.5mm.

We observe from this graph that the stress increases proportionally with strain until it reaches the value of the stress max $\sigma_{max} = 371\ MPa$ then it decreases with increase of strain till the rupture.

This rupture of the whole material occurred at the point where $\sigma_{rep} = 358\ MPa$ and $\varepsilon_{max} = 3.1\%$.

We can see that the curve progressed in a parabolic form in the interval [0;1.71] than it proceeded linearly in the region [1.71;2.94].

In the last region [2.94;3.1] the stress wiggled till the end of graph and that's because of the rupture of fibers and matrix before the total rupture of the specimen

The curve progressed approximately following the equation below

$F(x)= -5.7604x^4 + 27.925x^3 - 6.4174x^2 + 41.893x$

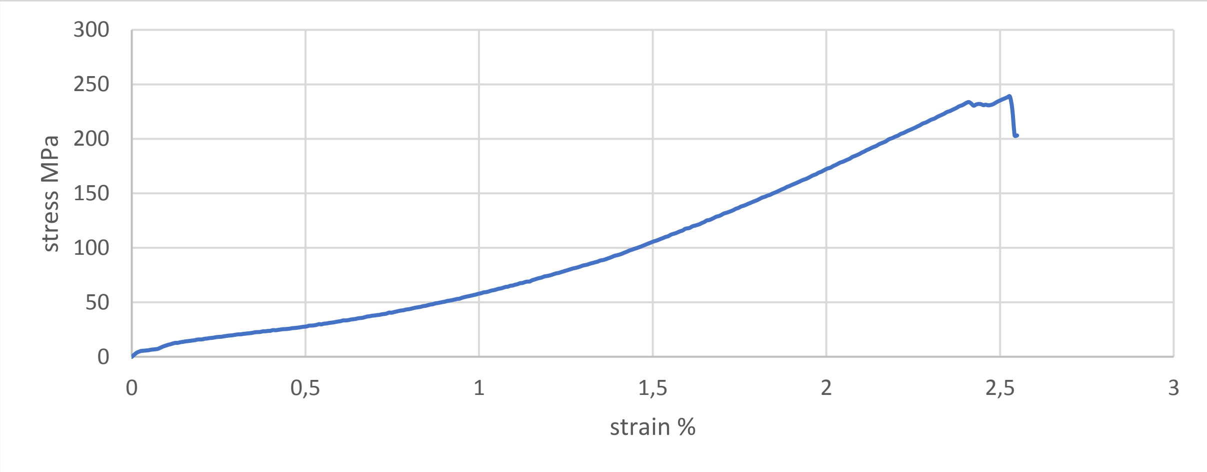

Figure. III.49 tensile test's graph of carbon/epoxy specimen with crack a=5mm.

We observe from this graph that the stress increases proportionally with strain until it reaches the value of the stress max $\sigma_{max} = 239\ MPa$ then it decreases with increase of strain till the rupture.

The rupture of the whole material occurred at the point where $\sigma_{rep} = 203 MPa$ and $\varepsilon_{max} = 2.54\%$

We can see that the curve progressed in a parabolic form in the interval [0;2.41].

In the second region [2.41;2.54] the stress wiggled till the end of graph and that's because of the rupture of fibers and matrix before the total rupture of the specimen

The curve progressed approximately following the equation below

$F(x) = -19,437x^6 + 138,97x^5 - 385,27x^4 + 523,96x^3 - 328,46x^2 + 127,84x$

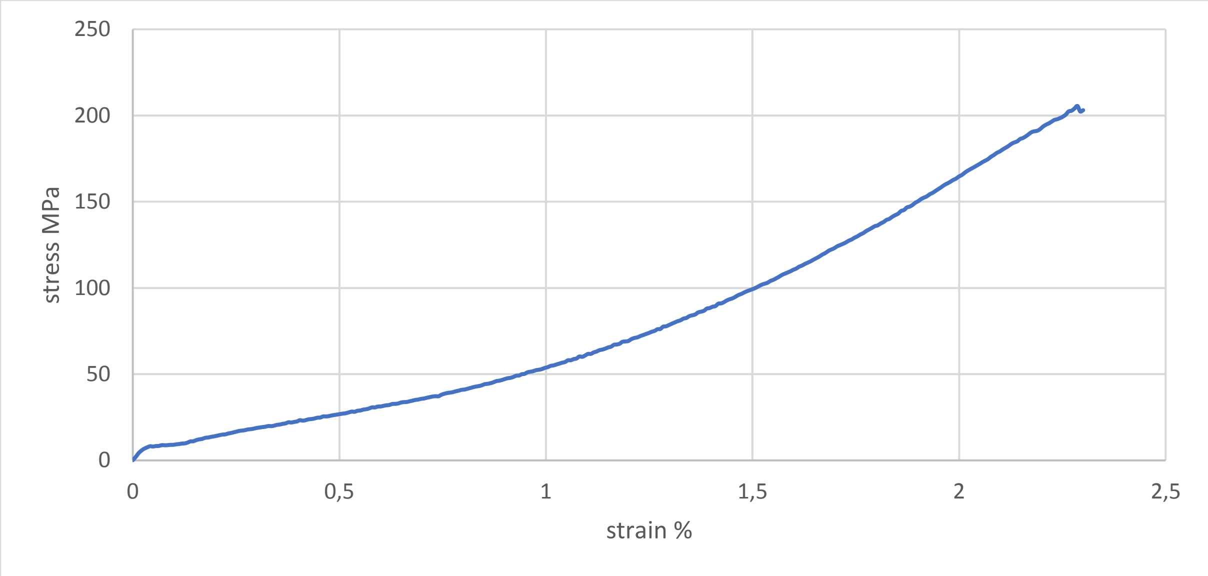

Figure. III.50 tensile test's graph of carbon/epoxy specimen with crack a=7.5mm.

We observe from this graph that the stress increased proportionally with strain until it reached the value of the stress max $\sigma_{max} = 205\ MPa$ then it decreases with increase of strain till the rupture.

The rupture of the whole material occurred at the point where $\sigma_{rep} = 202.33MPa$ and $\varepsilon_{max} = 2.29\%$.

We can see that the curve proceeded in a parabolic form in the interval [0;2.29] and this is because of the proprieties of the composite material and its defaults of production, measure and cut.

The curve progressed approximately following the equation below

$F(x)= -10.197x^4 + 51.344x^3 - 52.402x^2 + 61.376x + 3.5695$

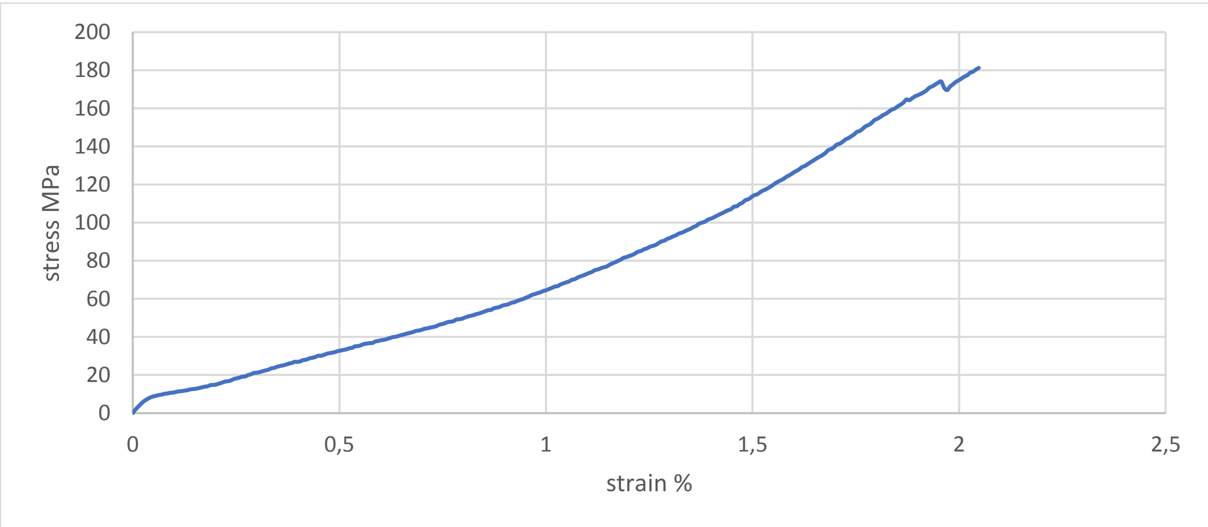

Figure. III.51 tensile test's graph of carbon/epoxy specimen with crack a=10mm.

We observe from this graph that the stress increases proportionally with strain until it reaches the value of the stress max $\sigma_{max} = 173\ MPa$ then it decreases a little bit to attain the stress value $\sigma = 169.61 MPa$ with increase of strain then it decreased another time to reach the maximum stress value $\sigma_{max} = 181\ MPa$.

This rupture of the whole specimen occurred at the point where $\sigma_{max} = 181 MPa$ and

$\varepsilon_{max} = 2.05\%$

We can see that the curve proceeded in a parabolic form in the interval [0;1.95] and this is because of the proprieties of the composite material and its defaults of production, measure and cut.

In the second region [1.95;2.05] we can see that the curve decreased than increased and that's because of both the weak adhesion of fiber matrix which caused the delamination and the micro crack of the matrix, and the big resistant of fibers which made the curve increase for the second time.

The curve progressed approximately following the equation below

$F(x)= -16.273x^4 + 71.837x^3 - 75.902x^2 + 82.07x$

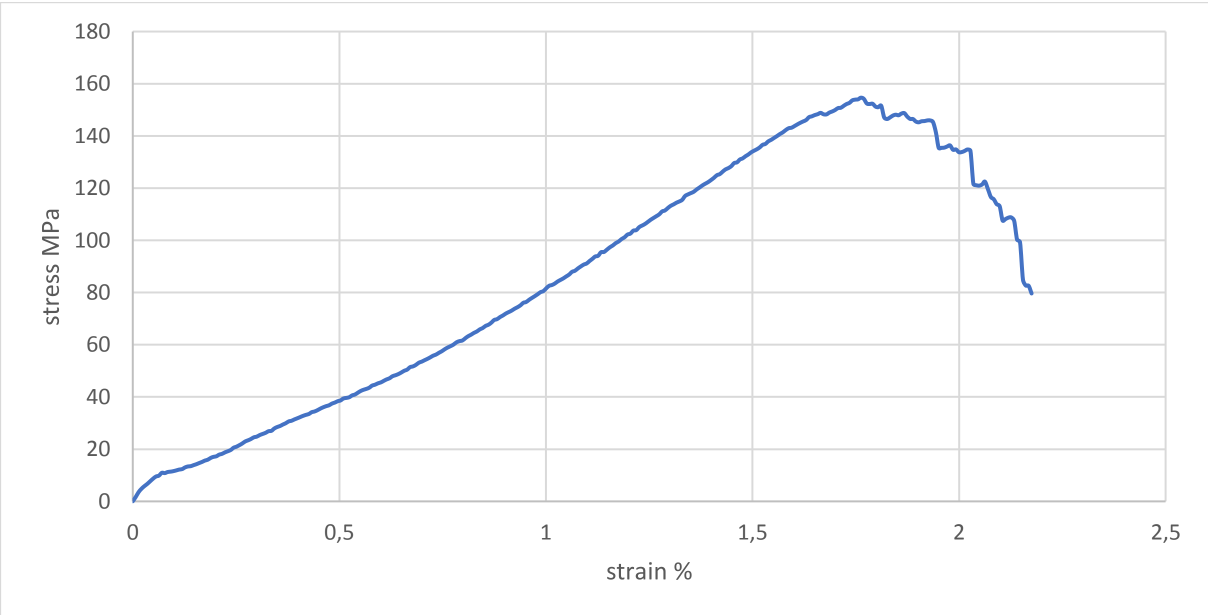

Figure. III.52 tensile test's graph of carbon/epoxy specimen with crack a=12.5mm.

We observe from this graph that the stress increases proportionally with strain until it reaches the value of the stress max $\sigma_{max} = 154.66 MPa$ then it decreases with increase of strain till the rupture.

the rupture of the whole material occurs at the point where $\sigma_{rup} = 76.65 MPa$ and

$\varepsilon_{max} = 2.18\%$

We note that the curve progressed approximately with a parabolic form except in the beginning to the point 0.07 where we can see that it progressed with a quick manner resulting of the slid between the specimen and its holders in the tensile test machine.

We can see also after the point 1.76 in the strain's axis that the curve decreased and submitted wiggles till the rupture and this is because of the rupture of fibers group by group that means that the fibers didn't break at once for all and that occurred till the rupture of the whole material.

The curve proceeded approximately following the equation below

$F(x)= -7.0554x^6 + 20.719x^5 - 35.518x^4 + 62.505x^3 - 43.193x^2 + 80.287x$

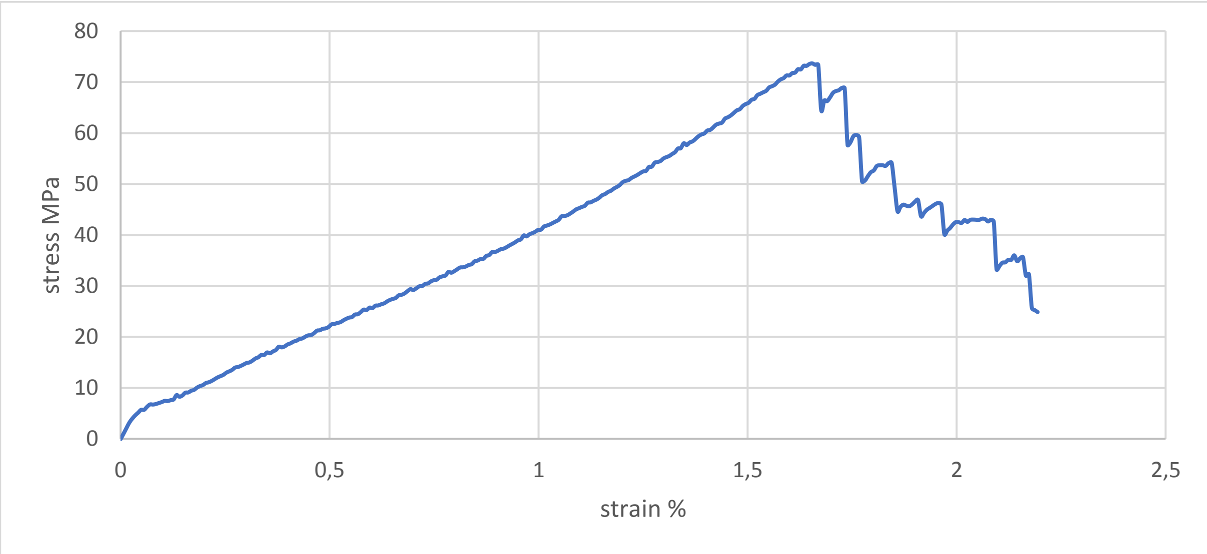

Figure. III.53 tensile test's graph of carbon/epoxy specimen with crack a=15mm.

We observe from this graph that the stress increased proportionally with strain until it reached the value of the stress max $\sigma_{max} = 73.55MPa$ then it generally decreased with increase of strain till the rupture.

the rupture of the whole material occurs at the point where $\sigma_{rup} = 24.88MPa$ and

$\varepsilon_{max} = 2.19\%$

We note that the curve progressed approximately with a parabolic form except in the beginning to the point 0.06 where we can see that it progressed with a quick manner resulting of a slid that occurred between the specimen and its holders in the tensile test machine.

We can see also after the point 1.76 in the strain's axis that the curve decreased and submitted wiggles till the rupture and this is because of the rupture of fibers group by group that means that the fibers didn't break at once for all and that occurred till the rupture of the whole material.

The curve proceeded approximately following the equation below

$F(x)= -19.029x^4 + 54.122x^3 - 48.595x^2 + 56.385x$

Table. III.4 results of tensile test on specimens of carbon/epoxy with different crack sizes

Carbon/epoxy composite material					
Crack size [mm]	Crack angle (degrees) (°)	Stress max [MPa]	Stress of rupture [MPa]	Strain of max stress %	Max strain [%]
0	0	690	690	4.19	4.19
2.5	90	371	358	3.09	3.1
5	90	239	203	2.53	2.55
7.5	90	205	202	2.29	2.3
10	90	181	181	2.05	2.05
12.5	90	155	79.7	1.76	2.18
15	90	73.4	24.9	1.66	2.19

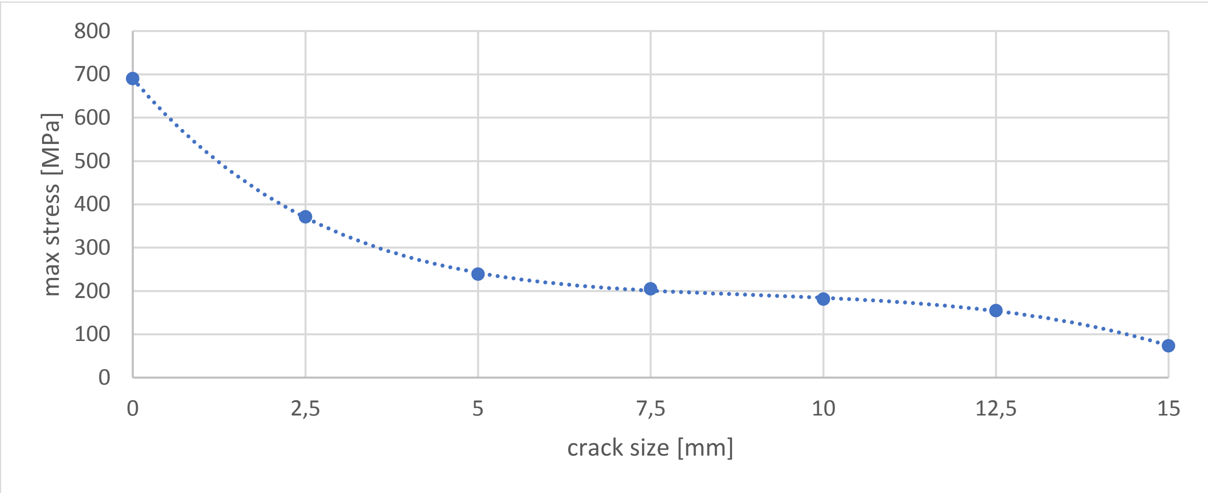

Figure. III.54 the effect of carbon fiber's different crack sizes on the maximum stress

We observe from this graph that the maximum stress decreased appositively with the increase of crack sizes.

The maximum stress has been reduced more than 9 times from the 0mm crack size to the biggest crack size which is 15 mm.

The stress reacts with the crack sizes following the equation below

$F(x) = -0.0018x^5 + 0.0932x^4 - 2.2501x^3 + 28.651x^2 - 187.13x + 690.21$

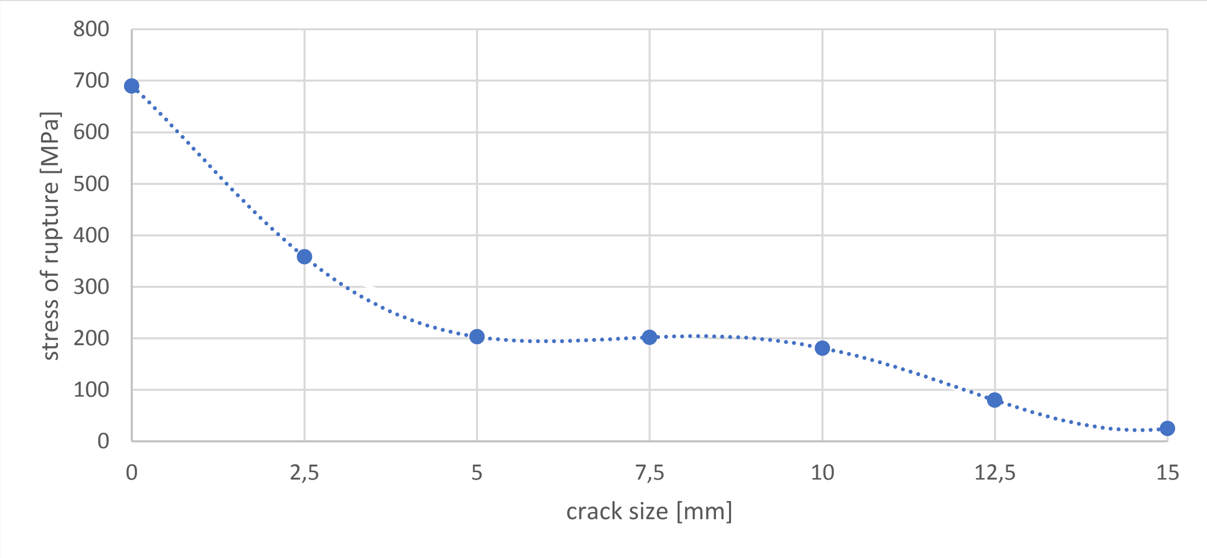

Figure. III.55 the effect of carbon fiber's different crack sizes on the stress of rupture

We observe from this graph that the stress of rupture decreases appositively with the increase of crack sizes till it reached the point 5 on the strain's axis then it stabilized approximately till the point 10 of the strain's axis then it decreased another time and always with the increase of the strain.

The stress variates with strain approximately following the equation below

$F(x)= -0.0011x^6 + 0.0634x^5 - 1.3039x^4 + 10.938x^3 - 24.368x^2 - 122.24x + 690$

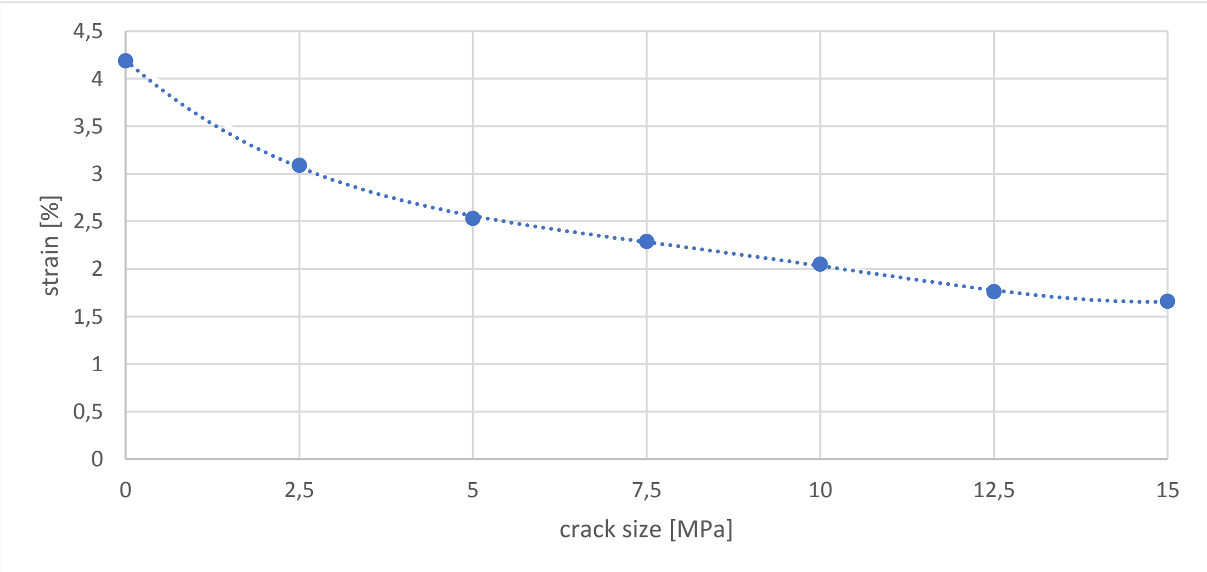

Figure. III.56 the effect of carbon/epoxy different crack sizes on the strain of maximum stress

We observe from the graph that the strain decreased appositively with increase of crack sizes, it decreased from 4.19% at crack size equals 0mm to reach 1.66% at the biggest crack size which is 15mm.

The strain has been reduced more than two times from the smallest to the biggest crack size.

The strain progressed with the crack size following the equation below

$F(x)= 0.0002x^4 - 0.0069x^3 + 0.0926x^2 - 0.6418x + 4.195$

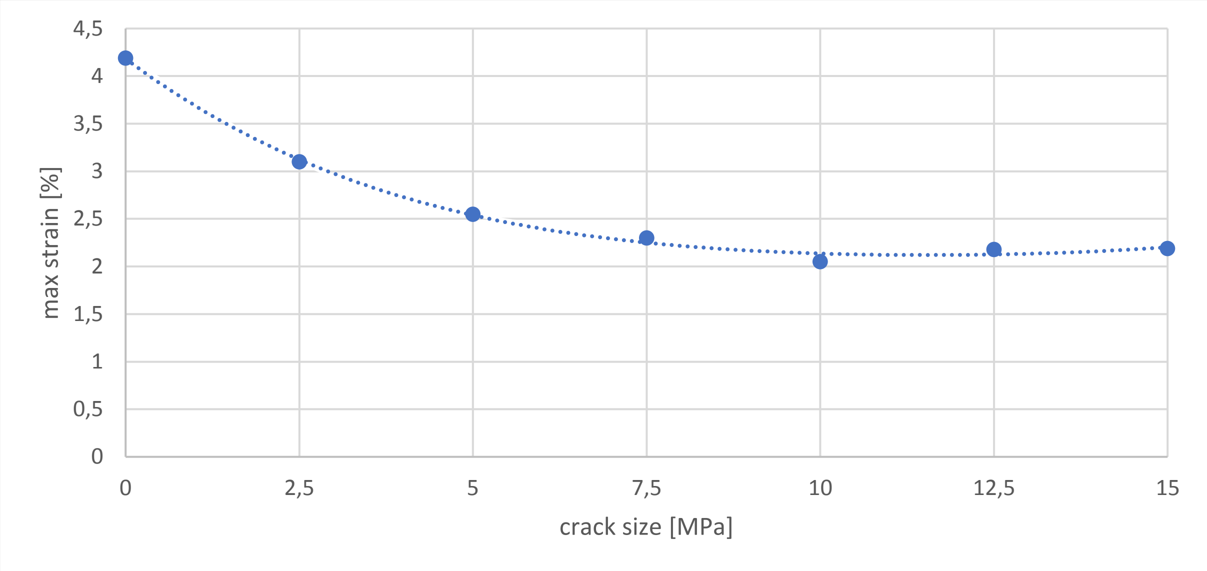

Figure. III.57 the effect of carbon/epoxy different crack sizes on the maximum strain

We observe from the graph that the maximum strain decreased appositively with increase of crack sizes from the beginning of the curve till the point 7.5 of the crack size axis then it approximately stabilized after the 7.5mm crack size it decreased from 4.19% at crack size equals 0mm to reach 2.19% at the biggest crack size which is 15mm.

The strain has been reduced more than two times from the smallest to the biggest crack size.

The maximum strain progressed with the crack size following the equation below

$F(x)= 6E\text{-}05x^4 - 0.0027x^3 + 0.0558x^2 - 0.5468x + 4.1827$

III.7.4. Carbon/epoxy result graphs (different crack sizes)

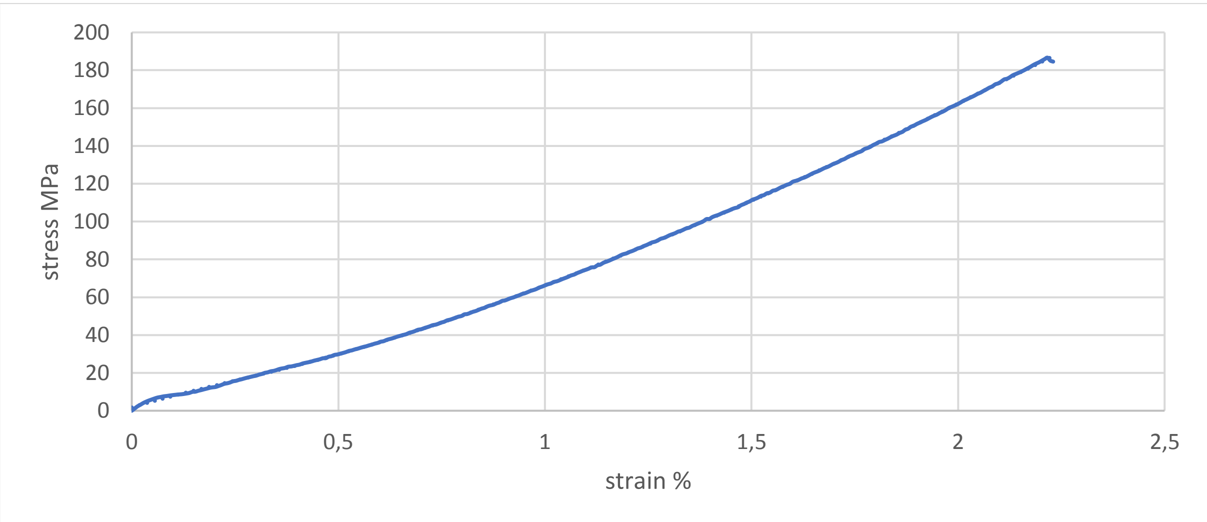

Figure. III.58 tensile test's graph of carbon/epoxy specimen with crack a=15mm, θ=30°

We observe from this graph that the stress increased proportionally with strain until it reached the value of the maximum stress $\sigma_{max} = 187\ MPa$ then it decreased with increase of strain till the rupture.

The rupture of the whole material occurred at the point where $\sigma_{rup} = 185MPa$ and

$\varepsilon_{max} = 2.23\%$

We can see that the curve proceeded parabolically following the equation below

F(x)= $-5.1278x^6 + 37.292x^5 - 104.4x^4 + 137.95x^3 - 67.733x^2 + 66.565x$

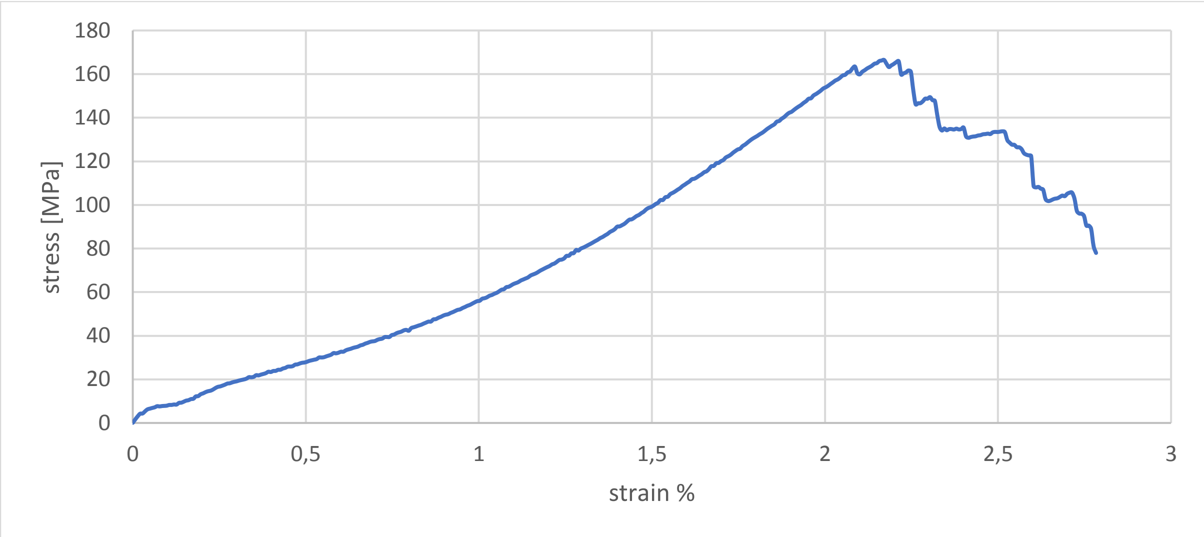

Figure. III.59 tensile test's graph of carbon/epoxy specimen with crack a=15mm, θ=45°

We observe from this graph that the stress increases proportionally with strain until it reaches the value of the stress max $\sigma_{max} = 165.88MPa$ then it decreases with increase of strain till the rupture.

The rupture of the whole material occurred at the point where $\sigma_{rep} = 77.98MPa$ and

$\varepsilon_{max} = 2.78\%$

We note that the curve progressed parabolically from the beginning of the curve till the point (2,09; 163.43) then it wiggled till it reached the maximum stress then it generally decreased and submitted so many wiggles until it reached the point of rupture of the whole material.

those wiggles are a result of a weak adhesion of fiber-matrix which made a mini and micro crack in the matrix, also it was because of the rupture of both fibers and matrix.

The rupture of fibers wasn't a total rupture but the fibers was breaking group by group till the end of the curve.

The curve progressed following the equation below

F(x)= $-22.87x^4 + 88.118x^3 - 85.539x^2 + 73.976x$

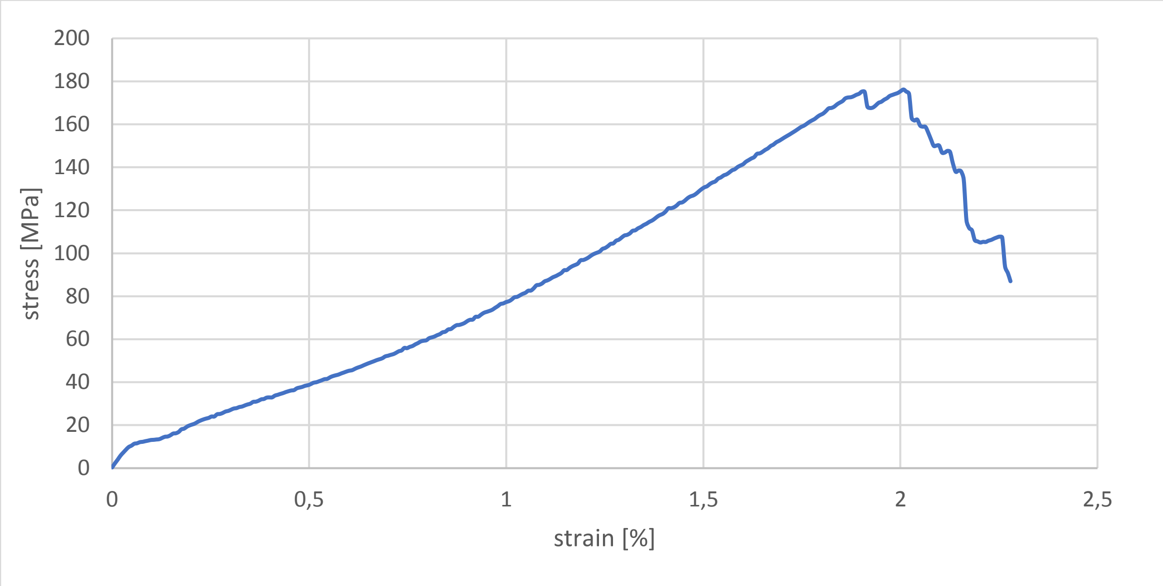

Figure. III.60 tensile test's graph of carbon/epoxy specimen with crack a=15mm, θ=60°

We observe from this graph that the stress increases proportionally with strain until it reaches the value of the stress max $\sigma_{max} = 176.2MPa$ then it decreases with increase of strain till the rupture.

The rupture of the whole material occurred at the point where $\sigma_{rep} = 86.98MPa$ and

$\varepsilon_{max} = 2.28\%$

We note that the curve progressed parabolically from the beginning of the curve till the point (1.91; 175.05) then it wiggled till it reached the maximum stress then it generally decreased and submitted so many wiggles until it reached the point of rupture of the whole material.

those wiggles are a result of a weak adhesion of fiber-matrix which made a mini and micro crack in the matrix, also it was because of the rupture of both fibers and matrix.

The rupture of fibers wasn't a total rupture but the fibers was breaking group by group till the end of the curve.

The curve progressed following the equation below

F(x)= $-26.233x^6 + 129.86x^5 - 257.21x^4 + 274.76x^3 - 150.29x^2 + 102.14x$

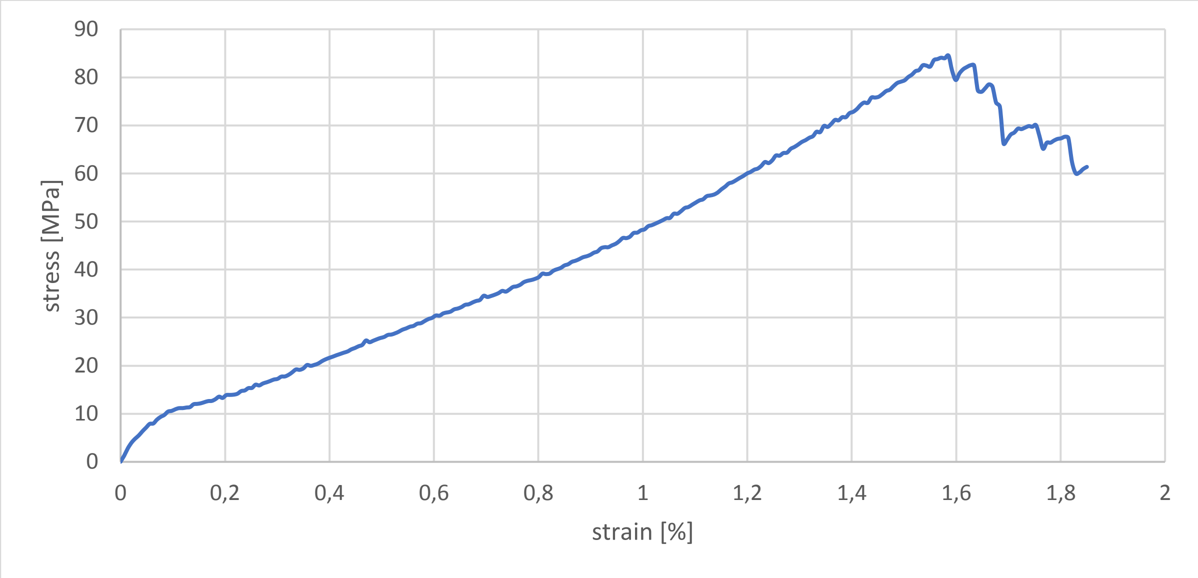

Figure. III.61 tensile test's graph of carbon/epoxy specimen with crack a=15mm, θ=90°

This point of rupture has a pick value of stress which is $\sigma_{repture} = 61.4\ MPa$

We observe from this graph that the stress increases proportionally with strain until it reaches the value of the stress max $\sigma_{max} = 84.49MPa$ then it decreases with increase of strain till the rupture.

The rupture of the whole material occurred at the point where $\sigma_{rep} = 61.37MPa$ and

$\varepsilon_{max} = 1.85\%$

We can see that the curve proceeded in a quick manner at the start of the graph in the interval [0;0.08] and this is because a slid happened between the specimen and its holders in the machine, we also note that the curve progressed parabolically from the beginning of the curve till the point (1.59; 84.49) then it generally decreased and submitted so many wiggles until it reached the point of rupture of the whole material.

those wiggles are a result of a weak adhesion of fiber-matrix which made a mini and micro crack in the matrix, also it was because of the rupture of both fibers and matrix.

The rupture of fibers wasn't a total rupture but the fibers was breaking group by group till the end of the curve.

The curve progressed following the equation below

$F(x)= -38.759x^5 + 118.97x^4 - 103.75x^3 + 19.209x^2 + 48.689x$

Table III.5 results of tensile test on specimens of carbon/epoxy with different crack angles

Carbon/epoxy reinforcement					
Crack size [mm]	Crack angle [°]	Max stress [MPA]	Stress of rupture [MPa]	Max stress strain [%]	Max strain [%]
0	0	690	690	4.19	4.19
15	30	187	185	2.22	2.23
15	45	165	78	2.16	2.78
15	60	176	87	1.9	2.28
15	90	82.5	61.4	1.59	1.85

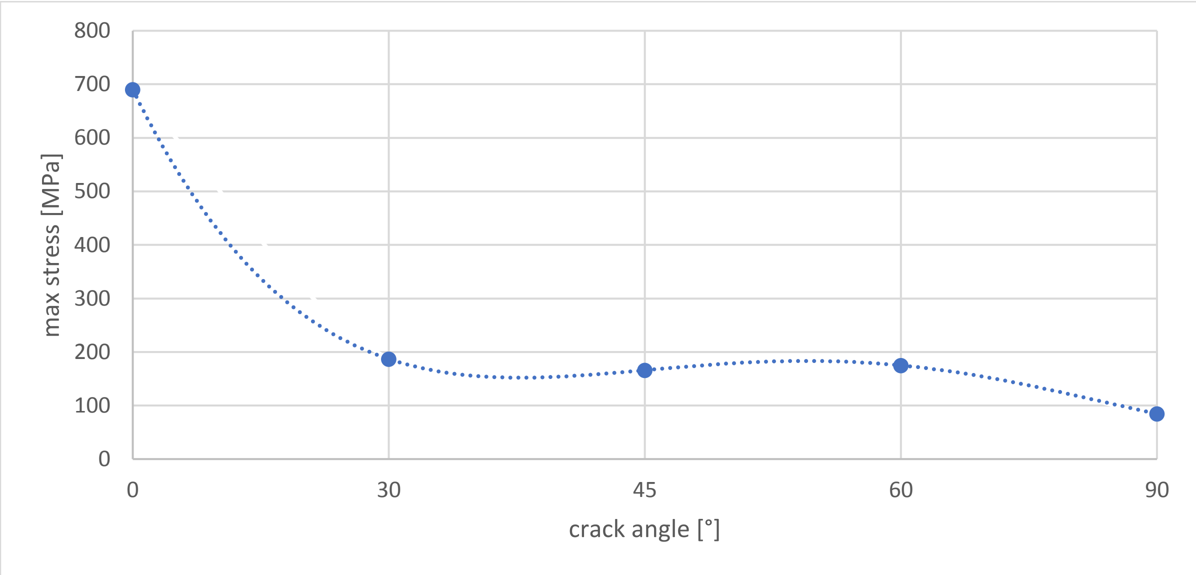

Figure. III.62 the effect of carbon fiber's different crack angles on the maximum stress

We observe from this graph that the maximum stress decreased appositively with the increase of crack angles until it reached the 30° then it approximatively stabilized until it attained 60° and it decreased another time to the end of the graph.

The maximum stress has been reduced more than 8 times from the 0° crack angle to the biggest crack angle which is 90°.

The maximum stress proceeded with crack angles following the equation below

$F(x)= 13.438x^4 - 209.71x^3 + 1163.3x^2 - 2726.5x + 690.23$

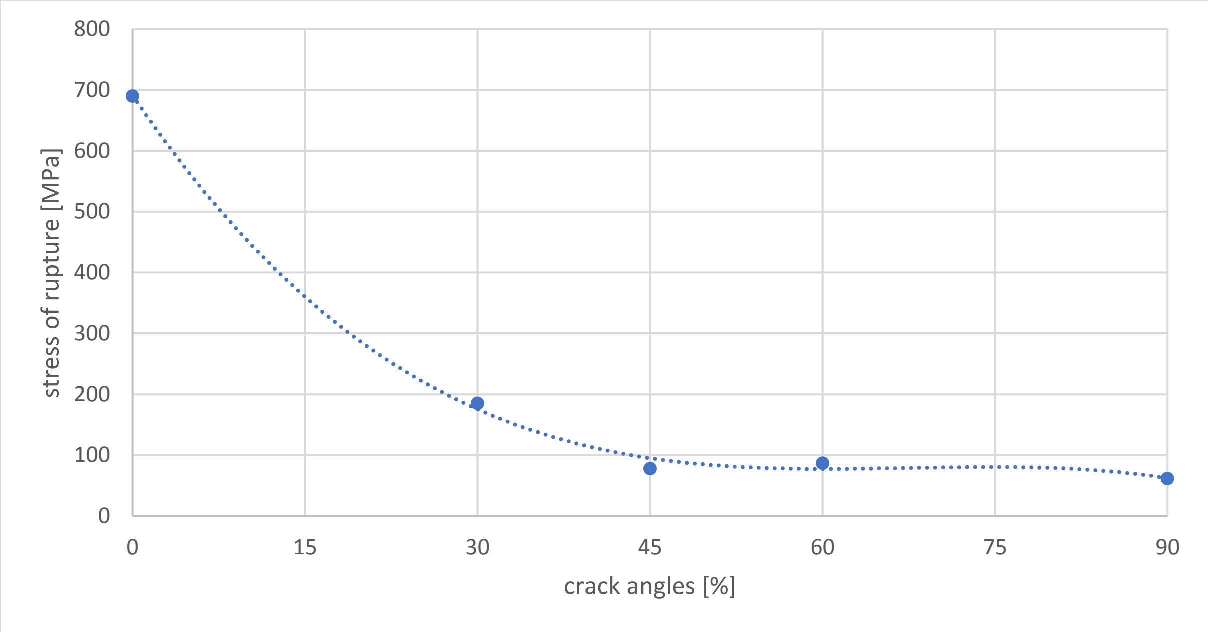

Figure. III.63 the effect of carbon/epoxy different crack angles on the stress rupture

We observe from this graph that the stress of rupture decreases appositively with the increasing of crack angles until it reaches the 45° then it stabilized till it arrived to 60° and it decreases another time to the end of the graph.

The stress of rupture has been reduced more than 11 times from the 0° crack angle to the biggest crack angle which is 90°.

The stress of rupture progressed with crack angles following the equation below

$F(x)= -0.0021x^3 + 0.4179x^2 - 27.868x + 691.07$

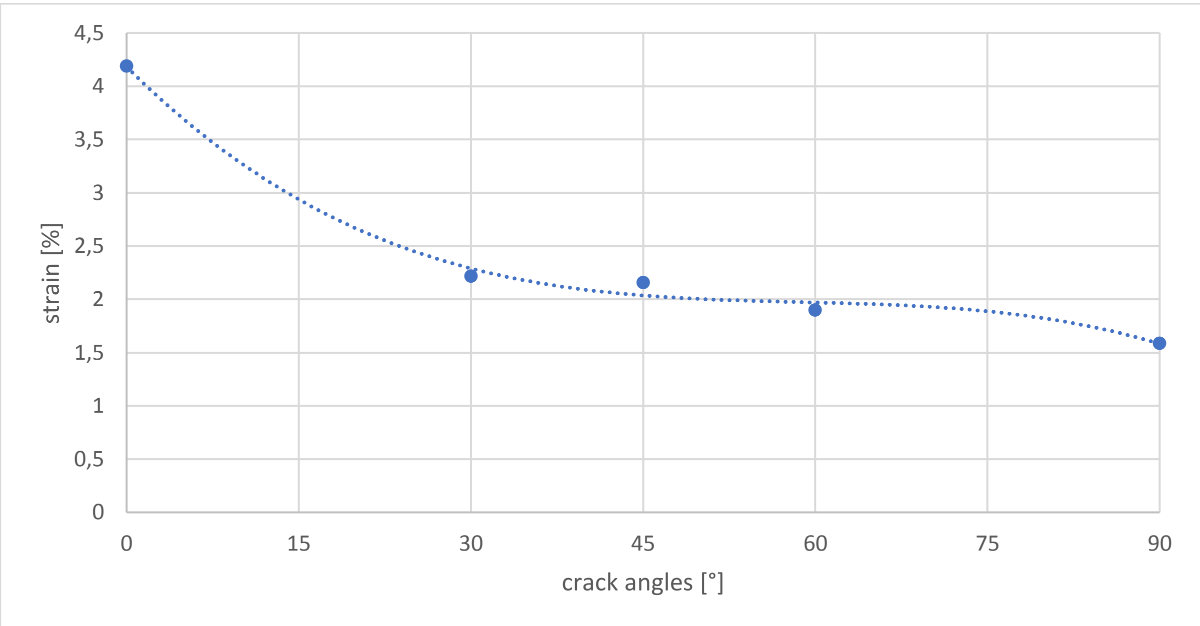

Figure. III.64 the effect of carbon/epoxy different crack angles on the stress rupture

We observe from this graph that the stress of rupture decreases appositively with the increasing of crack angles until it reaches the 45° then it approximately stabilized till it arrived to 60° and it decreases another time to the end of the graph.

The stress of rupture has been reduced more than 2 times from the 0° crack angle to the biggest crack angle which is 90°.

The stress of rupture progressed with crack angles following the equation below

$F(x)= -1E\text{-}05x^3 + 0.0018x^2 - 0.1075x + 4.1822$

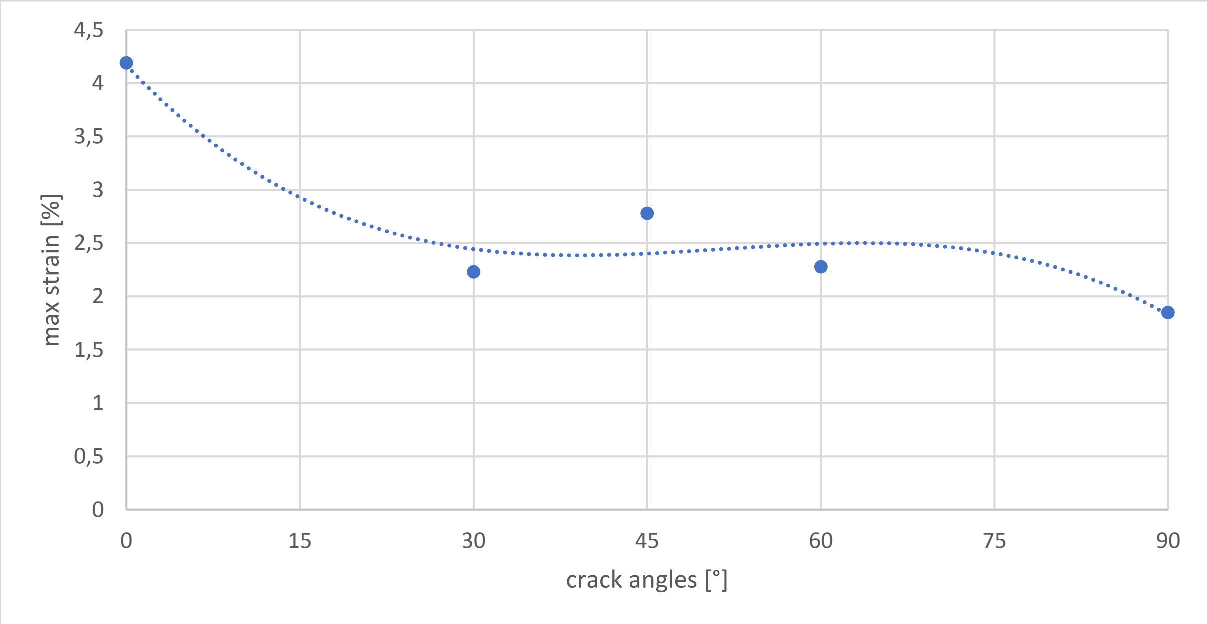

Figure. III.65 the effect of carbon/epoxy different crack angles on the stress rupture

We observe from this graph that the stress of rupture decreases appositively with the increasing of crack angles until it reaches the 30° then it approximately stabilized till it arrived to 60° and it decreases another time to the end of the graph.

The stress of rupture has been reduced more than 2 times from the 0° crack angle to the biggest crack angle which is 90°.

The stress of rupture progressed with crack angles following the equation below

$F(x)= -2E\text{-}05x^3 + 0.0024x^2 - 0.1147x + 4.1664$.

III.8. Conclusion

- We have seen in this work the different materials to make glass/epoxy and carbon/epoxy composite material and the different steps to produce it.
- We have seen also the manner that those materials react with tensile test and the propagation of the crack in these different specimens with different crack sizes and crack angles.
- Also, we observed from the obtained graphs, how does the stress reacts with strain, taking in consideration the different crack sizes and angles and how does this parameters effects on its progression.
- For stress strain's graphs, we can observe that the progress of the stress passes generally by two regions: the first region is where the stress increases with increase of the strain and the second region is that the stress decreases with increase of the strain.
- From the graphs of the progress of strain with crack sizes and the graphs of the progress of the strain with crack angles we deduce that the deformation decreases with the increase of the crack sizes and the increase of the crack angles
- From the given graphs and information, we deduce that the stress decreases with increase of the crack sizes and angles.

CHAPTER IV

NUMERICAL SIMULATION

IV.1. Introduction

ANSYS is a general purpose finite element modeling package for numerically solving a wide variety of mechanical problems. These problems include: static/dynamic structural analysis (both linear and non-linear), heat transfer and fluid problems, as well as acoustic and electro-magnetic problems.

In general, a finite element solution may be broken into the following three stages. This is a general guideline that can be used for setting up any finite element analysis.

1. Preprocessing: defining the problem; the major steps in preprocessing are given below:

- Define key points/lines/areas/volumes
- Define element type and material/geometric properties
- Mesh lines/areas/volumes as required

The amount of detail required will depend on the dimensionality of the analysis (i.e. 1D, 2D, axi-symmetric, 3D).

2. Solution: assigning loads, constraints and solving; here we specify the loads (point or pressure), stress (translational and rotational) and finally solve the resulting set of equations.
3. Post processing: further processing and viewing of the results; in this stage one may wish to see:

- Lists of nodal displacements
- Element forces and moments
- Deflection plots
- Stress contour diagrams

IV.2. Definition of ANSYS

ANSYS is the name commonly used for ANSYS mechanical, general-purpose finite element analysis (FEA) computer aided engineering software tools developed by ANSYS Inc. ANSYS mechanical is a self-contained analysis tool incorporating pre-processing such as creation of geometry and meshing. Solver and post processing modules in a unified graphical user interface. ANSYS is a general-purpose finite element-modeling package for numerically solving a wide variety of mechanical and other engineering problems. These problems include linear structural and contact analysis that is non-linear. Among the various FEA package, in this work ANSYS is used to perform the analysis.

IV.3. FEA of specimen using ANSYS WORKBENCH

The following steps are used in the solution procedure using ANSYS Workbench.

- The geometry of the specimen to be analyzed is made by ANSYS Workbench
- Material for specimen, wheel should be defined, material properties such as Young's modulus and Poisson's ration should be specified.
- Material strength such as ultimate tensile and yield strength need to be defined. Density of the material is required to be defined.
- Connection between wheel and pinion need to be defined.
- Meshing the three- dimensional gear model.
- The boundary conditions and external loads are applied.
- The solution is generated based on the previous input parameters.
- Finally, the solution is viewed in a variety of displays.

IV.4. Simulation process

IV.4.1. ACP (pre)

This section describes the composite modeling techniques for the use of shell, solid, and solid-shell elements.

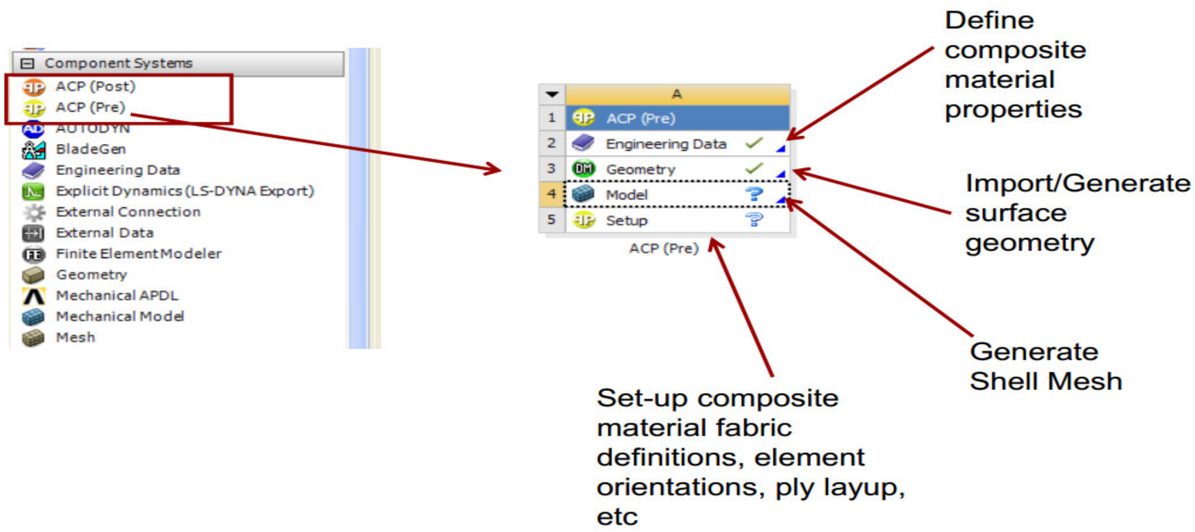

Figure IV.1 ACP (pre) ANSYS window information

IV.4.2. Engineering data

A part's response to etermined the material properties assigned to the part. Here we choose the specimen material and where we can edit the properties of it's like we see in the figures bellow.

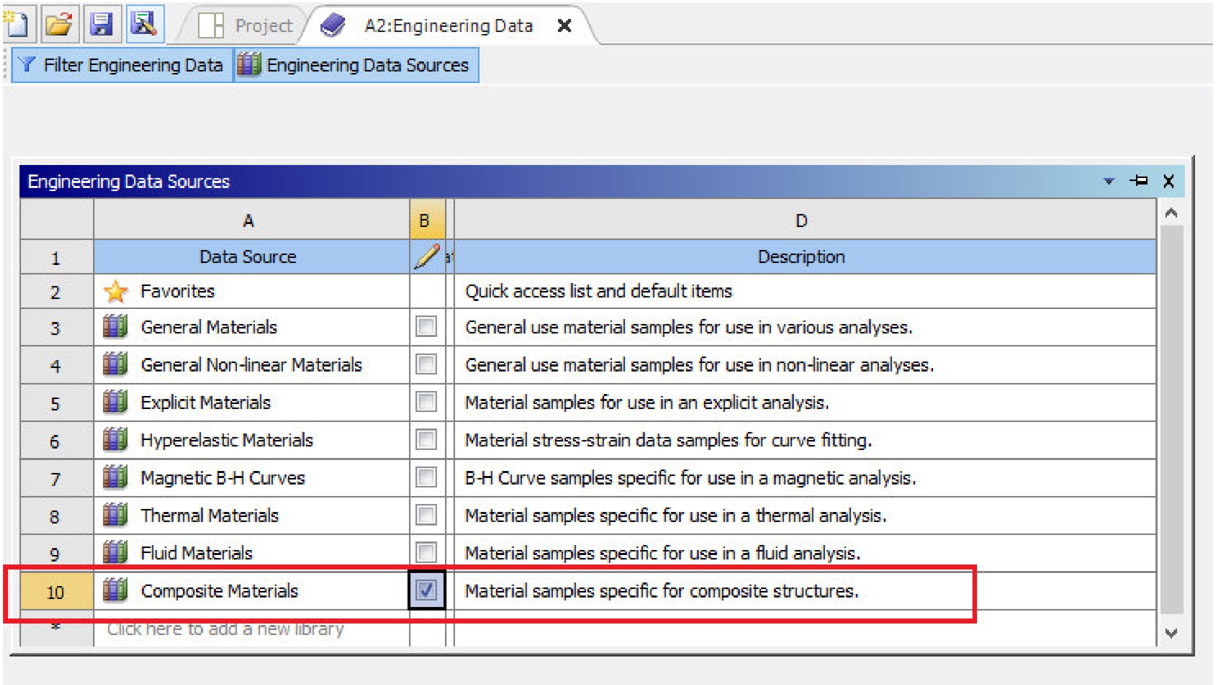

	A	B	D
1	Data Source		Description
2	Favorites		Quick access list and default items
3	General Materials	☐	General use material samples for use in various analyses.
4	General Non-linear Materials	☐	General use material samples for use in non-linear analyses.
5	Explicit Materials	☐	Material samples for use in an explicit analysis.
6	Hyperelastic Materials	☐	Material stress-strain data samples for curve fitting.
7	Magnetic B-H Curves	☐	B-H Curve samples specific for use in a magnetic analysis.
8	Thermal Materials	☐	Material samples specific for use in a thermal analysis.
9	Fluid Materials	☐	Material samples specific for use in a fluid analysis.
10	Composite Materials	☑	Material samples specific for composite structures.
*	Click here to add a new library		

Figure IV.2 Engineering Data Sources

Material does not need to be assigned to bodies in Mechanical. Material assignment is done in ACP .

All materials in Engineering Data are brought into ACP.

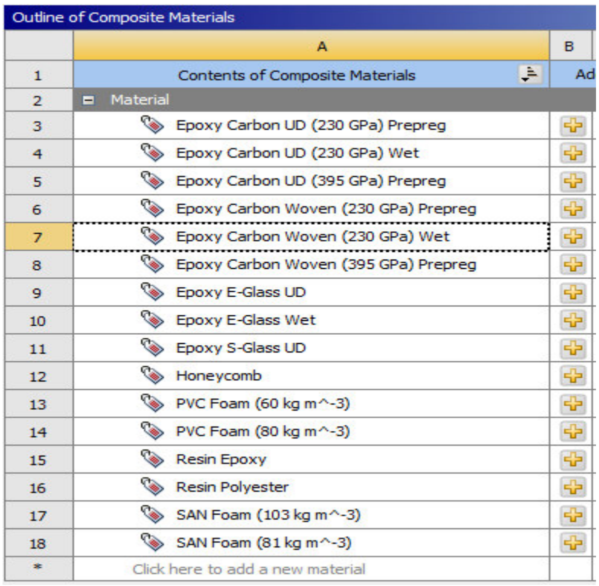

	A	B
1	Contents of Composite Materials	Ad
2	Material	
3	Epoxy Carbon UD (230 GPa) Prepreg	
4	Epoxy Carbon UD (230 GPa) Wet	
5	Epoxy Carbon UD (395 GPa) Prepreg	
6	Epoxy Carbon Woven (230 GPa) Prepreg	
7	Epoxy Carbon Woven (230 GPa) Wet	
8	Epoxy Carbon Woven (395 GPa) Prepreg	
9	Epoxy E-Glass UD	
10	Epoxy E-Glass Wet	
11	Epoxy S-Glass UD	
12	Honeycomb	
13	PVC Foam (60 kg m^-3)	
14	PVC Foam (80 kg m^-3)	
15	Resin Epoxy	
16	Resin Polyester	
17	SAN Foam (103 kg m^-3)	
18	SAN Foam (81 kg m^-3)	
*	Click here to add a new material	

Figure IV.3 outline of composite materials in engineering data source

IV.4.3. Geometry

The geometry of specimen was created with ANSYS Workbench for carrying out static structural analysis which is shown in figures bellow

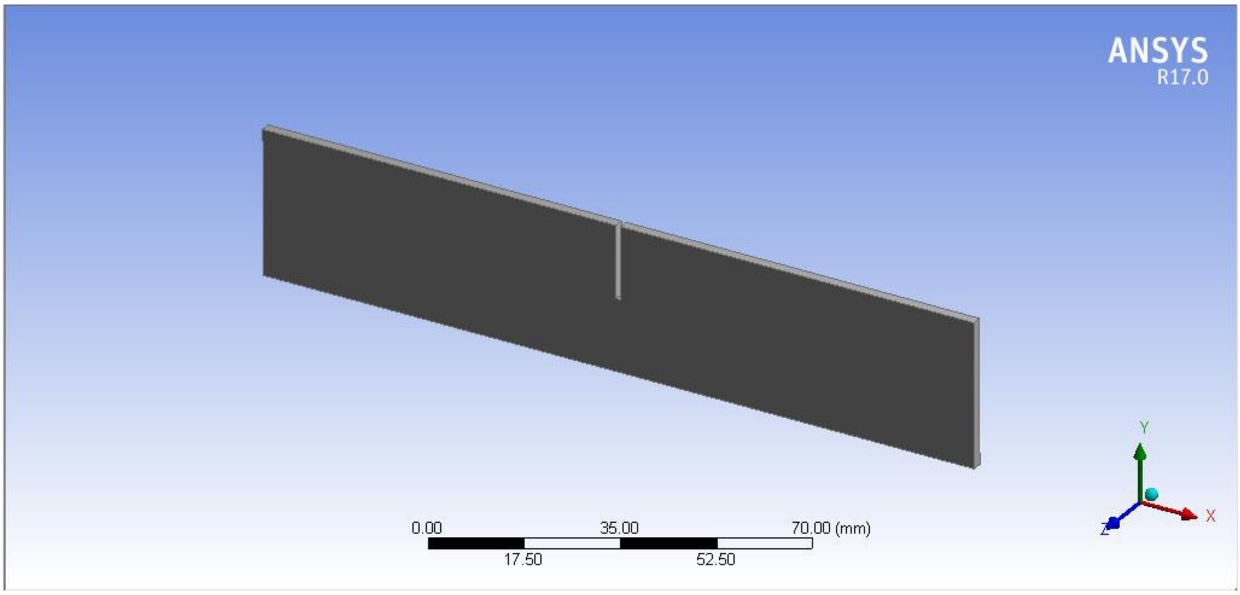

Figure IV.4 specimen with crack

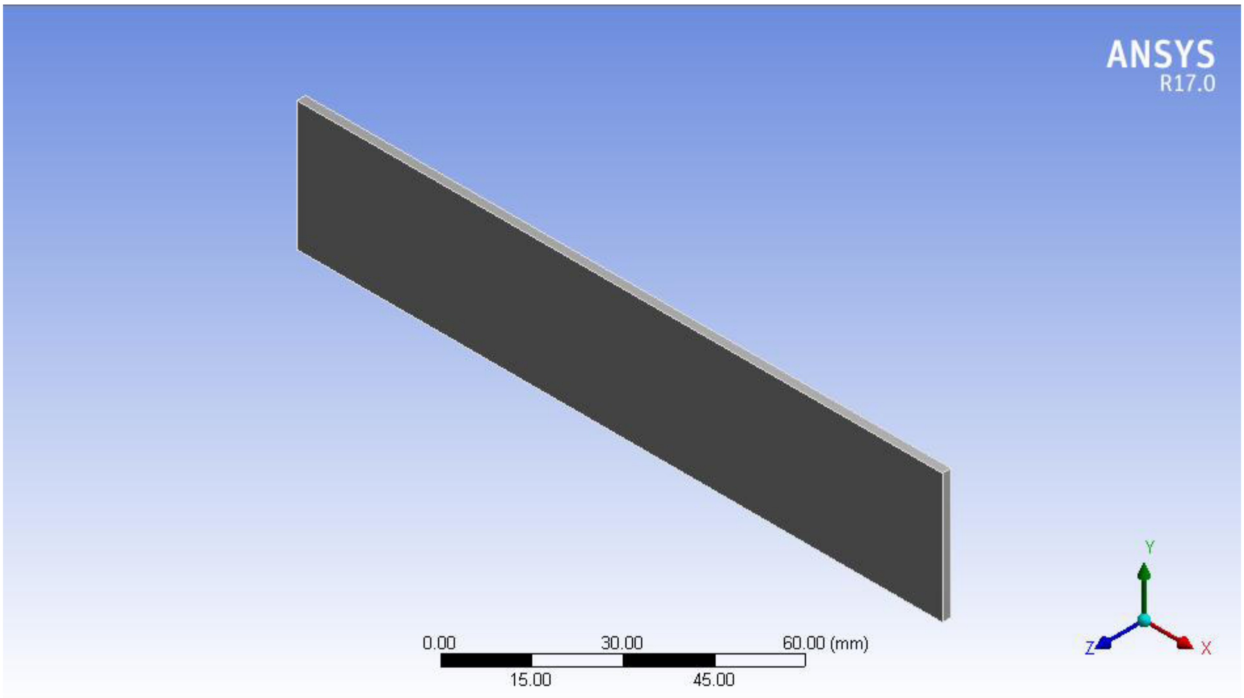

Figure IV.5 specimen without crack

IV.4.4. Meshing

Here the specimen is meshed in order to define the elements size . Mapped face meshing is done on specimen which is shown in figures bellow

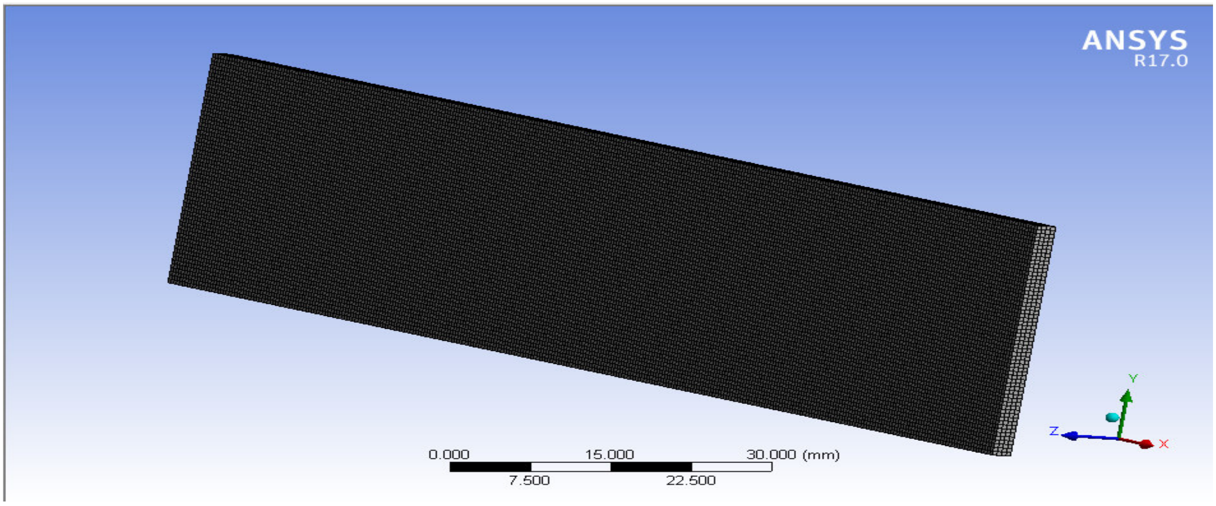

Figure IV.6 a meshed specimen (without crack)

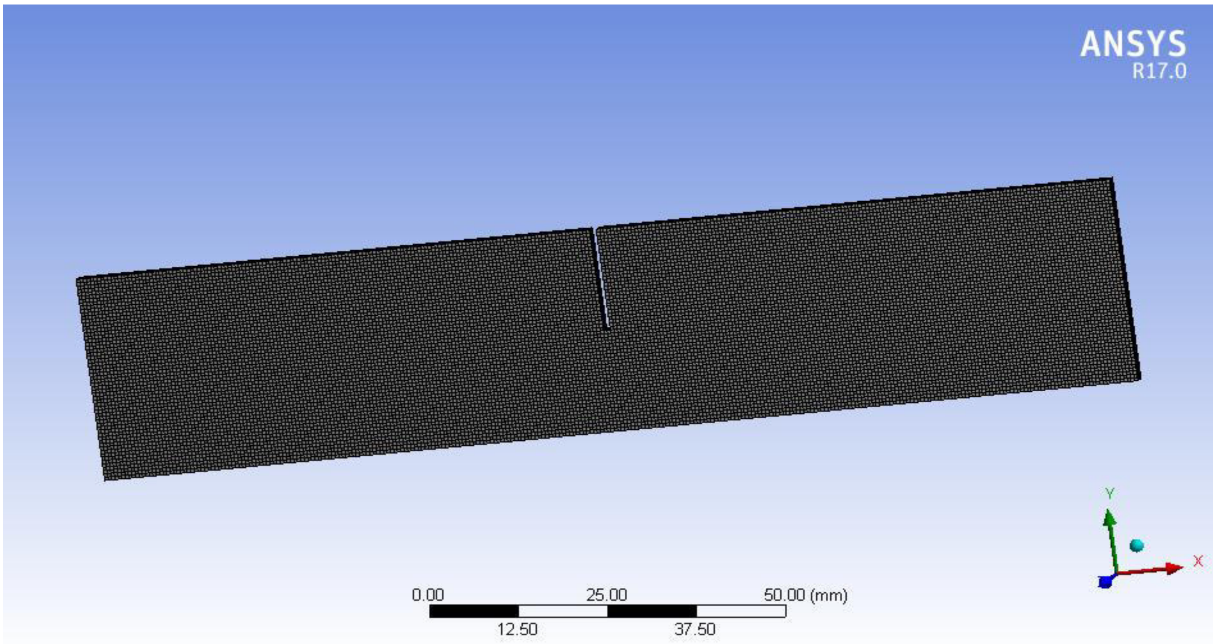

Figure IV.7 a meshed specimen (with crack)

- Type of mesh: quadratic
- Size: 1mm
- Nodes: 50400
- Elements: 9000

IV.4.5. Setup

Once shell mesh is generated and materials defined, ACP can be started by right click: Edit…

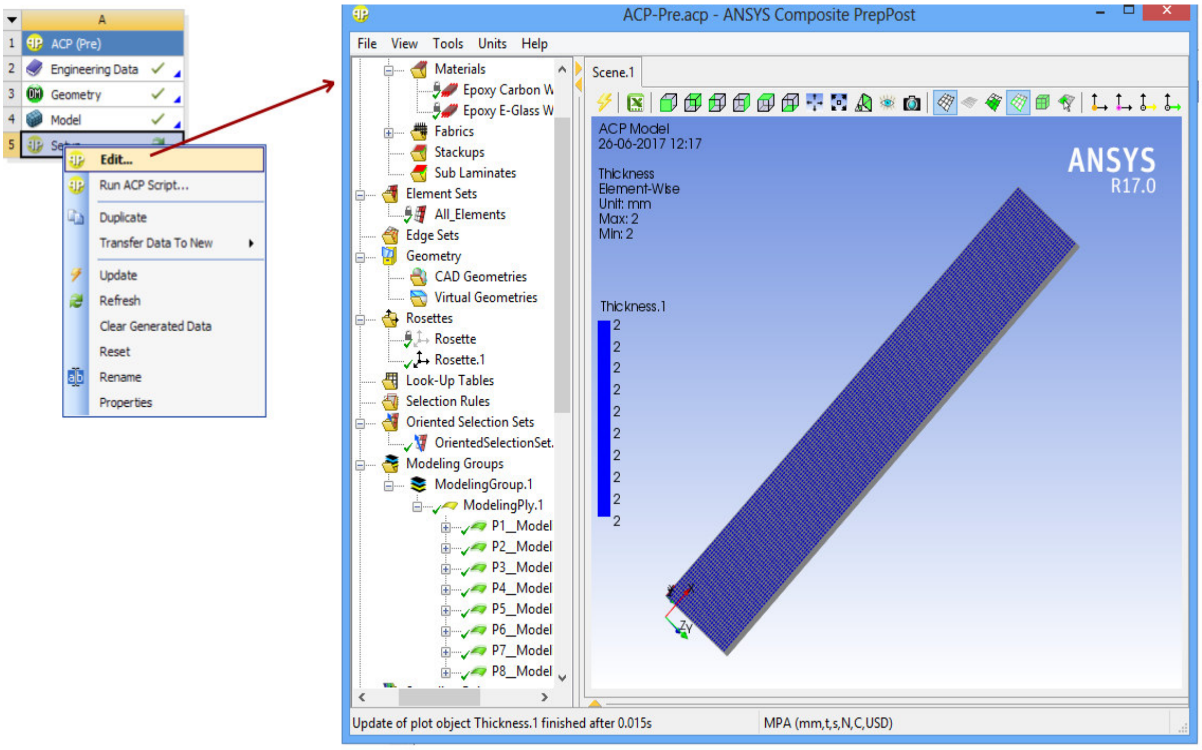

Figure IV.8 ACP Setup window

Once the model is setup in APC(Pre) it can be linked to whatever type of analyses we need to Solve.

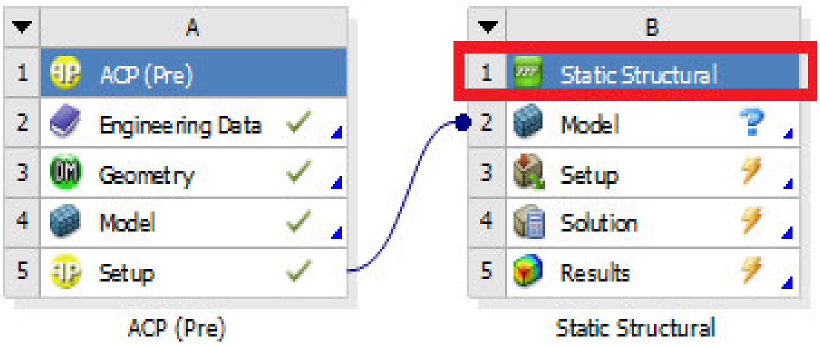

Figure IV.9 static structural as new window

IV.4.6. load and boundary conditions

The boundary condition such as fixed support and pressure applied in order to determine the solution information which is shown figures bellow.

(we introduced a ‘‘-’’ sign in the value of pressure to obtain a tensile force)

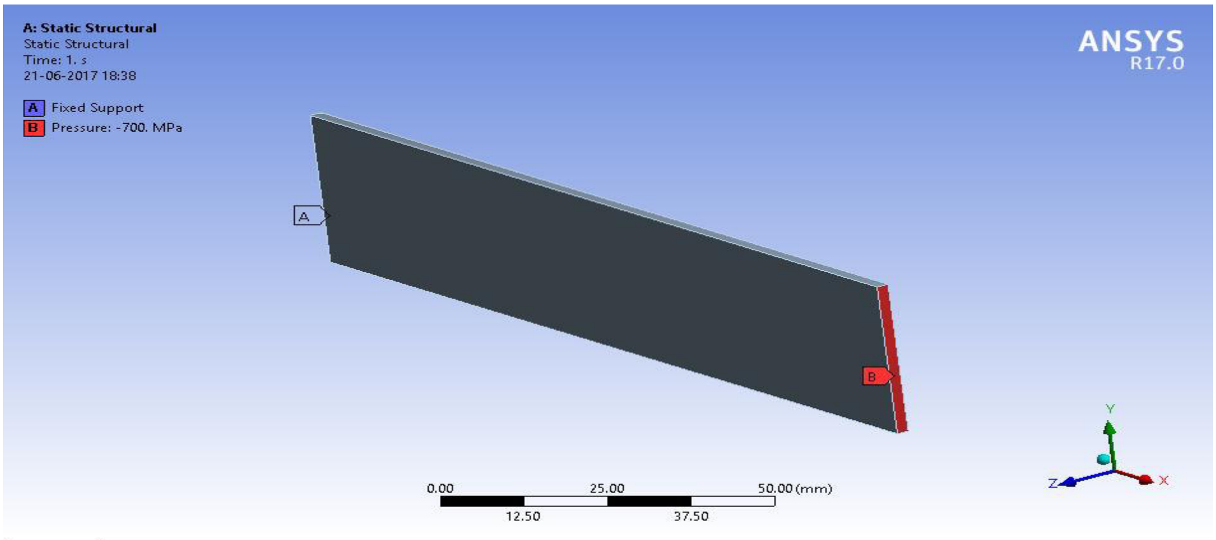

Figure IV.10 load and boundary condition (specimen without crack)

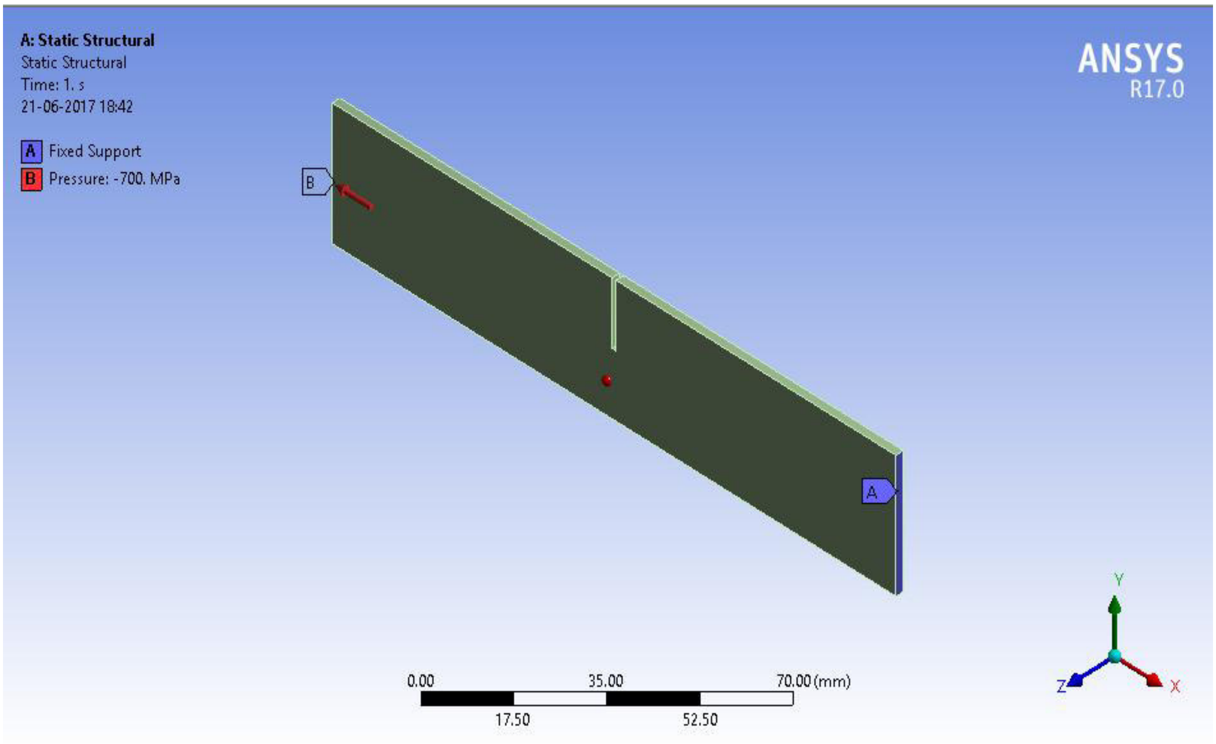

Figure IV.11 load and boundary condition (specimen with crack)

IV.5 Results and discussion of specimen in different crack angle

IV.5.1 Results for a carbon/epoxy specimen (without crack)

a) Total deformation

Total deformation of carbon epoxy specimen is 5.9501 mm which is shown in figure bellow

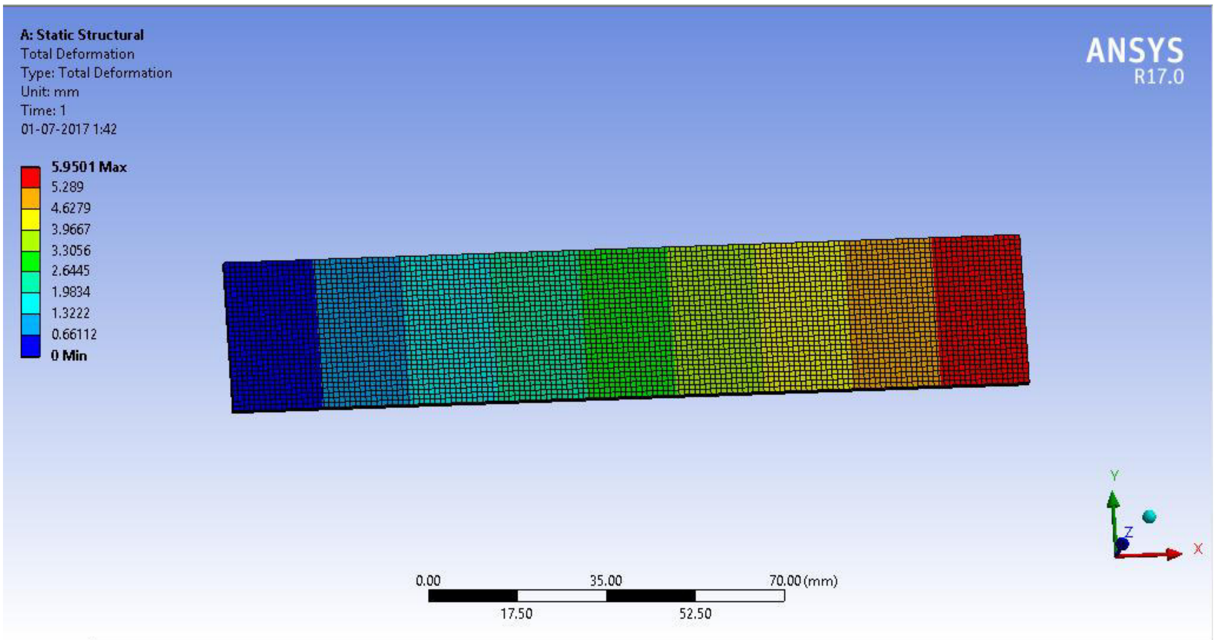

Figure IV.12 total deformation of carbon/epoxy specimen (without crack)

b) Maximum principal stress

Maximum principal stress acting on specimen is 671.67 MPa , which is shown in figure bellow

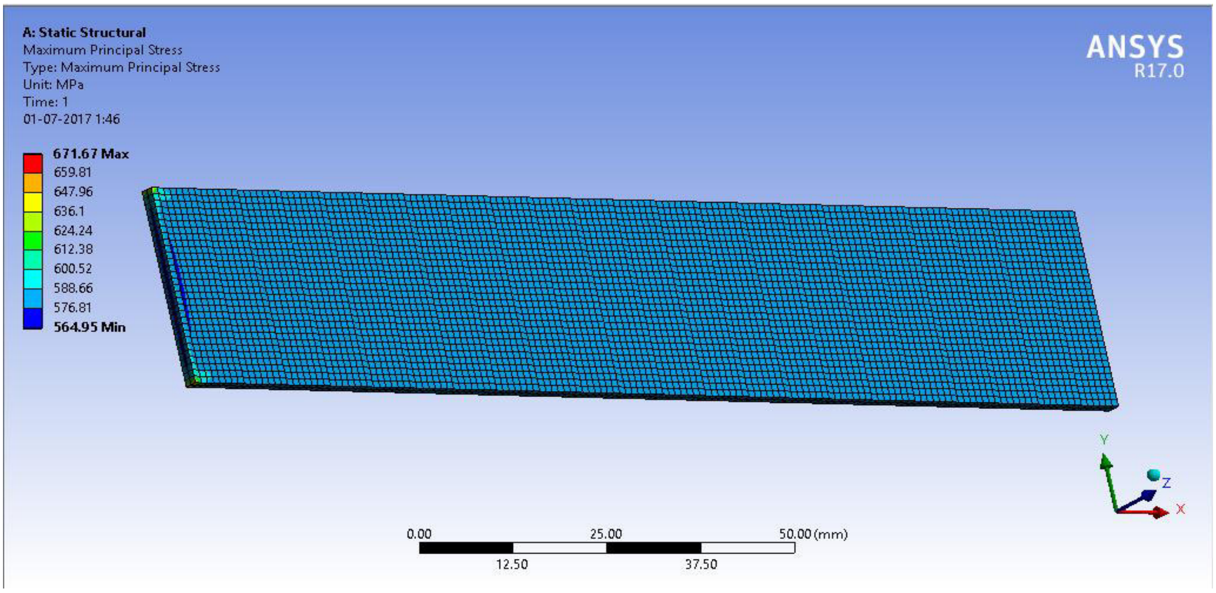

Figure IV.13 Maximum principal stress of carbon/epoxy specimen (without crack)

c) Normal elastic strain

Normal elastic strain acting on the specimen is 0.04507 which is shown in figure bellow

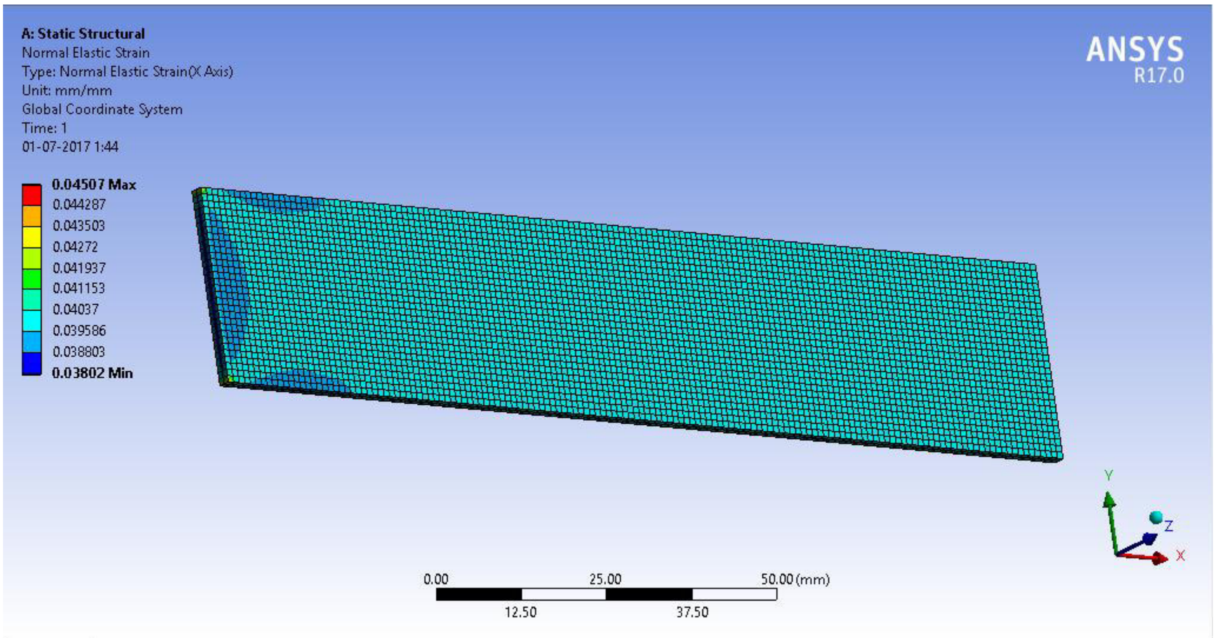

Figure IV.14 normal elastic strain of carbon/epoxy specimen (without crack)

IV.5.2 Results for a carbon/epoxy specimen with a=15mm & θ=90° crack

a) Total deformation

Total deformation of carbon epoxy specimen is 2.9308 mm which is shown in figure bellow

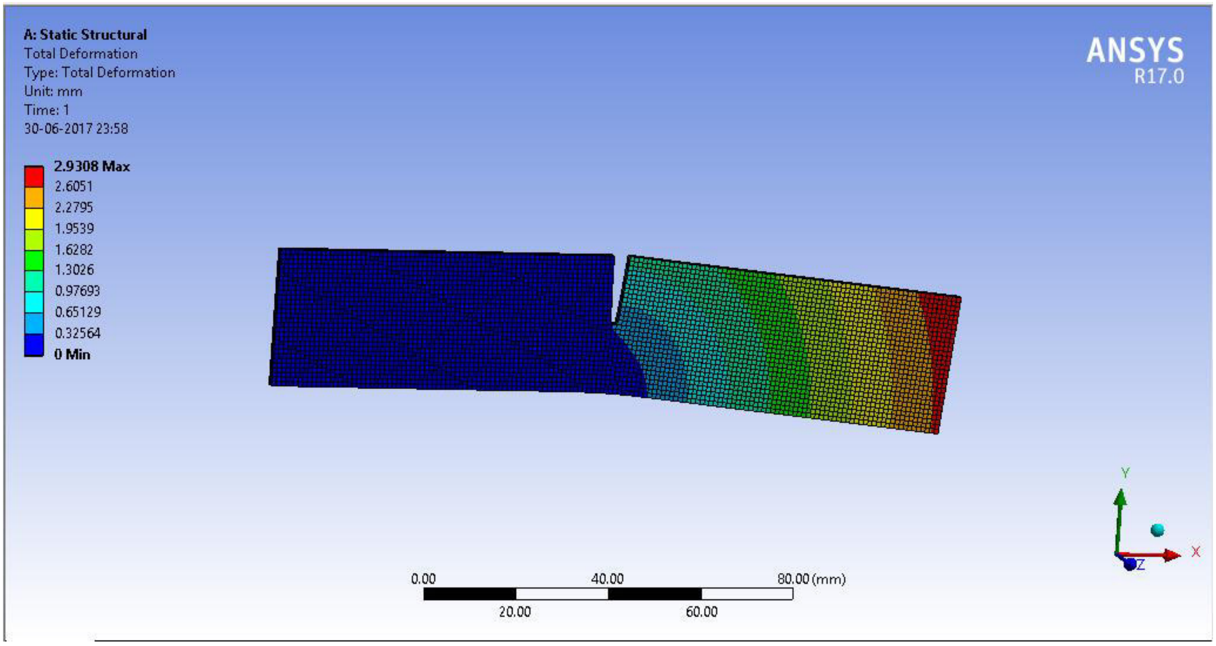

Figure IV.15 total deformation of carbon/epoxy specimen (with a=15mm & θ=90° crack)

b) Maximum principal stress

Maximum principal stress acting on specimen is 87.857 MPa , which is shown in figure bellow

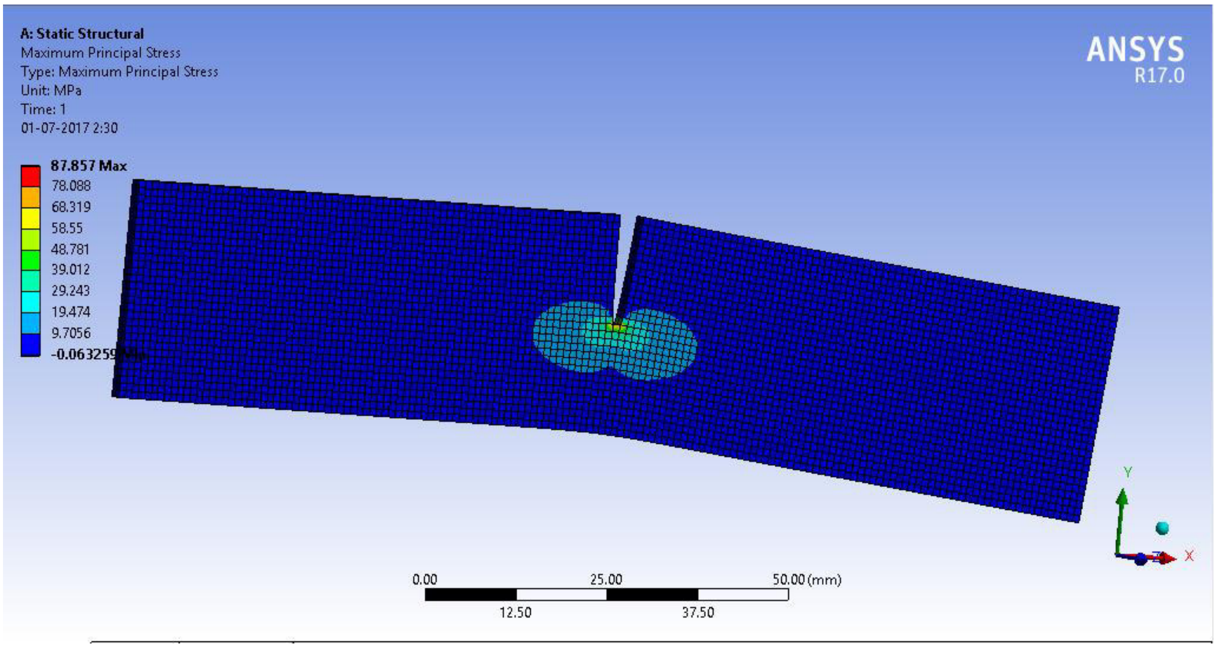

Figure IV.16 Maximum principal stress of carbon/epoxy specimen (with a=15mm & θ=90° crack)

c) Normal elastic strain

Normal elastic strain acting on the specimen is 0.014734 which is shown in figure bellow

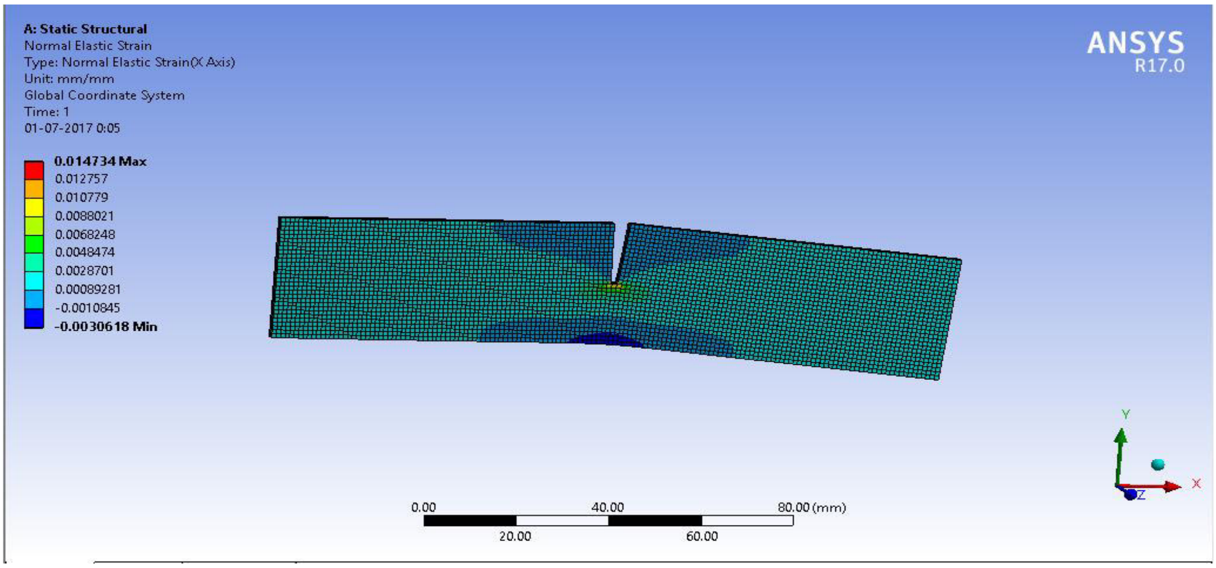

Figure IV.17 normal elastic strain of carbon/epoxy specimen (with a=15mm & θ=90° crack)

IV.5.3 Results for a carbon/epoxy specimen (with a=15mm & crack θ=60°)

a) Total deformation

Total deformation of carbon epoxy specimen is 3.1568 mm which is shown in figure bellow

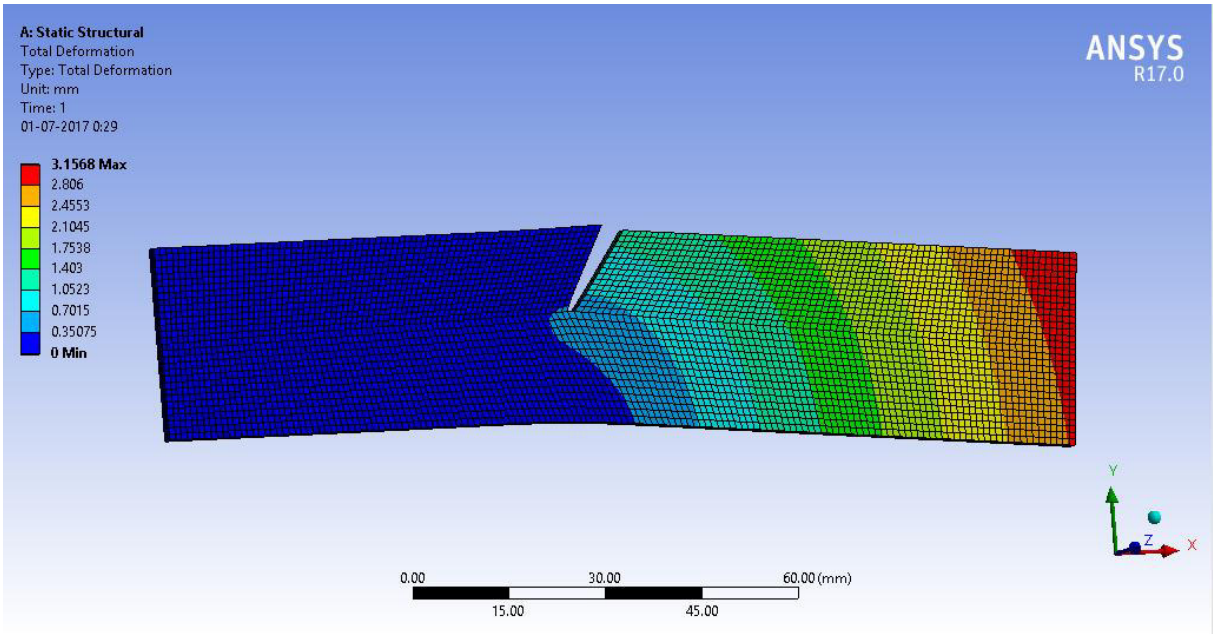

Figure IV.18 total deformation of carbon/epoxy specimen (with a=15mm & θ=60° crack)

b) Maximum principal stress

Maximum principal stress acting on specimen is 187.46 MPa , which is shown in figure bellow

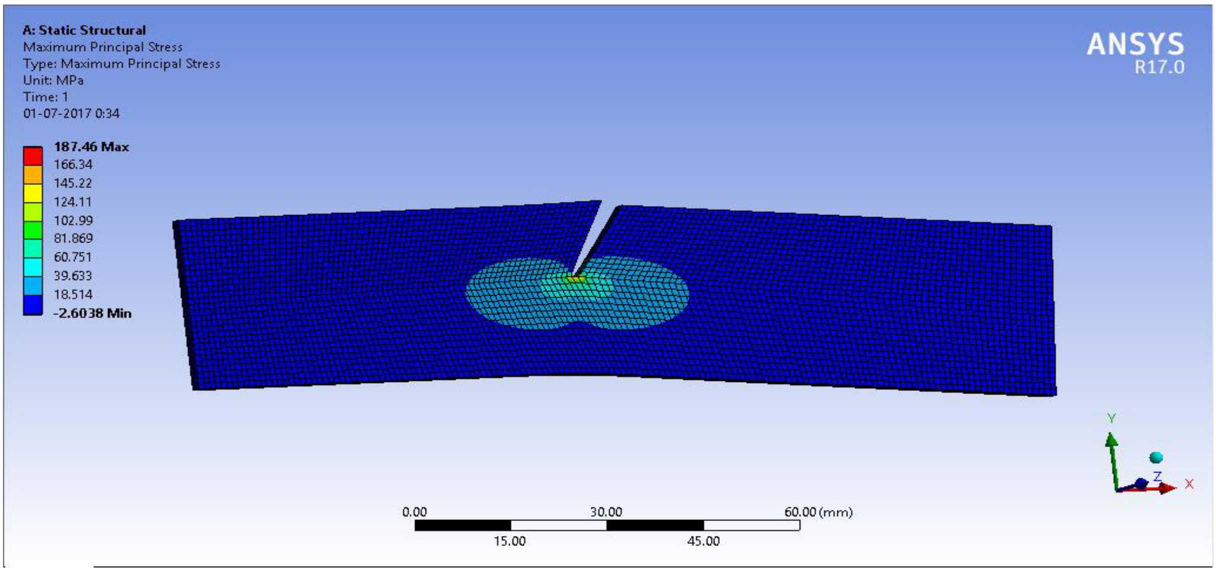

Figure IV.19 Maximum principal stress of carbon/epoxy specimen (with a=15mm & θ=60° crack)

c) Normal elastic strain

Normal elastic strain acting on the specimen is 0.021272, which is shown in figure bellow

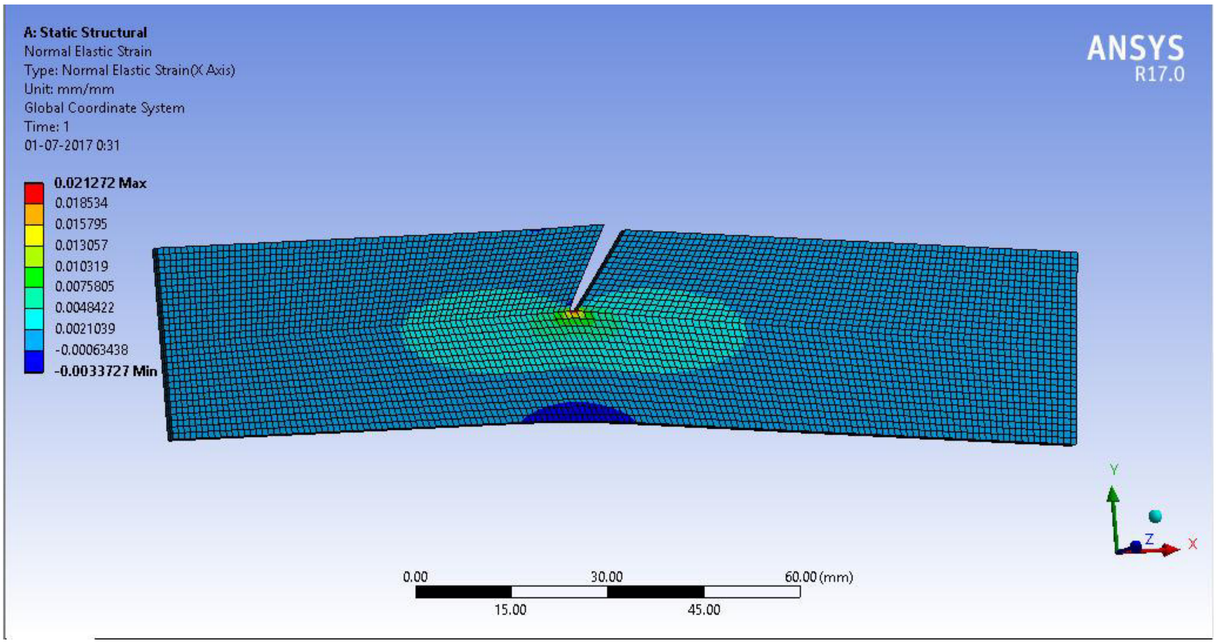

Figure IV.20 normal elastic strain of carbon/epoxy specimen (with a=15mm & θ=60° crack)

IV.5.4 Results for a carbon/epoxy specimen with a=15mm & θ=45°crack

a) Total deformation

Total deformation of carbon epoxy specimen is 3.8097 mm which is shown in figure bellow

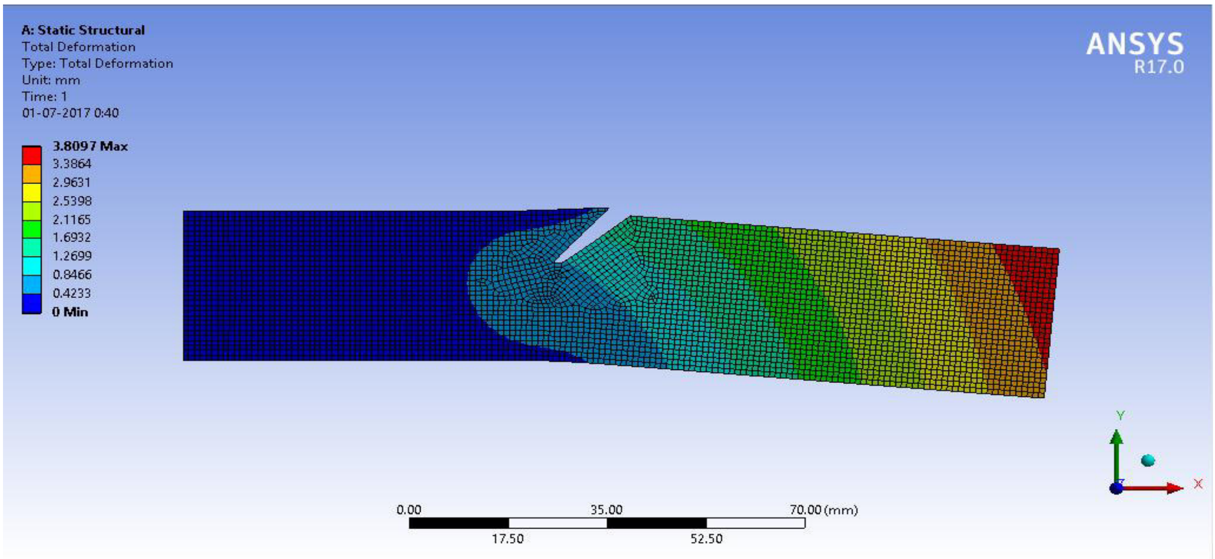

Figure IV.21 total deformation of carbon/epoxy specimen (with a=15mm & θ=45° crack)

b) Maximum principal stress

Maximum principal stress acting on specimen is 170.15 MPa , which is shown in figure bellow

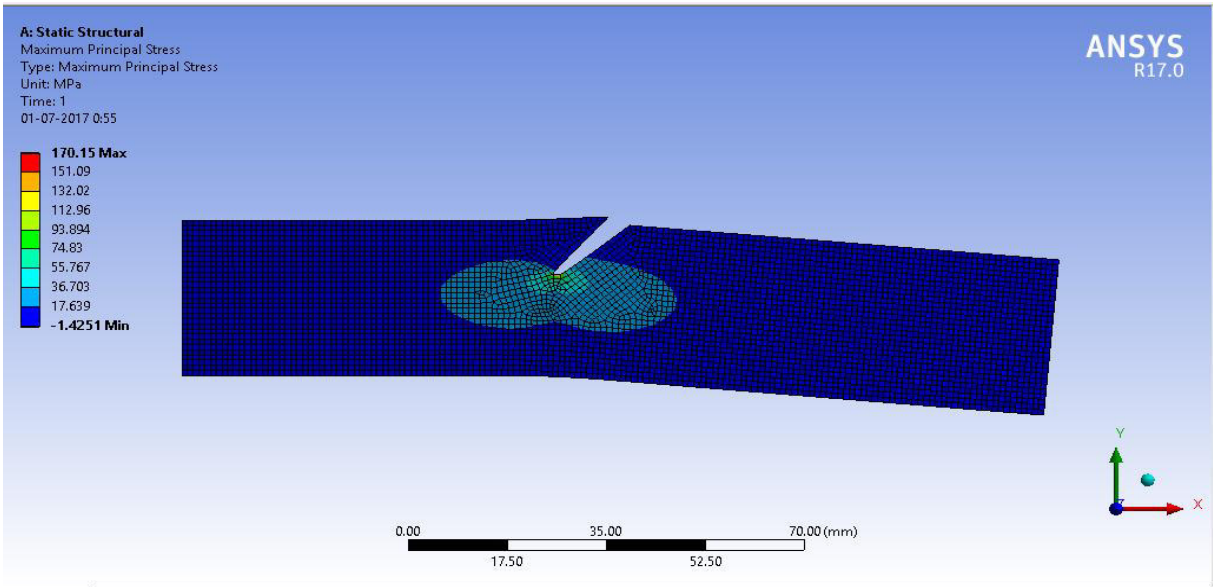

Figure IV.22 Maximum principal stress of carbon/epoxy specimen (with a=15mm & θ=45°crack)

c) Normal elastic strain

Normal elastic strain acting on the specimen is 0.025224, which is shown in figure bellow

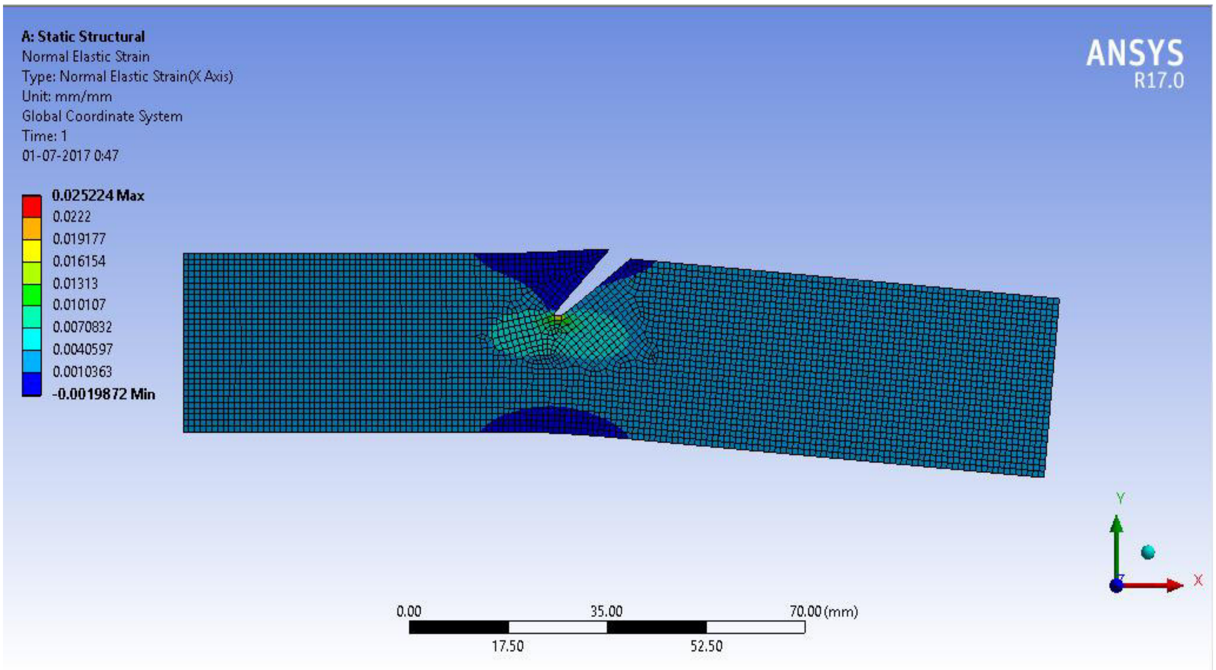

Figure IV.23 normal elastic strain of carbon/epoxy specimen (with a=15mm & θ=45° crack)

IV.5.5 Results for a carbon/epoxy specimen with a=15mm & θ=30° crack

a) Total deformation

Total deformation of carbon epoxy specimen is 3.2203 mm which is shown in figure bellow

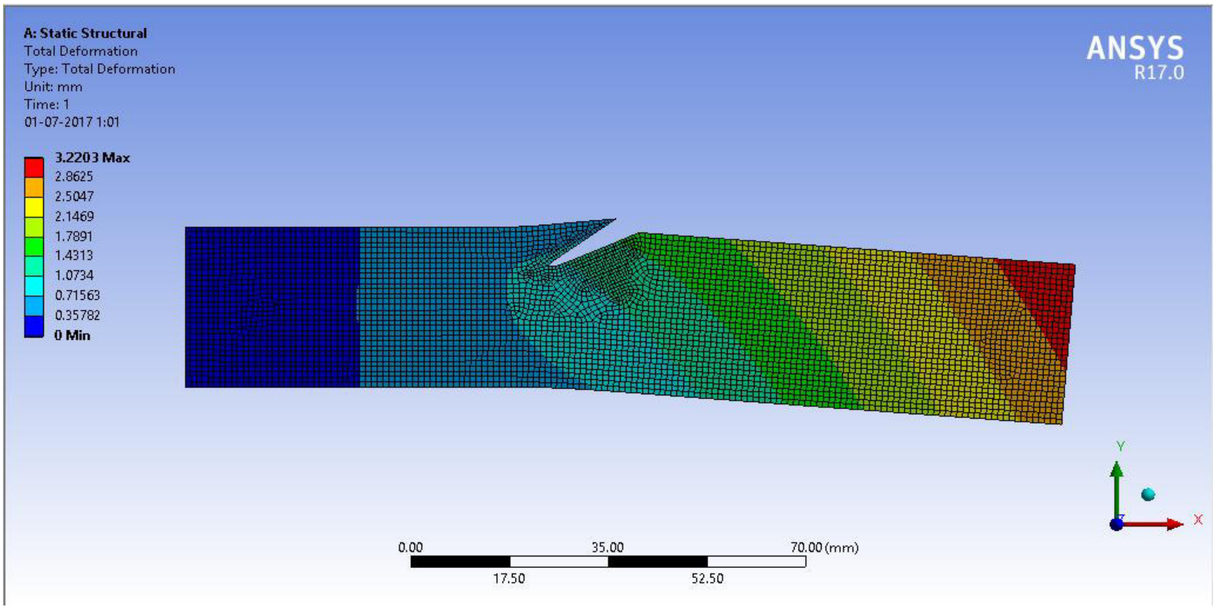

Figure IV.24 total deformation of carbon/epoxy specimen (with a=15mm & θ=30° crack)

b) Maximum principal stress

Maximum principal stress acting on specimen is 196.54 MPa , which is shown in figure bellow

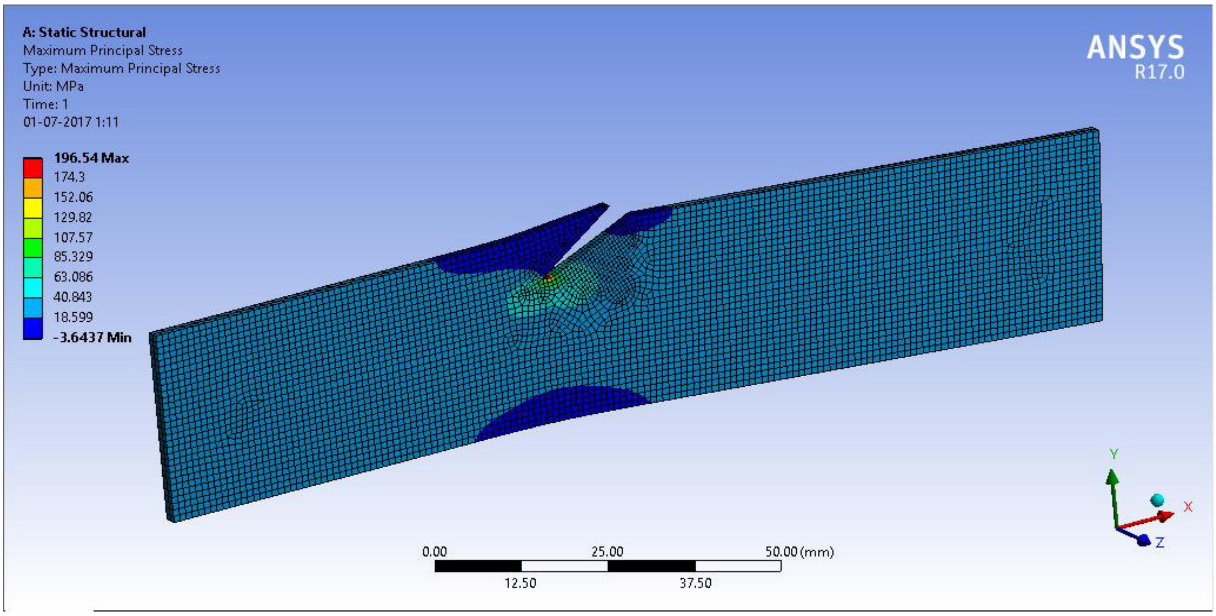

Figure IV.25 Maximum principal stress of carbon/epoxy specimen (with a=15mm & θ=30°crack)

c) Normal elastic strain

Normal elastic strain acting on the specimen is 0.002024, which is shown in figure bellow

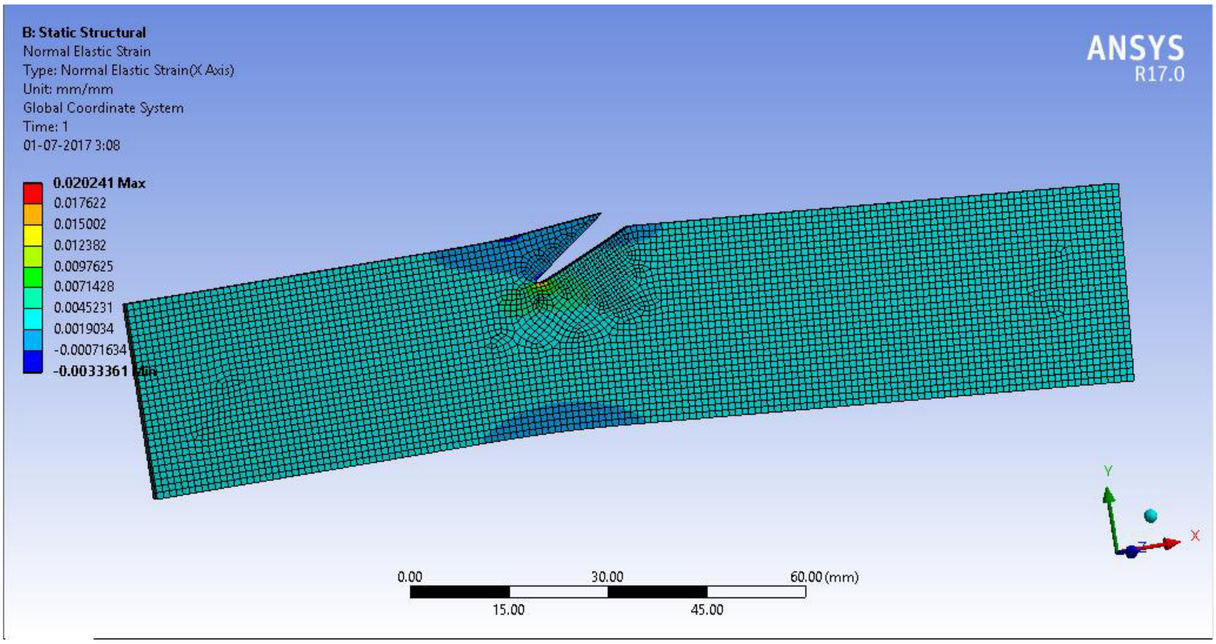

Figure IV.26 normal elastic strain of carbon/epoxy specimen (with a=15mm & θ=30° crack)

Note:

We didn't make the result of glass/epoxy cracked specimens with different angles because we have the same work, but we changed the material of specimens.

IV.5.6 Discussion

a) Total deformation [mm]

Table IV.1 total deformation of cracked specimen in different angle of crack

	0°	30°	45°	60°	90°
Carbon/epoxy	5.9501	3.2203	3.8097	3.1568	2.9308
Glass/epoxy	5.6452	1.6319	1.5908	2.6401	2.6612

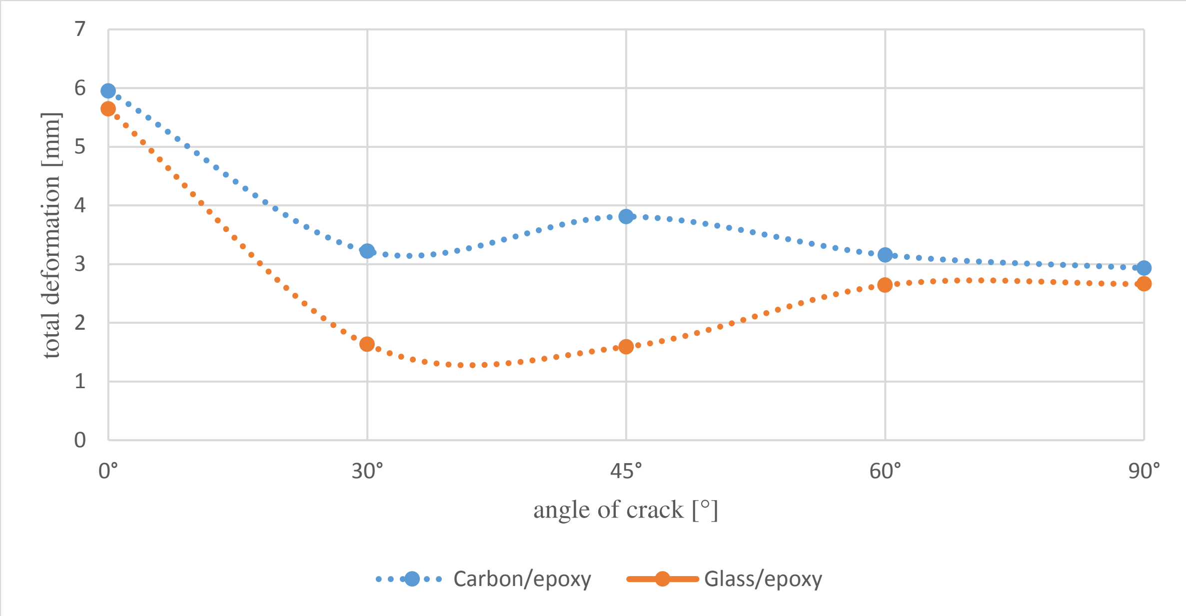

Figure IV.27 total deformation for carbon/epoxy & glass/epoxy specimens under tensile

Test with different angle of crack

The graph IV.27 represent the curves of total deformation of carbon/epoxy & glass/epoxy specimen under tensile test vs angle of crack, we can clearly see that the total deformation in both cases decreases with the angle of crack decrease.

b) Maximum principal stress [MPa]

Table IV.2 total maximum principle stress of cracked specimen in different angle of crack

	0°	30°	45°	60°	90°
Carbon/epoxy	671.67	196.54	170.15	187.46	87.857
Glass/epoxy	249.62	89.46	44.78	62.58	79.15

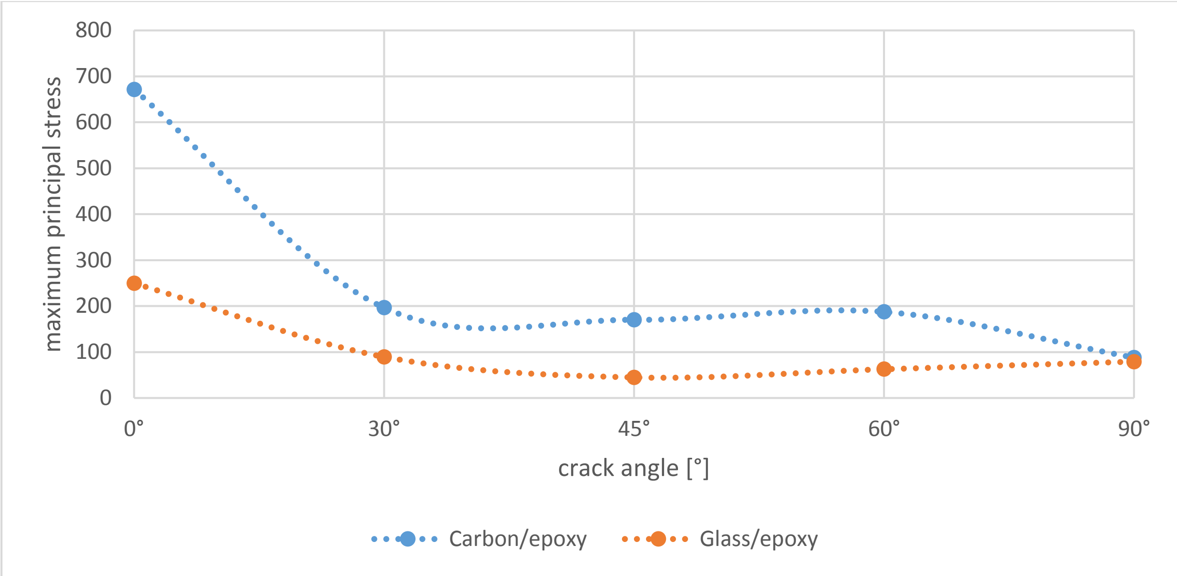

Figure IV.28 Maximum principal stress of carbon/epoxy &glass/epoxy specimen vs different angle of crack under tensile test

The graph IV.28 represent the curves of Maximum principal stress of carbon/epoxy & glass/epoxy specimen under tensile test, we can clearly see that the maximum principal stress decrease with the angle of crack decrease

c) Normal elastic strain

Table IV.3 total Normal elastic strain cracked specimen in different angle of crack

	0°	30°	45°	60°	90°
Carbon/epoxy	0.0450	0.02024	0.02522	0.02127	0.01473
Glass/epoxy	0.0386	0.0176	0.0101	0.0178	0.0086

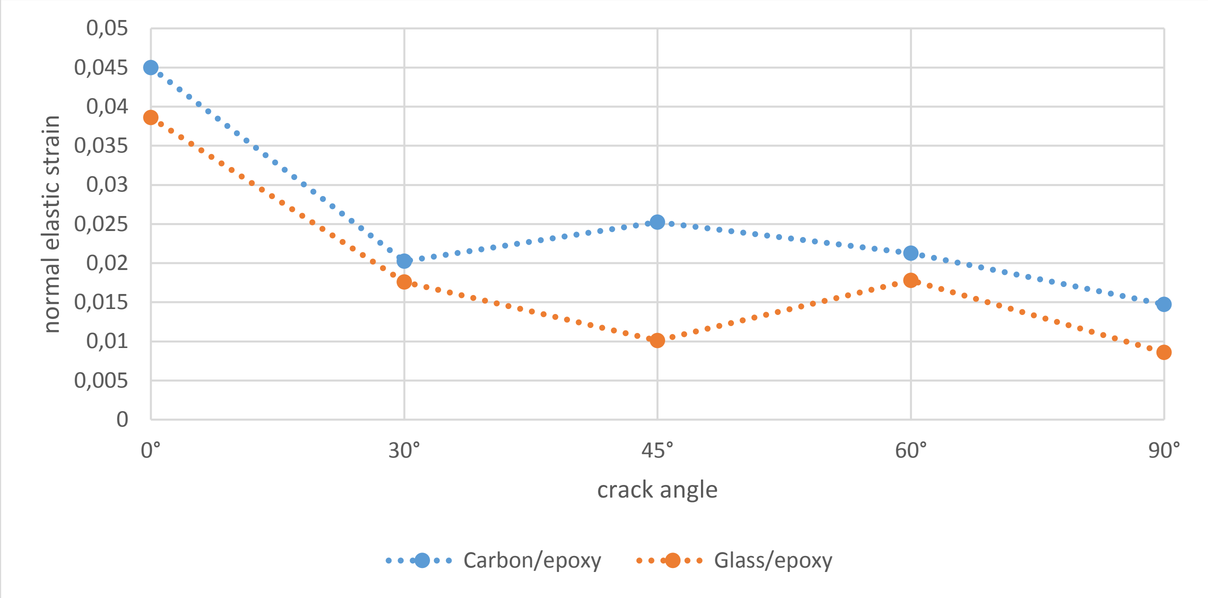

Figure IV.29 Normal elastic strain carbon/epoxy & glass/epoxy specimens under tensile test with different angle of crack

The graph IV.29 illustrate the values of the normal elastic strain evolution according to the different crack angle. we observe that the normal elastic strain decreases when the angle of crack decrease

IV.6 Results and discussion of specimen in different crack size

IV.6.1 Results for a glass/epoxy specimen with a=10mm & θ= 90° crack

a) Total deformation

Total deformation of glass epoxy specimen is 2.8083 mm which is shown in figure bellow

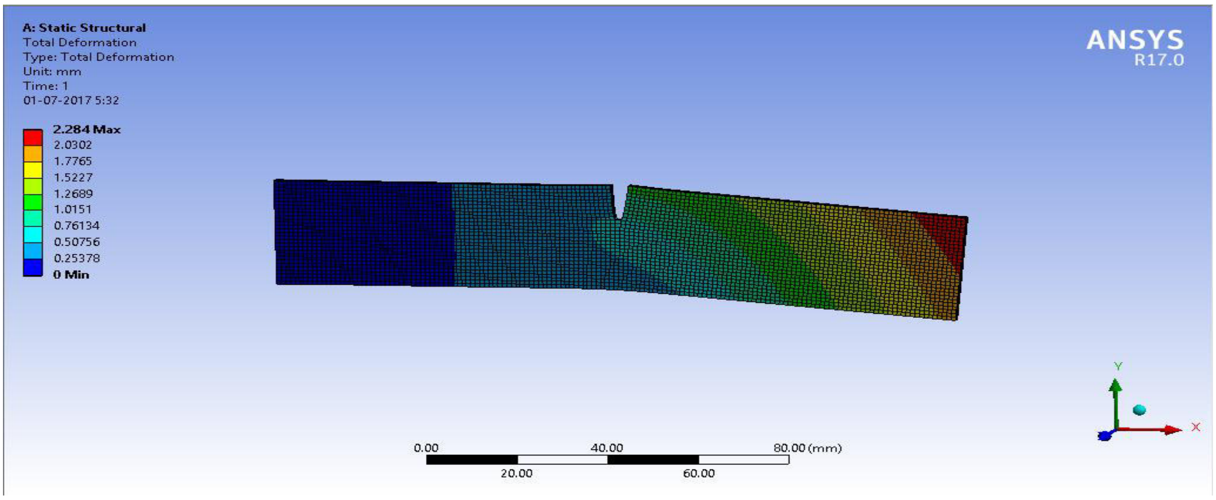

Figure IV.30 total deformation of glass /epoxy specimen (with a=10mm & θ=90° crack)

b) Maximum principal stress

Maximum principal stress acting on specimen is 69.664 MPa , which is shown in figure bellow

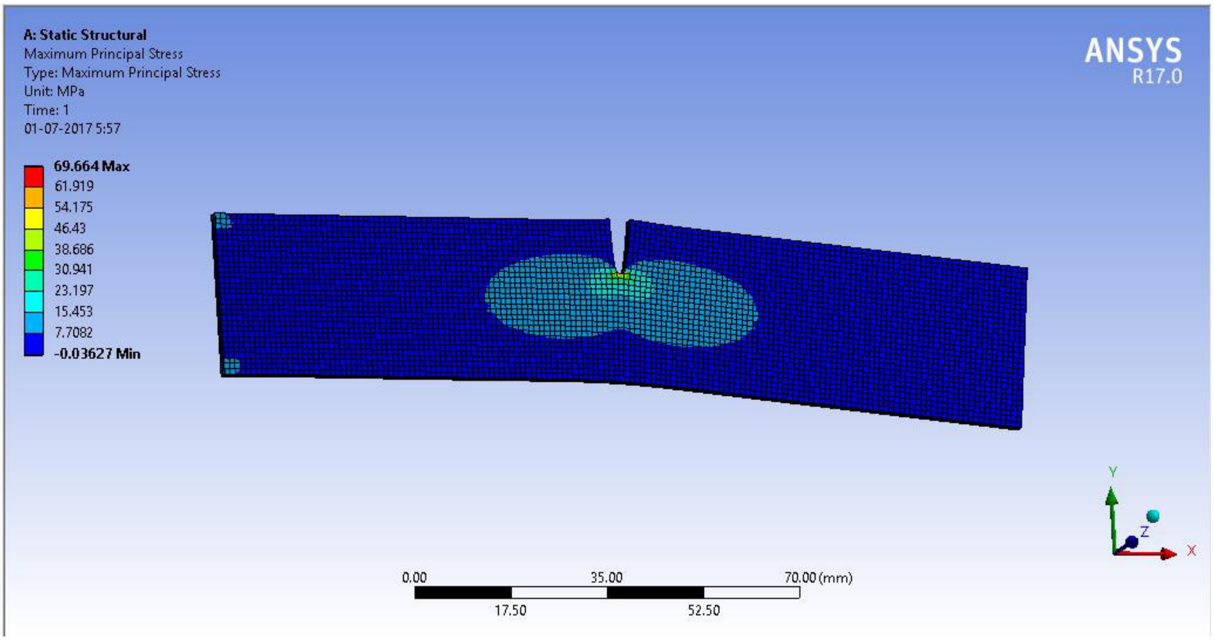

Figure IV.31 Maximum principal stress of glass /epoxy specimen (with a=10mm & θ=90° crack)

c) Normal elastic strain

Normal elastic strain acting on the specimen is 0.014592 which is shown in figure bellow

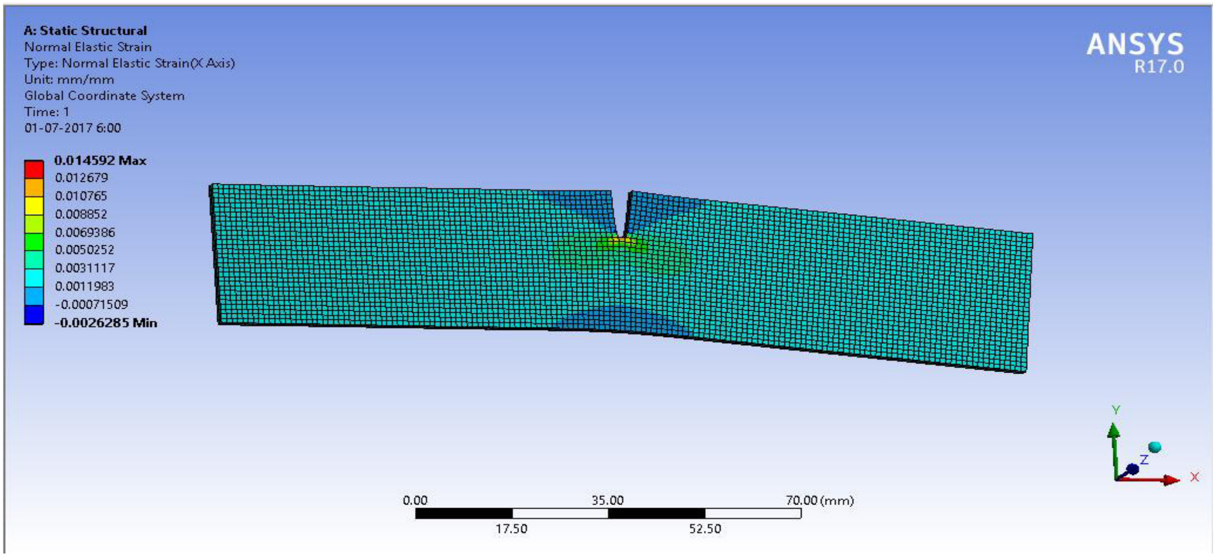

Figure IV.32 normal elastic strain of glass /epoxy specimen (with a=10mm & θ=90° crack)

IV.6.2 Results for a glass/epoxy specimen with a=5mm & θ=90° crack

a) Total deformation

Total deformation of glass epoxy specimen is 3.3837 mm which is shown in figure bellow

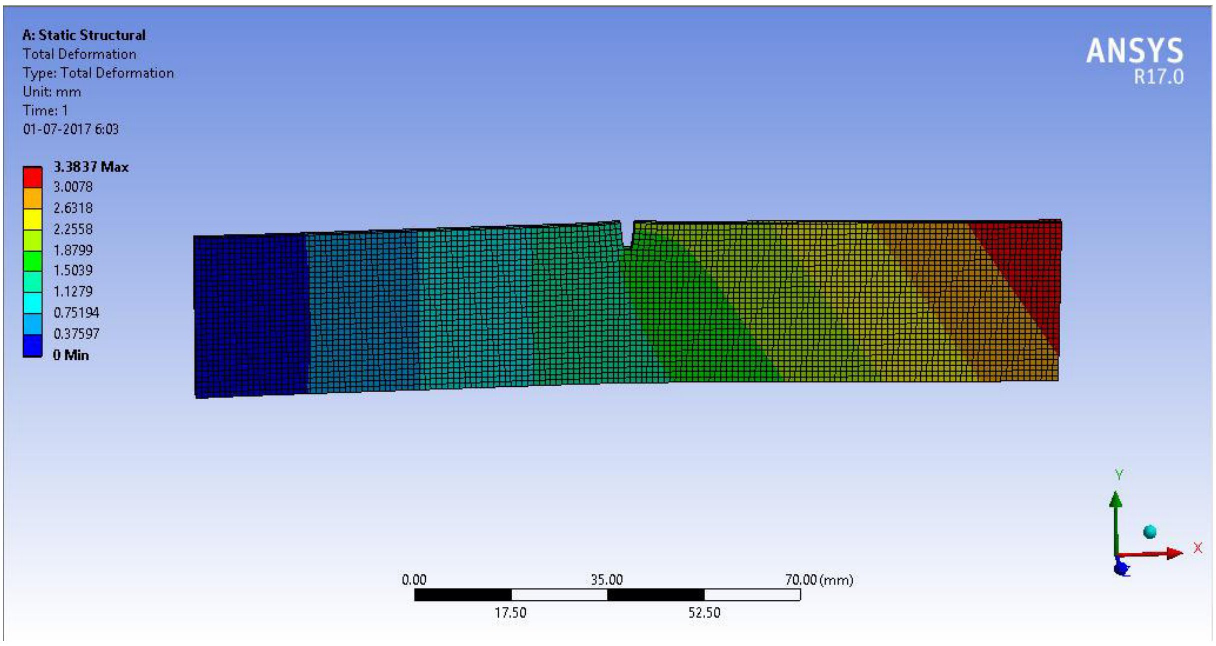

Figure IV.33 total deformation of glass /epoxy specimen (with a=5mm & θ=90° crack)

b) Maximum principal stress

Maximum principal stress acting on specimen is 138.69 MPa , which is shown in figure bellow

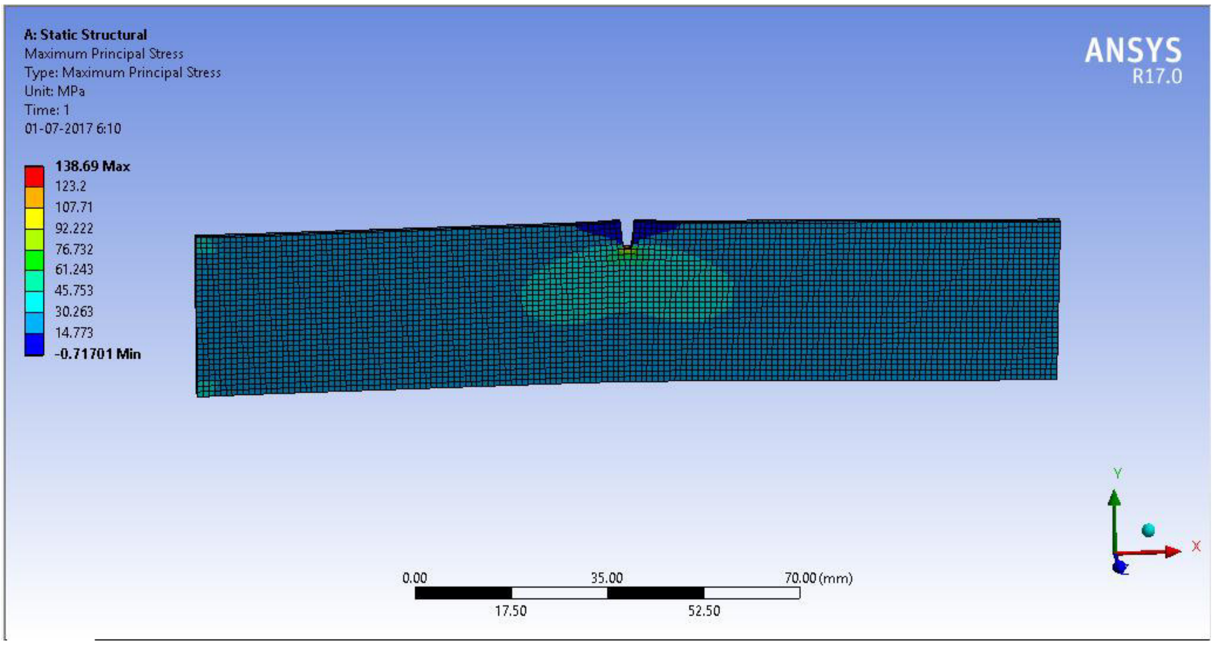

Figure IV.34 Maximum principal stress of glass /epoxy specimen (with a=5mm & θ=90° crack)

c) Normal elastic strain

Normal elastic strain acting on the specimen is 0.022313 which is shown in figure bellow

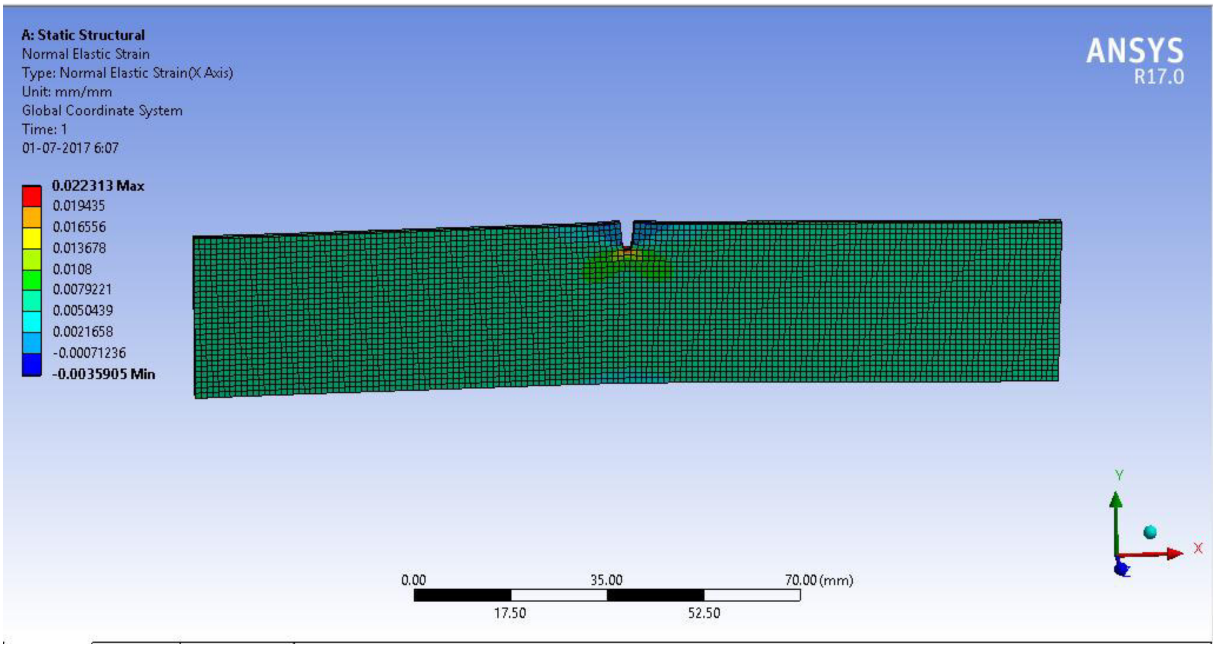

Figure IV.35 normal elastic strain of glass /epoxy specimen (with a=5mm & θ=90° crack)

IV.6.3 Results for a glass/epoxy specimen without crack

a) Total deformation

Total deformation of glass epoxy specimen is 5.6451 mm which is shown in figure bellow

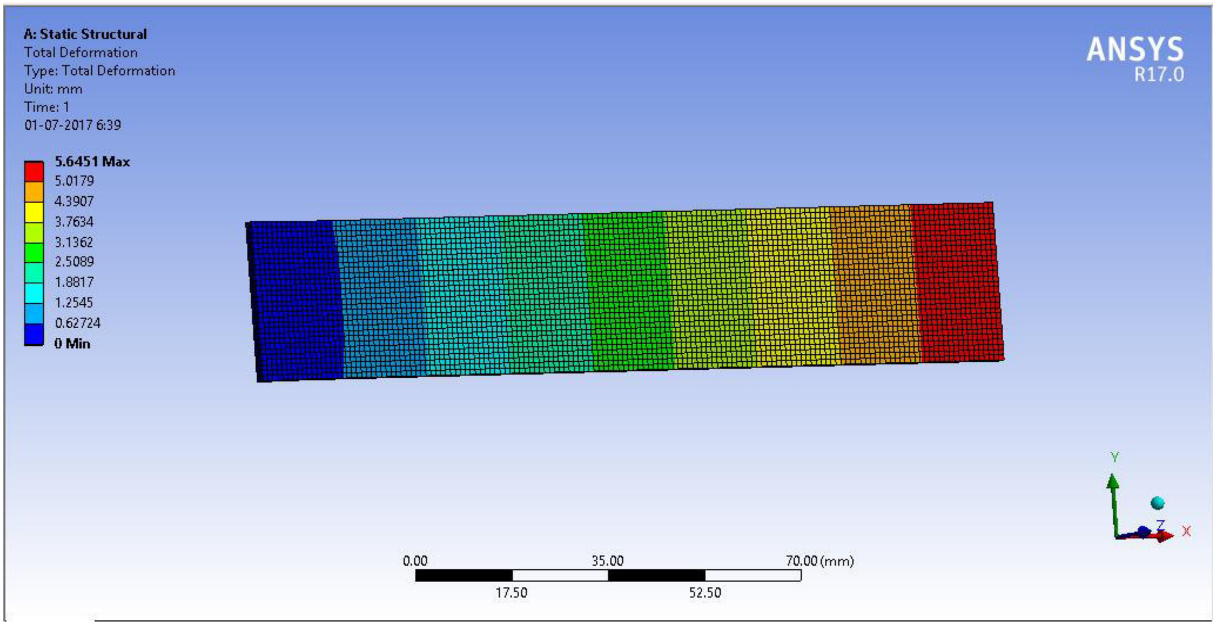

Figure IV.36 total deformation of glass /epoxy specimen (without crack)

b) Maximum principal stress

Maximum principal stress acting on specimen is 249.62 MPa , which is shown in figure bellow

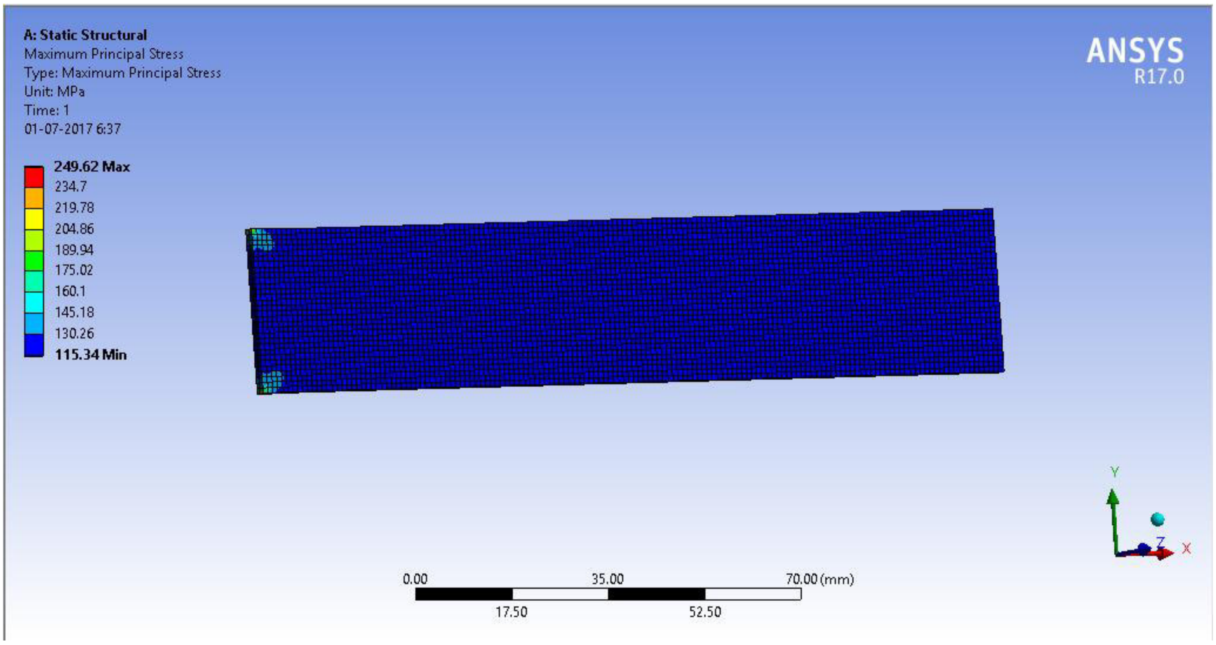

Figure IV.37 Maximum principal stress of glass /epoxy specimen (without crack)

c) Normal elastic strain

Normal elastic strain acting on the specimen is 0.0386 which is shown in figure bellow

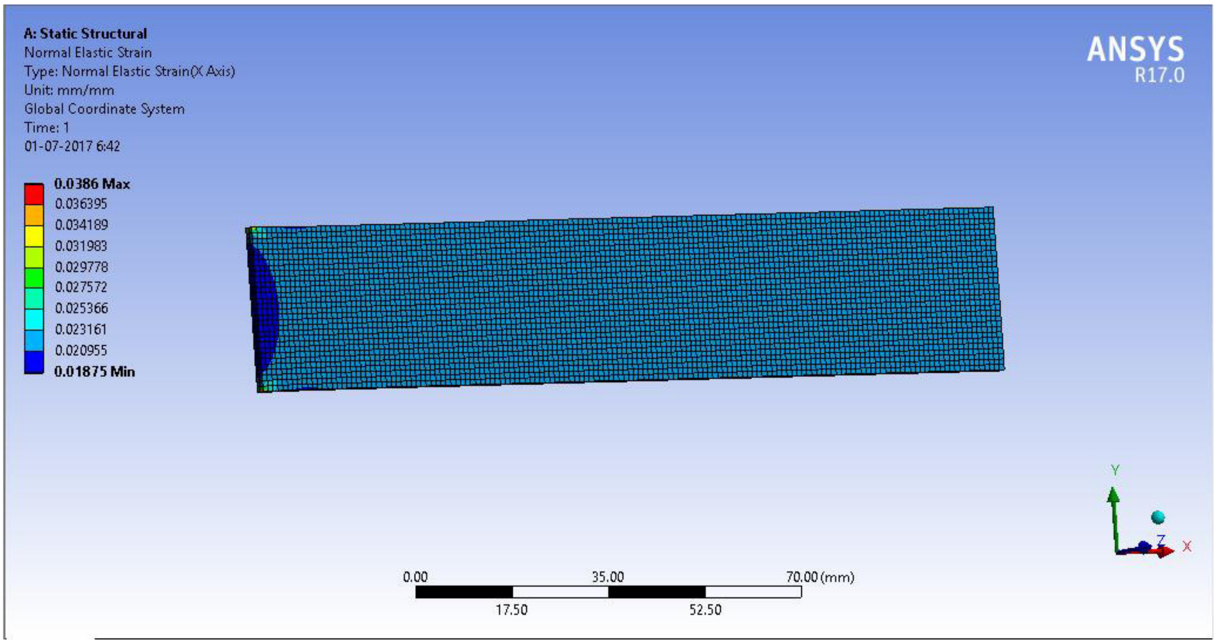

Figure IV.38 normal elastic strain of glass /epoxy specimen (without crack)

IV.6.4 Discussion

Note:

For the carbon/epoxy specimens we did the same work but we changed the material and we took the boundary conditions from the experimental study.

a) Total deformation [mm]

Table IV.4 total deformation of cracked specimen in different size of crack

	0 mm	5 mm	10 mm	15 mm
Carbon/epoxy	5.9501	3.6710	2.857	2.9308
Glass/epoxy	5.6451	3.3837	2.8083	2.6612

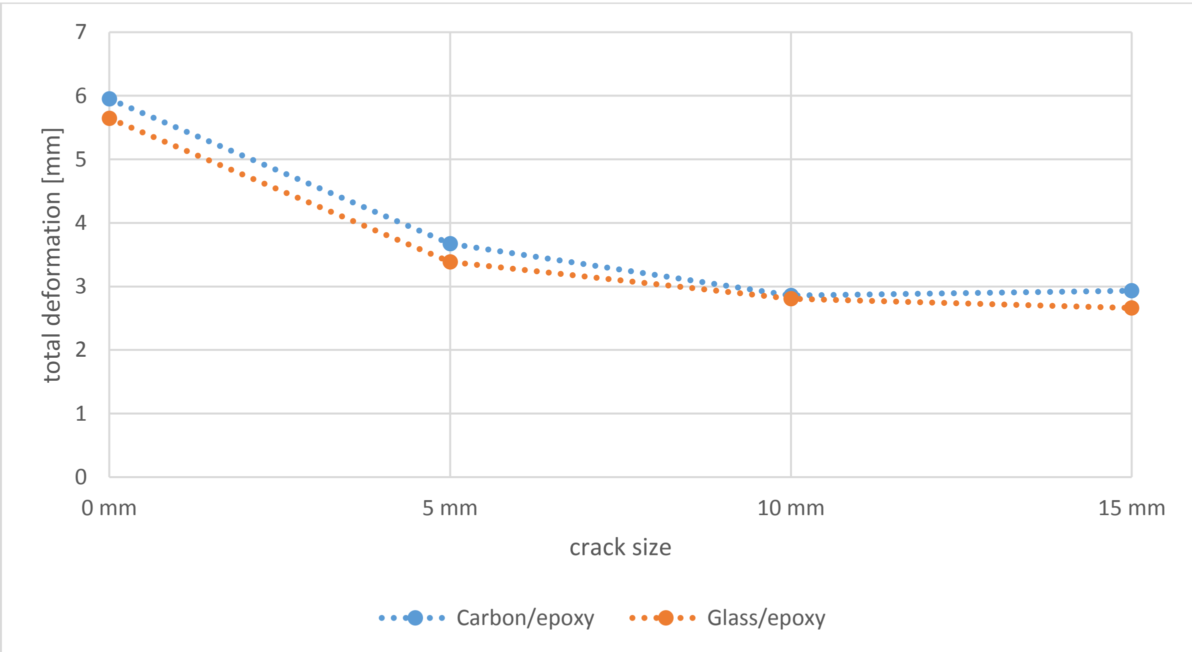

Figure IV.39 total deformation for carbon/epoxy & glass/epoxy specimens under tensile test with different angle crack

This graph represents the curves of the total deformation values of carbon/epoxy and glass/epoxy specimens as a function of different crack size of a specimen. We can clearly see that the deformation decrease when the crack size decrease.

b) Maximum principal stress

table IV.5 Maximum principal stress of carbon/epoxy and glass/epoxy in different size of crack

	0	5	10	15
Carbon/epoxy	671.67	243.12	186.74	87.857
Glass/epoxy	249.62	138.69	69.664	79.15

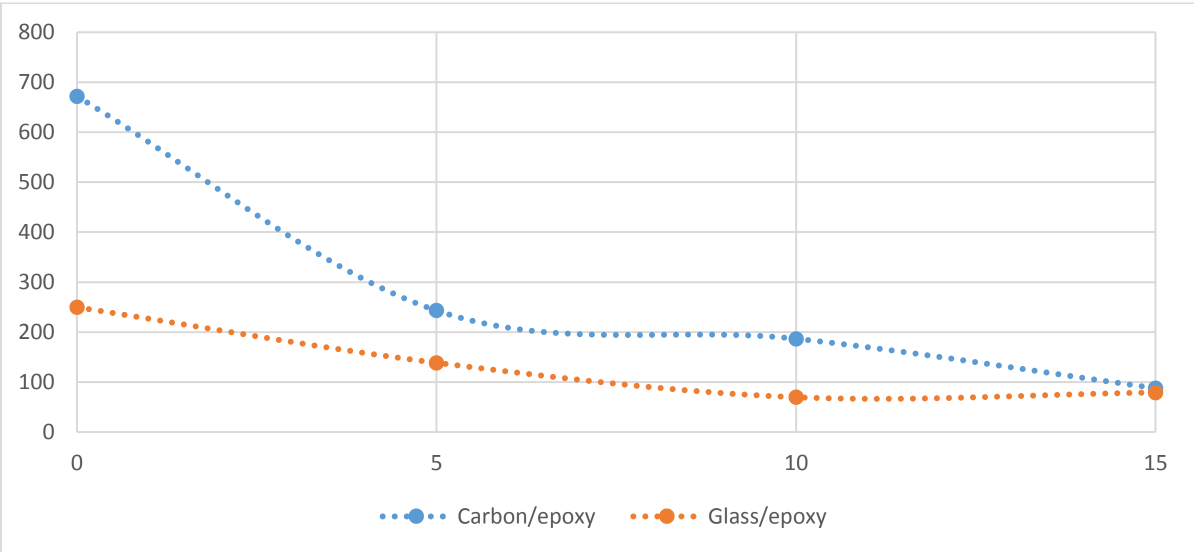

Figure IV.40 Maximum principal stress of carbon/epoxy & glass/epoxy in different size of crack

The same discussions can be drawn for the distribution of maximum principal stress as crack size for both of carbon/epoxy and glass/epoxy specimens .

The both of this graphs decrease in maximum principal stress when the crack size decrease.

c) Normal elastic strain

table IV.6 normal elastic strain of glass/epoxy and glass/epoxy in different size of crack

	0	5	10	15
Carbon/epoxy	0.0450	0.0249	0.01945	0.01473
Glass/epoxy	0.0386	0.022313	0.014592	0.0086

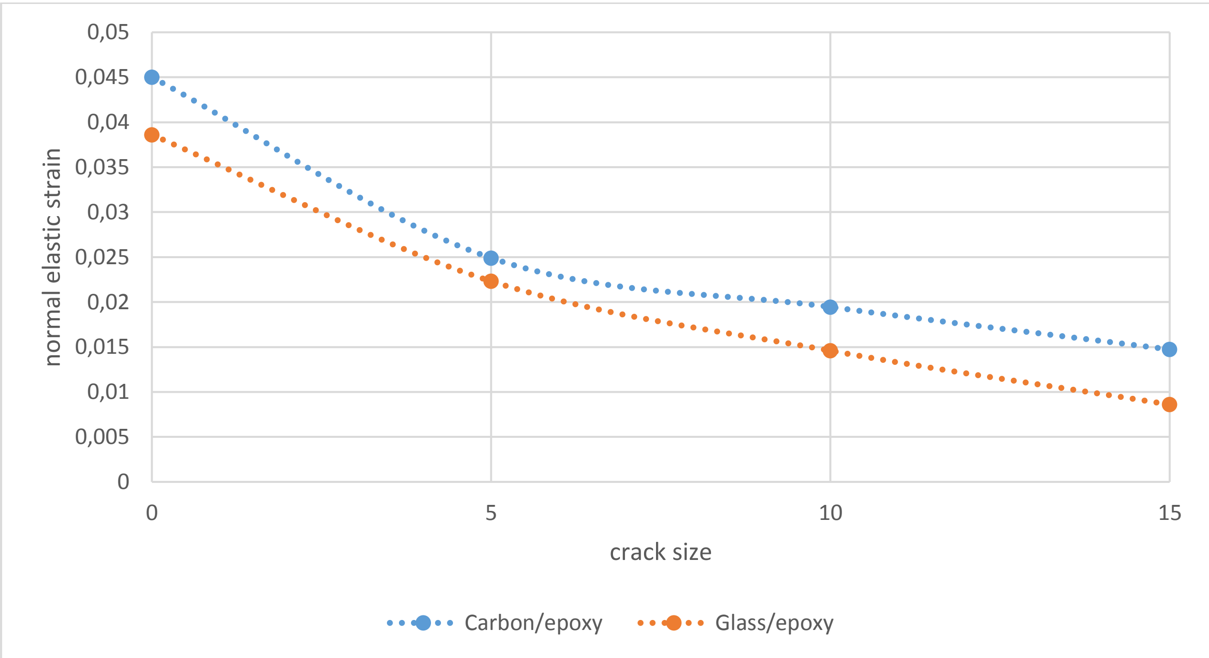

Figure IV.41 Normal elastic strain carbon/epoxy & glass/epoxy specimens under tensile test with different crack size

The graph IV.41 illustrate the values of the normal elastic strain evolution according to the different crack size. we observe that the normal elastic strain decreases when the size of crack decrease.

IV.7 Conclusion

- We have simulated in this chapter some different cracked carbon/epoxy and glass/epoxy specimens to observe the effects of different crack sizes and crack angles on the propagation of cracks and the progress of stress, strain and deformation.

- We have seen in a general manner that the stress decreases with the increase of crack sizes and angles.
- We have seen also that the deformation decreases with the increase of both crack sizes and crack angles.
- Also, the strain decreases with the increase of crack sizes and angles.
- All of those results (the decrease of all of the stress, strain and deformation due to the increase of crack that causes the decrease of materials resistant to stress which makes the failure of those specimens faster every time the crack grows).

GENERAL CONCLUSION

General conclusion

We saw firstly a concept on composite materials and its existence from long years ago, its benefits and limits in several fields of use also we have touched its components from reinforcement and matrix and their types, define mechanical proprieties of the composite material and have an idea about the laminae and the laminate.

Such as every material on this planet, the composite material give in to fracture that can damage it, each composite material can handle a maximum stress that it depends on the characteristics of each material and after it gets above his maximum stress the fracture occurs.
Cracks decreases the materials characteristics, strength and performance.
For the experimental part, we have seen the different materials to make glass/epoxy and carbon/epoxy composite material and the different steps to produce it, as We saw also the manner that those materials react with tensile test and the propagation of the crack in these different specimens with different crack sizes and crack angles, then we observed from the obtained graphs, how does the stress reacts with strain, taking in consideration the different crack sizes and angles and how does this parameters effects on its progression.

For stress strain's graphs, we could observe that the progress of the stress passes generally by two regions: the first region is where the stress increases with increase of the strain and the second region is that the stress decreases with increase of the strain then we had graphs of the progress of strain with crack sizes and the graphs of the progress of the strain with crack angles we deduced from it that the deformation decreases with the increase of the crack sizes and the increase of the crack angles because of the relation between strain and deformation.

In the last chapter, we have simulated some different cracked carbon/epoxy and glass/epoxy specimens to observe the effects of different crack sizes and crack angles on the propagation of cracks and the progress of stress, strain and deformation.

We have seen in a general manner that the stress decreases with the increase of crack sizes and angles, the same thing for the deformation decreases with the increase of both crack sizes and crack angles, also for the strain, where we found that it decreases with the increase of crack sizes and angles.

All of those results (the decrease of all of the stress, strain and deformation due to the increase of crack) causes the decrease of materials resistant to stress which makes the failure of those specimens faster every time the crack grows.

According to this work, we deduce that the experimental study and the numerical simulation are very important to observe the defects and the loads on the fractured composite material.

From the obtained results, we founded that the results of the experimental study goes the same way that the numerical study gave us.

The aim of this study is to detect the influence of different fracture sizes and angles on the composite materials and determinate its behaviors in three cases: simple specimen (without crack), with different crack sizes and different crack angles and this what was proved in this work.

REFERENCES

Reference

[1] Toughening Mechanisms in Composite Materials by Qinghua Qin and Jianqiao Ye Woodhead Publishing is an imprint of Elsevier. 80 High Street, Sawston, Cambridge, CB22 3HJ, UK. 225 Wyman Street, Waltham, MA 02451, USA. Langford Lane, Kidlington, OX5 1GB, UK. 2015.

[2] Laminar Composites Second Edition George H. Staab. Butterworth-Heinemann The Boulevard, Langford Lane, Kidlington, Oxford OX5 1GB, UK. 225 Wyman Street, Waltham, MA 02451, USA. 2015 Elsevier.

[3] Modeling Damage, Fatigue and Failure of Composite Ramesh TALREJA and Chandra VEER SINGH. 2012. Printed in the United Kingdom at the University Press, Cambridge.

[4] Composite materials: Engineering and sciences, F. L. Matthews and R. D. Rawlings, Woodhead Publishing is an imprint of Elsevier. 80 High Street, Sawston, Cambridge, CB22 3HJ, UK. 225 Wyman Street, Waltham, MA 02451, USA. Langford Lane, Kidlington, OX5 1GB, UK. 1994.

[5] Mechanics of composite materials second edition by Robert M. JONES Printing by Edwards Brothers, Ann Arbor, Ml, 1998.

[6] The Behavior of Structures Composed of Composite Materials by Jack R. VINSON and Robert L. IERAKOWSKI Print ©2002 Kluwer Academic Publishers Dordrecht.

[7] https://en.m.wikipedia.org/wiki/composite_materials

[8] Mechanics of composite materials second edition by Autar K. Kaw © 2006 by Taylor & Francis Group, LLC.

[9] https://en.wikipedia.org/wiki/Composite_material#/media/File:Composite_3d.png. 2017-04-09/09:43.

[10] http://www.3mb.asia/composites-ancient-times.2017-04-09/09:44.

[11] https://bashny.net/t/en/291097#. 2017-0.4-09/09:44

[12] https://es.wikipedia.org/wiki/Contrachapado#/media/File:Plywood.jpg. Date of use: 2017-04-29/09:44.

[13] http://www.essentialchemicalindustry.org/materials-and-applications/composites.html. Date of use: 2017-04-09/09:44

[14] http://www.regmedia.co.uk/2013/06/27/drayson.jpg. Date of use: 2017-07-13/11:30

[15] http://slidrplayer.com/slide/10855692/ date of use: 2017-07-13/11:51

[16] http://upload.wikipedea.org/wikipedia/1/1f/king%27s_collage_chapel_-_fan_vaulted_ceiling_-_Cambridge_-_UK_2007.jpg. date of use: 2017-07-13/11:54.

APPENDIX

Proprieties of Materials:

Matrix

Table: The epoxy resin properties

Properties	RESINE EPOCAST 50_A1
Color	straw
Density (g/cm^3)	1.21
Viscosity (mg/cm. s)	77.7
Temperature of life has 25 c ° and without opening of container (less)	12

The hardener

The hardener used is reference hardener 964, it is compatible with Epocast resin 50_A1

Table: The Hardener properties

Properties	HARDENER 964
Colour	Orange Gold
Density (g/cm^3)	1.05
Viscosity (mg/cm. s)	4000
Temperature of life has 25 c ° and without opening of container (less)	12

Reinforcements:

The reinforcements used are carbon fabrics and bidirectional glass (see figure), these characteristics are mentioned in the tables below:

Table: General property of carbon fibers

	Carbone HR
Density(kg/m^3)	1750
Modulus of longitudinal elasticity [MPa]	230000
Shear Modulus [MPa]	50000
Poisson v coefficient	0.3
Tensile Breaking Stress [MPa]	3200
Elongation at rupture [%]	1.3

Coefficient of thermal expansion	0.02
Temperature limit	>1500

Table: General property of glass fibers

	Glass R
Density (kg/m^3)	2500
Longitudinal elasticity Modulus [MPa]	86000
Shear Modulus [MPa]	36000
Poisson coefficient ν	0.2
Tensile Breaking Stress [MPa]	3200
Elongation at rupture [%]	4
Coefficient of thermal expansion	0.3
Temperature limit	800